


Politecnico di Torino

**Politecnico di Torino**

Corso di Laurea Magistrale in Ingegneria civile
A.a. 2025/2026
Sessione di laurea Mese 2026

# Fish habitat suitability in a hydropower-regulated river reach

## An ecohydraulic study of brown trout (*Salmo trutta*) and European grayling (*Thymallus thymallus*)

Relatori:

Paolo Vezza

Schicheng Li

Candidato:

Emanuela Servetti

# English abstract

Freshwater ecosystems face major global threats, with flow regulation a primary cause of river habitat alteration. In hydropower-regulated rivers, discharge changes directly affect water depth, flow velocity and hydraulic energy, which in turn affect fish habitat and ecosystem function.

This thesis examines how regulated discharge shapes physical habitat suitability in the Ume River's bypass reach, just downstream of the Stornorrfors dam. Using two-dimensional ecohydraulic modelling, it evaluates habitat availability for brown trout (*Salmo trutta*) and European grayling (*Thymallus thymallus*) at different life stages. The study links hydraulic modelling with habitat assessment, focusing on water depth and flow velocity as principal drivers of habitat quality.

Habitat response to discharge variation is highly species- and stage-specific. No single discharge scenario fits all ecological components. Brown trout generally showed a reduction in suitable habitat with increasing discharge, especially for fry, juvenile and adult stages, whereas adult European grayling benefited from higher-flow conditions. Early life stages, especially fry, were the most vulnerable, relying on low-velocity marginal habitats and struggling with increased hydraulic energy. Low discharge best protected these stages, while intermediate flows offered a more balanced compromise for the fish community. In particular, $Q_{21}$ emerged as the most protective scenario for limiting life stages, while $Q_{30}$ represented the best multi-objective compromise. Short-term flow variations further reduced habitat stability, emphasising the need for environmental flow assessments to address both discharge magnitude and timing.

This study shows that two-dimensional ecohydraulic modelling is an effective tool for managing regulated rivers. By connecting hydraulic processes with species specific requirements, the approach exposes ecological trade-offs that standard discharge-focused methods can miss.

***Keywords:*** *ecohydraulic modelling, regulated rivers, habitat suitability, environmental flow, brown trout, European grayling, Ume River, Weighted Usable Area, hydropeaking*

# Italian abstract

Gli ecosistemi d'acqua dolce sono esposti a gravi minacce globali, e la regolazione delle portate rappresenta una delle principali cause di alterazione degli habitat fluviali. Nei fiumi regolati da impianti idroelettrici, le variazioni di portata influenzano direttamente la profondità dell'acqua, la velocità della corrente e l'energia idraulica, che a loro volta influenzano l'habitat dei pesci e il funzionamento degli ecosistemi.

Questa tesi esamina come la portata regolata influenzi l'idoneità fisica dell'habitat nel tratto bypassato del fiume Ume, subito a valle della diga di Stornorrfors. Attraverso una modellazione eco-idraulica bidimensionale, viene valutata la disponibilità di habitat per la trota fario (*Salmo trutta*) e il temolo europeo (*Thymallus thymallus*) in diverse fasi del ciclo vitale. Lo studio collega la modellazione idraulica alla valutazione dell'habitat, concentrandosi sulla profondità dell'acqua e sulla velocità della corrente come principali fattori che determinano la qualità dell'habitat.

La risposta dell'habitat alle variazioni di portata è fortemente specifica per specie e fase vitale. La trota fario ha mostrato generalmente una riduzione dell'habitat idoneo con l'aumento della portata, soprattutto per avannotti, giovani e adulti, mentre gli adulti di temolo europeo hanno beneficiato di condizioni di portata più elevata. Le prime fasi di vita, in particolare gli avannotti, sono risultate le più vulnerabili, poiché dipendono da habitat marginali a bassa velocità e faticano a adattarsi all'aumento dell'energia idraulica. Le basse portate hanno protetto meglio queste fasi, mentre portate intermedie hanno offerto un compromesso più equilibrato per la comunità ittica. In particolare, $Q_{21}$ è emerso come lo scenario più protettivo per le fasi di vita limitanti, mentre $Q_{30}$ ha rappresentato il miglior compromesso multi-obiettivo. Le variazioni di portata di breve durata hanno ulteriormente ridotto la stabilità dell'habitat, sottolineando la necessità che le valutazioni dei deflussi ecologici considerino sia l'entità della portata sia la sua variabilità temporale.

Questo studio mostra che la modellazione eco-idraulica bidimensionale è uno strumento efficace per la gestione dei fiumi regolati. Collegando i processi idraulici ai requisiti specifici delle specie, l'approccio permette di evidenziare compromessi ecologici che i metodi tradizionali basati esclusivamente sulla portata possono non cogliere.

***Parole chiave:*** *modellazione eco-idraulica, fiumi regolati, idoneità dell'habitat, deflusso ecologico, trota fario, temolo europeo, fiume Ume, area utilizzabile ponderata, picco di portata*

# Acknowledgements

This thesis was carried out during my Erasmus period at KTH Royal Institute of Technology as part of my Master's degree in Civil Engineering at Politecnico di Torino.

I would like to express my sincere gratitude to my supervisors for their guidance and support throughout the development of this thesis. I am particularly grateful to Shicheng Li, who patiently supported me over the past months and helped me address the doubts and challenges that arose during this work. I would also like to sincerely thank Paolo Vezza for his valuable advice, encouragement and support throughout the development of this thesis, despite the distance.

I would also like to thank Politecnico di Torino for the academic path that made this thesis possible, as well as KTH Royal Institute of Technology for the opportunity to spend an enriching Erasmus period in Stockholm, which contributed significantly to both my academic and personal growth.

Finally, I am deeply grateful to my family and friends for their encouragement, patience and support throughout this journey.

.

# Contents

**Figure index** ..... **xii**

**1 Introduction** ..... **1**

1.1 Context and problem definition ..... 1

1.2 Aim and objectives of the thesis ..... 4

1.3 Scope and limitations ..... 5

**2 Background** ..... **7**

2.1 The Ume River system ..... 7

2.1.1 River management and ecological restoration ..... 8

2.1.2 Target fish species ..... 9

2.2 Ecohydraulics and habitat assessment ..... 12

2.3 Habitat Suitability Theory ..... 13

2.3.1 Habitat suitability methodology ..... 14

1.1.1 Weighted usable area and related index ..... 16

2.4 Hydrodynamic modelling ..... 17

2.4.1 Governing equations ..... 17

2.4.2 Numerical approach ..... 18

2.4.3 HEC-RAS software ..... 18

**3 Materials and methods** ..... **21**

3.1 Study area ..... 21

3.2 Hydraulic model setup ..... 22

3.2.1 Geometry and topographic data ..... 22

3.2.2 River geometry creation ..... 23

3.2.3 Computational mesh ..... 25

3.2.4 Boundary conditions ..... 27

3.2.5 Numerical parameters ..... 28

3.3 Model calibration and validation ..... 29
3.3.1 Validation data ..... 29
3.3.2 DEM anomalies and uncertainties ..... 31
3.3.3 Calibration procedure ..... 31
3.4 Scenario simulations ..... 32
3.5 Data extraction and post-processing ..... 33
3.6 Habitat assessment framework ..... 34
3.6.1 Habitat Suitability Curves ..... 34
3.6.2 Habitat Suitability Index ..... 36
3.6.3 Weighted Usable Area ..... 37
3.6.4 Habitat suitability classes ..... 37
3.7 Ecological flow assessment ..... 39
3.7.1 Limiting factor analysis ..... 39
3.7.2 Multi-objective optimisation ..... 39

**4 Results and analysis ..... 41**
4.1 Model calibration and validation ..... 41
4.2 Hydraulic results ..... 44
4.3 Steady-state simulations ..... 49
4.3.1 Habitat suitability spatial distribution ..... 49
4.3.2 Quantitative habitat analysis ..... 53
4.3.3 Qualitative habitat analysis ..... 55
4.3.4 Habitat response to discharge variations ..... 57
4.3.5 Optimal discharge identification ..... 57
4.4 Unsteady simulation ..... 63
4.4.1 Temporal evolution of habitat availability ..... 63
4.4.2 Habitat quality dynamics ..... 67

**5 Discussion ..... 73**
5.1 Model reliability ..... 73
5.2 Ecological differences between species and life stages ..... 74
5.3 Optimal discharge and ecological conflicts ..... 75
5.4 Effects of hydropeaking ..... 76
5.5 Practical implications, study limitations and future directions ..... 77

**6 Conclusion ..... 81**

**Bibliography** ..... **86**

# Figure index

Figure 1.1. The Living Planet Index by ecosystem type from 1970 to 2020 based on 16,909 populations of 1,472 freshwater species [3] ..... 2
Figure 1.2. Expected result of the implementation of the Emergency Recovery Plan [4] ..... 2
Figure 2.1. Maps showing the position of dams and hydropower stations in the Ume River catchment [8]..... 7
Figure 2.2. Life cycle of Atlantic salmon (source: Atlantic Salmon Trust). The general life cycle structure is representative of salmonoid species [22]. ..... 10
Figure 2.3. Brown trout - Salmo trutta [26] .....11
Figure 2.4. European grayling - Thymallus Thymallus [28].....11
Figure 2.5. Physical habitat as an intersection of geomorphology and hydrology [29] ..... 12
Figure 3.1.Position of Stornorrfors in Sweden and map of the hydropower plant [42]. ..... 21
Figure 3.2. Digital Elevation Model of the study reach in the Ume River. The colour scale represents the elevation. ..... 23
Figure 3.3. Final banklines overlaid on the Lantmäteriet map ..... 24
Figure 3.4. Final banklines overlaid on the Google Maps satellite map..... 25
Figure 3.5. Computational mesh of the study domain generated in HEC-RAS ..... 27
Figure 3.6. Boundary condition setup in the HEC-RAS Unsteady Flow Data editor . 28
Figure 3.7. 2D mesh with upstream (Boundary line 2) and downstream (Boundary line 1) boundary lines locations. ..... 28
Figure 3.8. Key locations in the study reach extracted from HEC-RAS ..... 30
Figure 3.9. Unsteady flow hydrograph, based on a hydropeaking scenario with 30 flow changes per day .....33
Figure 3.10. Habitat suitability curves for water depth and flow velocity for Grayling species [34], [43] .....35
Figure 3.11. Habitat suitability curves for water depth and flow velocity for brown trout species [34], [43]..... 36
Figure 4.1. Preliminary WSE distribution obtained from HEC-RAS simulation..... 41
Figure 4.2. Water surface elevation difference (ΔWSE) obtained from the parametric sweep of Manning's roughness coefficients. ..... 42
Figure 4.3. Spatial distribution of calibrated Manning's roughness coefficients implemented as a Land Cover layer ..... 43
Figure 4.4. Comparison between measured and simulated WSE ..... 44

Figure 4.5. Spatial distribution of flow velocity for Q = 21 m³/s obtained from HEC-RAS ..... 45
Figure 4.6. Spatial distribution of water depth for Q = 21 m³/s obtained from HEC-RAS ..... 46
Figure 4.7. Boxplot of depth and velocities for different flow scenarios: a) complete depth analysis with outliers, b) detail of depth below 3m, c) velocity distribution... 47
Figure 4.8. Cumulative Distribution Functions (CDF) for depth ..... 48
Figure 4.9. Cumulative Distribution Functions (CDF) for velocity ..... 49
Figure 4.10. HSI distribution for the fry stage at each discharge scenario for the European grayling ..... 49
Figure 4.11. HSI distribution for the juvenile stage at each discharge scenario for the European grayling ..... 50
Figure 4.12. HSI distribution for the spawning stage at each discharge scenario for the European grayling ..... 50
Figure 4.13. HSI distribution for the adult stage at each discharge scenario for the European grayling ..... 50
Figure 4.14. HSI distribution for the fry stage at each discharge scenario for the brown trout ..... 51
Figure 4.15. HSI distribution for the juvenile stage at each discharge scenario for the brown trout ..... 52
Figure 4.16. HSI distribution for the spawning stage at each discharge scenario for the brown trout ..... 52
Figure 4.17. HSI distribution for the adult stage at each discharge scenario for the brown trout ..... 52
Figure 4.18. Variation of WUA with the discharge: comparison between the two species ..... 54
Figure 4.19. Habitat quality composition for brown trout: percentage distribution of High (HSP), Medium (MSP), and Low (LSP) Suitability Proportions as a function of discharge ..... 55
Figure 4.20. Habitat quality composition for European grayling: percentage distribution of High (HSP), Medium (MSP), and Low (LSP) Suitability Proportions as a function of discharge. ..... 56
Figure 4.21. Hydraulic niche shift analysis: displacement of habitat centroids in the depth-velocity space for each species and life stage across the simulated discharge scenarios ..... 57
Figure 4.22. Total Weighted Usable Area (Grayling + Trout) as a function of discharge ..... 59
Figure 4.23. General Pareto trade-off curve ..... 60
Figure 4.24. Pareto trade-off curve per life stages ..... 61
Figure 4.25. Limiting factor analysis ..... 62
Figure 4.26. Multi-objective compromise ..... 63
Figure 4.27. Distribution of WUA values during the central 12 h of ramping for the different life stages of European grayling ..... 64
Figure 4.28. Distribution of WUA values during the central 12 h of ramping for the different life stages of brown trout ..... 65
Figure 4.29. Evolution of WUA over time for European grayling: comparison between the stages ..... 66

Figure 4.30. Evolution of WUA over time for brown trout: comparison between the stages..... 67
Figure 4.31. Temporal dynamics of habitat quality for Brown Trout during the unsteady simulation, showing the evolution of suitability classes (HSP, MSP, LSP) over time..... 68
Figure 4.32. Temporal dynamics of habitat quality for European Grayling during the unsteady simulation, showing the evolution of suitability classes (HSP, MSP, LSP) over time..... 69
Figure 4.33. Habitat class boxplot for brown trout..... 70
Figure 4.34. Habitat class boxplot for European grayling ..... 70

# Chapter 1

# Introduction

## 1.1 Context and problem definition

Rivers represent complex systems in which hydrological, hydraulic, and ecological processes interact on different temporal and spatial scales. The physical habitat that aquatic populations inhabit is shaped by physical processes such as channel morphology, flow, and sediment transport. In turn, the biological community adjusts to these conditions in response to changes in water flow, depth, speed, and habitat. These interactions and their effects on the environment occur on various levels of complexity, from the scale of global river systems down to the smallest physical phenomena to which the habitat is directly exposed. Moreover, temporal variation, whether cyclic, such as seasonality, or episodic events, further influences both the nature of river processes and ecological reaction. As a result, understanding these interactions is especially essential in regulated rivers, where human activities have significantly altered natural processes.

Freshwater ecosystems are among the most threatened environments in the world. Despite representing a very small fraction of the world's waters, about 0.01%[1], and covering less than 1% of the Earth's surface, they support a significant amount of global diversity, harbouring more than 10% of all known species [2]. Recent global assessments highlight the severity of biodiversity loss in these systems and indicate that the decline is often more severe than that observed in terrestrial ecosystems. The Living Planet Report of WWF states that populations of freshwater vertebrates have declined by 85% since 1970 [3]. Furthermore, approximately one third of fish species that are dependent on freshwater are at risk of extinction [4]. These trends result from multiple factors that can be grouped into five categories: flow regulation, overexploitation, habitat fragmentation, water pollution and invasive species, combined with global environmental changes [3], [5]. But it is widely recognised that one of the primary causes of ecological degradation is the alteration of natural flow, which makes it essential to better understand how to manage river systems.

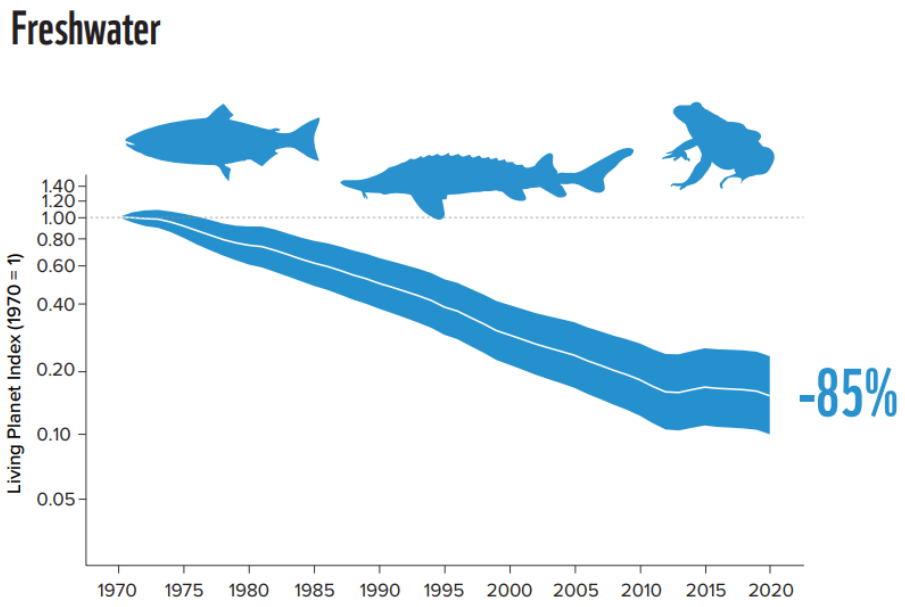



*Figure 1.1. The Living Planet Index by ecosystem type from 1970 to 2020 based on 16,909 populations of 1,472 freshwater species [3]*

In response to this ongoing global crisis of freshwater biodiversity, scientists and international organisations have worked together and developed the Emergency Recovery Plan [4]. The implementation is intended to reverse the trends of species decline through six key strategies that aim to: naturalise river flow, improve water quality, conserve essential habitat, regulate sustainable fishing and sand extraction, control invasive species, and remove obsolete river barriers (Figure 1.2).

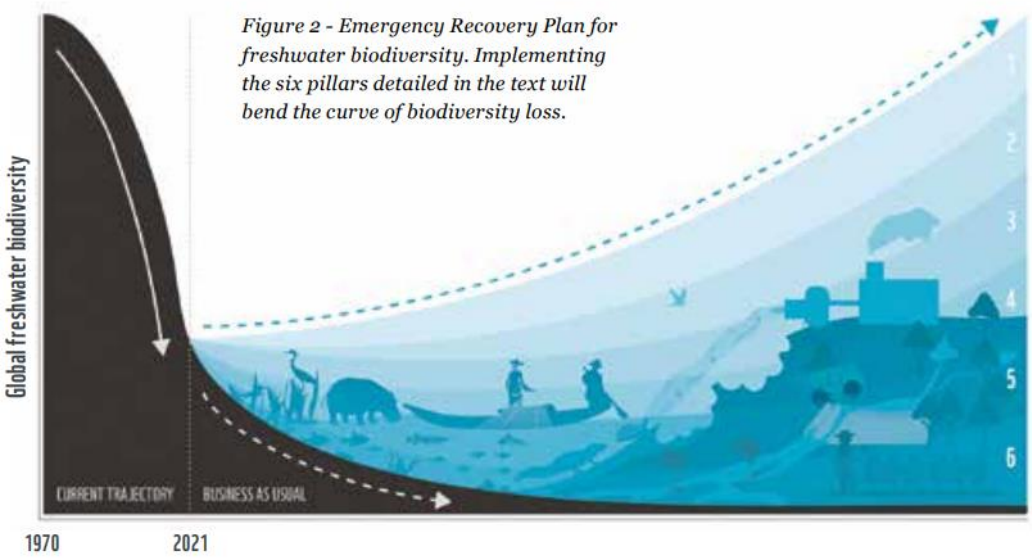



*Figure 1.2. Expected result of the implementation of the Emergency Recovery Plan [4]*

The flow regime plays a fundamental role in shaping river ecosystems, controlling not only hydraulic conditions but also sediment transport, channel morphology and ecological processes. Alterations of these flow regimes, through changes in magnitude, frequency, duration and timing, can cause ecological problems, influencing the availability of habitats and the distribution and life-cycle processes of

many species. This has effects not just on the fish community, but also on macroinvertebrates, riparian vegetation and the functioning of the whole ecosystem. As a consequence, regulated rivers often exhibit simplified habitats, reduced connectivity and decreased ecological resilience [6], [7].

In Sweden and across the Scandinavian countries, large river systems have undergone profound transformations during the twentieth century, primarily due to the expansion of hydroelectric power generation. The Ume River represents a clear example of this industrial evolution.

However, the human footprint on these rivers predates the advent of electricity. In the past, the rivers of Scandinavia were heavily modified to facilitate timber floating. This involved systematic channel clearing, resulting in a long-term reduction in the river's natural complexity. Later, the evolution of hydropower has further played a great part in the shaping of these systems. Today, the Ume River is fragmented by several artificially created channels, reservoirs and dams, which altogether transform the natural flow regime and, in doing so, its spatial and temporal discharge variability [8]. Besides long-term variation, rapid short-term flow fluctuations, usually referred to as hydropeaking, are commonly recorded in regulated rivers due to hydropower operations. Sudden changes in discharge may cause rapid changes in river level and water flow velocity, affecting the stability of habitats and fish behaviour. In many studies, hydropeaking has been directly related to fish mortalities due to stranding and reduction in benthic macroinvertebrate diversity, emphasising its ecological significance beyond the simple gradual alteration of water flow [9]. Although hydropower provides a key element of energy production in Sweden and contributes to the transition to renewable energy, flow regulation has led to profound alterations in flow dynamics.

At the river scale, dams influence the flow regime by reducing the frequency and intensity of natural floods, altering low-water conditions and modifying seasonal variability. These modifications have cascading ecological consequences. Studies conducted in Northern Sweden have demonstrated that flow regulation can greatly alter the aquatic system, the abundance and diversity of fish in the ecosystem [10]. These modifications can also affect sediment compositions, channel morphology and the structure of fish communities.

In a regulated system, such as the Ume River, the physical habitat represents the connection between hydraulic alterations and ecological responses. Local conditions, such as water depth and flow velocity, affect benthic species distribution and fish life processes, including swimming costs, foraging efficiency, and spawning success [10].

Habitat selection in salmonids, for example, often reflects a compromise between the energetics of feeding and the risk of predation in high-velocity habitats [11]. Moreover, different life stages of the same species may occupy distinct habitats, requiring specific conditions for spawning, juveniles, and adults. For example, experimental and field studies have shown that brown trout early life stages generally prefer shallow areas with relatively higher flow velocities, whereas juveniles and adults tend to select deeper habitats associated with lower velocities. [12].

A crucial aspect is that fish respond to local conditions rather than to average values calculated at the research scale. For this reason, mean values evaluated at the scale of the whole river are not sufficient to describe the complexity of the real habitat. It is instead necessary to use spatially distributed information about depth

and velocity to represent the heterogeneity of the microhabitat. This spatial heterogeneity plays a fundamental role in maintaining biodiversity, providing a range of ecological niches and supporting species coexistence within a single river reach.

In this context, habitat modelling tools are useful to provide numerical quantification of the relationship between hydraulic parameters and habitat suitability. By integrating hydraulic simulations with responses of the species of interest, these tools allow the assessment of habitat conditions under different flow scenarios and support river management and restoration strategies. Although modelling tools are increasingly becoming available, accounting for this spatial variability and translating it into an ecologically meaningful indicator remains a significant challenge. Two-dimensional hydraulic models are particularly suitable because they allow the simulation of spatially distributed flow fields at scales relevant to aquatic species.

In recent years, river restoration and ecological rehabilitation have become more important in environmental policies. As a clear example of this trend, the European Union has recently adopted the Nature Restoration Law. The regulation is designed to counteract the degradation driven by human activities and requires Member States to restore at least 20% of terrestrial and marine areas by 2030 and to progressively expand restoration actions in the following decades. The overall aim of the regulation is to promote the recovery of freshwater biodiversity, halt further ecosystem loss and restore the functioning and resilience of natural systems to climate change by 2050 [13]. These policies demonstrate the importance of adopting quantitative tools capable of linking hydrological management with ecological responses in river systems, and ecohydraulic modelling represents one of the most promising approaches to achieve this goal [7].

In this context, the present study aims to apply a two-dimensional hydraulic model integrated with habitat suitability analysis to a regulated river system, contributing to a better understanding of the relationship between hydraulic dynamics and ecological conditions.

## 1.2 Aim and objectives of the thesis

This thesis aims to evaluate the influence of regulated discharge conditions on physical habitat conditions in the Ume River bypass reach. The study develops a two-dimensional ecohydraulic modelling approach to assess habitat availability and quality for selected fish species under different flow scenarios and to support environmental flow assessment in regulated rivers.

To achieve this aim, the following objectives are defined:

- investigating how regulated discharges shape hydraulic habitat characteristics in the selected river reach;
- assessing habitat suitability for brown trout (*Salmo trutta*) and European grayling (*Thymallus thymallus*) under different flow conditions;
- comparing habitat responses among species and life stages to identify ecological trade-offs associated with flow regulation;

- evaluating the potential of two-dimensional ecohydraulic modelling as a decision-support tool for environmental flow assessment in regulated rivers

## 1.3 Scope and limitations

The following thesis presents several limitations that should be emphasised in order to ensure clarity in the reading phase and interpretation of the results.

The hydraulic modelling of the Ume River is located downstream of the Stornorrfors dam, which is not modelled, but is taken into account when selecting the simulated discharge. The analysed reach is therefore not representative of the entire river system, but only of the bypass section between the dam and the city of Umeå.

It is also important to underline that habitat conditions will be evaluated from a hydraulic perspective only. In particular, the study will focus on habitat modelling using velocity and depth, while the substrate will not be included in the analysis. Likewise, morphological changes will not be analysed due to a lack of reliable data.

Although hydraulic variables such as velocity and depth are key factors in defining habitat suitability, other environmental variables can also influence habitat conditions. Factors such as temperature, ice presence, food availability and substrate composition can play an important role in defining habitat quality [7]. These aspects are not considered in this work but may represent potential directions for future research.

In addition, the habitat suitability curves adopted in this study were derived from published literature and expert-based sources rather than from site-specific observations collected in the Ume River. Consequently, the represented hydraulic preferences may not fully reflect the local behaviour of brown trout and European grayling populations in the study reach. Furthermore, biological validation data, such as observed fish densities, habitat use surveys, or spawning success measurements, were not available. Therefore, the resulting Habitat Suitability Index (HSI) and Weighted Usable Area (WUA) values should be interpreted as indicators of potential hydraulic habitat rather than direct measures of ecological condition or population performance.

# Chapter 2

# Background

## 2.1 The Ume River system

The Ume River is situated in the northern part of Sweden (Figure 2.1). It starts in the Scandinavian mountains of northern Swedish Lapland, then runs eastwards through Västerbotten County.
After receiving water from its biggest tributary, the Vindel River, it continues in the coastal area and flows into the Bothnia Bay of the Baltic Sea. The river is approximately 467 km long and drains a catchment area of 26,800 km². It represents one of the most important fluvial systems in the region, with an annual discharge of around 242 m³/s [14].

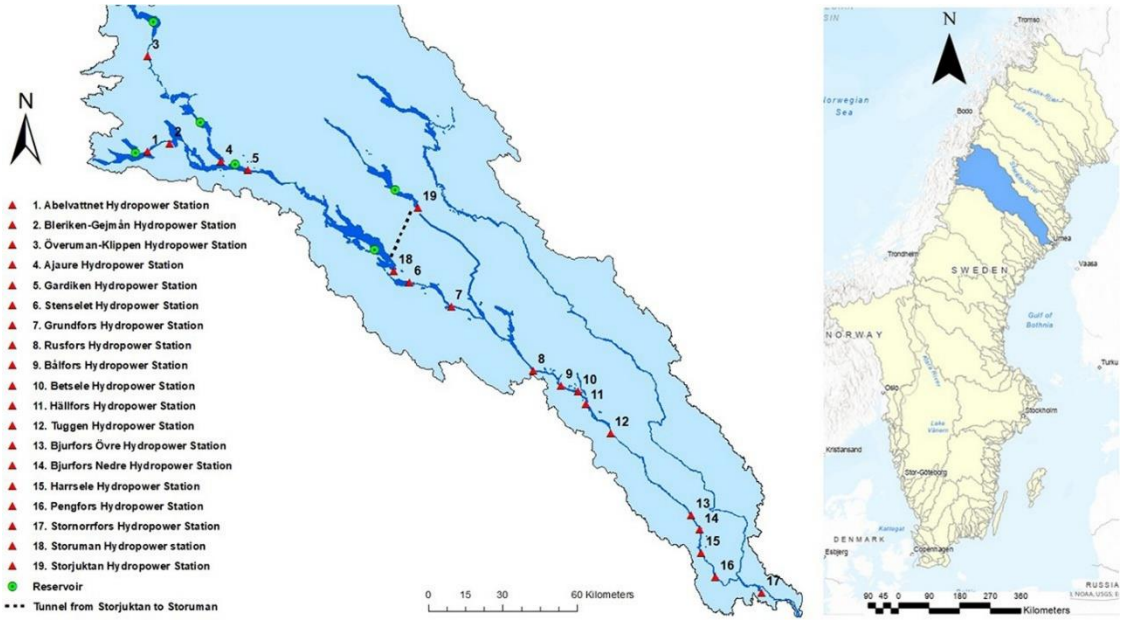



*Figure 2.1. Maps showing the position of dams and hydropower stations in the Ume River catchment [8]*

Between the 1950s and 1960s, the river was regulated through the construction of 19 dams and hydropower stations distributed along its course, exploiting most of the available head of the main channel. Today, it represents the third-largest hydropower producer in Sweden, with a mean annual production of 7.9 TWh [8]. Among these

facilities, the Stornorrfors hydropower station is the second largest in Sweden in terms of production capacity, with a head of 75 m and an installed capacity of 591 MW. The power plant is equipped with four turbines and began operation in 1958.

Six of the hydropower facilities present on the Ume River operate as storage reservoirs, while the remaining plants are run-of-river dams arranged in cascade, many of which are affected by hydropeaking. The extensive exploitation of the available head has resulted in substantial alteration of the natural flow regime and a loss of longitudinal connectivity. One of the most important consequences is the drastic reduction of fast-flowing habitats, such as riffles and rapids, which have decreased from 39% before regulation to only 1% in the current system [15]. In addition, due to flow diversion, several river sections have been bypassed, resulting in reaches that are either dry or characterised by strongly reduced discharge. This is the case for the reach downstream of the Stornorrfors dam, which is the focus of the present study.

These hydromorphological changes, combined with historical river modifications for timber floating activities[1], have led to substantial ecological impacts, affecting fish communities, microvertebrate fauna and riparian vegetation.

### 2.1.1 River management and ecological restoration

In response to these impacts, several management and restoration strategies have been adopted. Historically, the regulation of the Ume River was carried out with limited consideration of ecological consequences, leading to the loss of natural spawning habitats and interruptions of migratory pathways. To compensate for these impacts, several measures have been adopted. Hydropower operators are required to implement stocking programs to support fish populations, involving species such as Atlantic salmon (*Salmo salar*), brown trout (*Salmo trutta*), European grayling (*Thymallus thymallus*) and Arctic char (*Salvelinus alpinus*) [15].

In this context, Vattenfall, one of the main hydropower operators on the river, conducts extensive fish stocking to sustain populations affected by regulation. Near Stornorrfors hydropower plant, it annually releases approximately 80000 salmon fry, 20000 sea trout and 20000 graylings [17]. In addition to stocking, some structural measures have been implemented to restore connectivity. At the Stornorrfors hydropower plant, a fish ladder is present to allow the upstream migration toward the Vindel River and the downstream passage of juvenile dispersal toward the Baltic Sea.

In 2012, the Ume River Project was initiated to promote an integrated and collaborative approach. This initiative involves cooperation among local communities, research institutions, environmental organisations, hydropower companies and public authorities, with the aim of restoring riverine ecosystems in accordance with the European Water Framework Directive (2000/60/EC). The project

[1] Timber floating was a major activity in Sweden from around 1850 to 1970, resulting in extensive modification to rivers, such as the removal of boulders and woody debris, cutting off secondary channels, and flow pattern simplification. These changes reduced habitat complexity and negatively impacted the fish and invertebrate communities, and may still show the effects today [16]

is based on adaptive and strategic management and integrates various restoration actions, including habitat restoration and environmental monitoring [15].

Complementary restoration efforts in tributaries also contribute to improving ecological status. For example, in the Vindel River LIFE project, previously channelised tributaries impacted by timber drifting were restored to improve habitat structure and accessibility for important fish species. This has enhanced connectivity among stream networks and increased the diversity of habitats for salmonids and other species [18]. More recently, small dams in four tributaries were removed to restore longitudinal and lateral connectivity. This has allowed migratory and resident species to recolonise upstream habitats, re-establish sediment and nutrient dynamics and support riparian vegetation [19].

Despite these efforts, flow management remains an important determinant of ecological status, and artificial stocking continues to play a key role in maintaining fish populations. This highlights the need for quantitative tools capable of assessing habitat conditions across multiple scenarios, thereby providing useful information for more effective and ecologically robust management strategies.

### 2.1.2 Target fish species

The fish community in the Ume River is diverse with regard to the following aspects: resident fish, which live in the river year-round, and migratory fish, which spend at least part of their lives in other parts of the river system or in the sea. Migratory species include Atlantic salmon (*Salmo salar*) and brown trout (*Salmo trutta*), while resident species include Arctic char (*Salvelinus alpinus*) and European grayling (*Thymallus thymallus*)[15]. However, during the summer months, Atlantic salmon, brown trout and European grayling are all known to reside within the reach, utilizing it as a seasonal habitat [20].

For the purpose of this study, two species were selected due to their ecological relevance and sensitivity to flow regulation: brown trout and European. Both species are salmonids and exhibit complex life cycles characterised by strong ontogenetic variability in habitat preferences. Salmonids generally go through several developmental stages, as shown in Figure 2.2, including egg, alevin, fry, juvenile (parr/smolt), adult and spawning [21]. To capture the full ecological footprint of flow regulation, this study considers four distinct life stages for each species: fry, juvenile, adult and spawning.

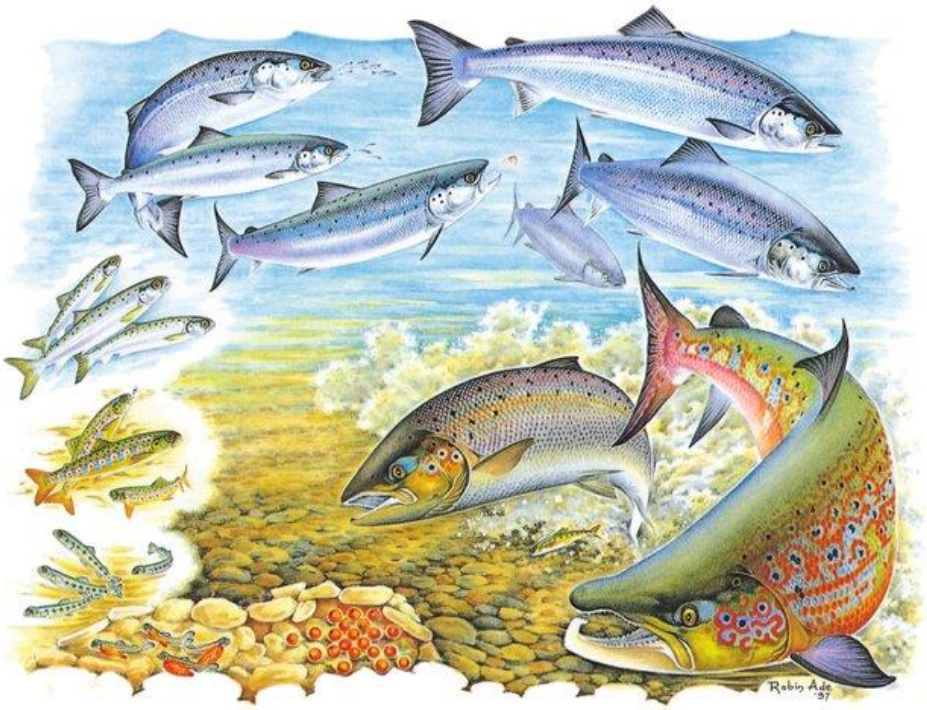


*Figure 2.2. Life cycle of Atlantic salmon (source: Atlantic Salmon Trust). The general life cycle structure is representative of salmonoid species [22].*

The transition between the different stages of the life cycle is not simply a change in size but involves morphological transformations that determine the fish's interaction with the river. In the early stage, fry exhibit limited muscle development and incomplete fin morphology, resulting in very limited swimming ability and making them easily swept away by the current [21]. As they grow, their bodies become more streamlined and muscular, allowing them to move from sheltered areas to habitats with faster currents, thus optimising energy intake [23]. As adults, they reach maximum hydrodynamic efficiency and their larger size allows them to maintain their position even in deeper and stronger currents [12]. During spawning, individuals require sufficient energy to move to the substrate and build nests, making them dependent on specific combinations of depth and speed to ensure an adequate oxygen supply to the embryos [22].

The brown trout is a temperate salmonid native to continental Eurasia and found in most European river systems, North Africa, and the British Isles. The species is highly adaptable and widely distributed in Sweden, occurring in rivers, lakes, and coastal environments. Young individuals typically prefer shallow rapids (20-30 cm deep) with moderate velocities (20-50 cm/s) and finer substrates, while older individuals prefer deeper pools (>30 cm) with slow velocities (<20 cm/s) and coarser substrates [11], [23]. Riparian cover is an important resource, as it provides shelter through rocks, vegetation, and overhanging banks, and its presence increases fish abundance, while its removal leads to population decline [11]. It is also evident that seasonal changes occur; for example, in winter, brown trout retreat into interstitial spaces with coarse substrate or into deep, slow-flowing pools, narrowing their spatial niche [11], [23].

The brown trout spawning season typically runs from late autumn to early winter, usually from November to December. Empirical observations indicate that

nests are typically found at depths of 15 to 45 cm, with water velocities ranging from 20 to 55 cm/s. They also require well-oxygenated gravel with a grain size of 16 to 64 mm and a constant flow of high-quality water [24], [25].



*Figure 2.3. Brown trout - Salmo trutta [26]*

European grayling is a native species belonging to the order Salmoniformes, sometimes classified within the family Thymallidae [24]. It is widely distributed in northern Sweden and northern Europe, occurring in both rivers and lakes, and occasionally in estuaries. They tend to inhabit medium-sized boreal rivers with well-oxygenated waters and predominantly gravelly substrates, preferring clear, fast-flowing stretches.

Studies have shown that optimal breeding habitat is found at depths of 30-40 cm, with average velocities of 40-70 cm/s and substrate dimensions of 16-32 mm [27]. Spawning occurs in early spring, typically between March and April, when water temperatures range between 4°C and 8°C. After hatching, the larvae initially remain in slower water before moving to benthic habitats. Juveniles feed on aquatic invertebrates and floating insects, so their habitat choice is strongly influenced by both substrate structure and flow conditions [24].

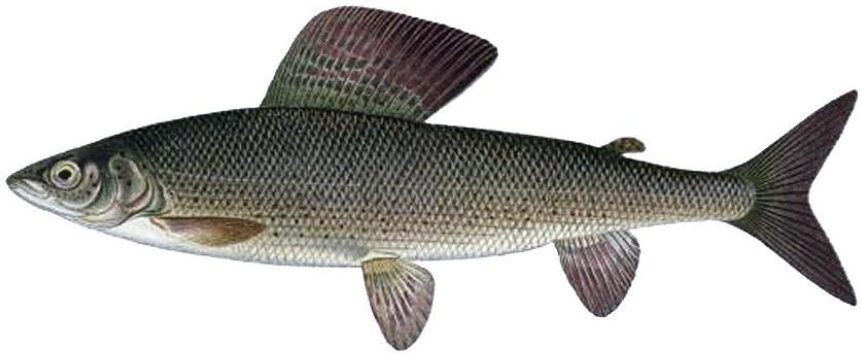


*Figure 2.4. European grayling - Thymallus Thymallus [28]*

Both species require a mosaic of habitats that offer appropriate combinations of depth, velocity, substrate and cover. Their dependence on specific hydraulic

conditions at different life stages makes them ideal species for habitat suitability analysis.

## 2.2 Ecohydraulics and habitat assessment

In recent decades, the need to understand the interactions between flow processes and aquatic ecosystems has grown. This has led to the development of ecohydraulics. Ecohydraulics is a discipline at the intersection of hydraulic ecology and fluid dynamics, with the objective of understanding and quantifying the relationship between flow regimes and habitat quality [29]. It provides quantitative tools to support the management and conservation of freshwater ecosystems, including the definition of environmental flows, the design of habitat restoration strategies and the evaluation of the impacts of human activities on aquatic biodiversity, particularly in regulated rivers where natural flow regimes are strongly modified [7].

Rivers are, by definition, the most dynamic environment. In fact, variations in discharge, sediment transport, temperature and river morphology result in a wide range of hydraulic conditions. This leads to a range of habitats capable of supporting diverse aquatic fauna [30]. Ecohydraulic studies aim to quantify river health through the use of multiple indicators. Some of them are ecological status, water quality, hydrology, channel geometry and, above all, the availability of physical habitat. Physical habitat is the environment in which aquatic species live. It is composed of the combination of flow regime and river morphology [29]. This interaction governs the spatial distribution of hydraulic variables, which directly influence swimming effort, feeding efficiency and spawning success, and therefore control the distribution and behaviour of aquatic species.




*Figure 2.5. Physical habitat as an intersection of geomorphology and hydrology [29]*

A fundamental contribution to understanding the relationships between flow and ecology is provided by Bunn and Arthington (2002), who identified four key principles regarding the impacts of flow modification in rivers. The first principle states that hydrology determines physical habitat, which, in turn, determines community structure and life-history patterns. The second affirms that aquatic organisms have evolved in response to natural flow variability and channel conditions. The third remark is that maintaining longitudinal and lateral connectivity within river systems is essential for population persistence. Finally, the last states that alterations in flow regimes tend to facilitate the spread of non-native species. Together, these principles demonstrate that variable, natural flow conditions are vital to biodiversity and

ecosystem functioning, which are the cornerstones of the natural flow paradigm (Poff et al., 1997).

Ecohydraulics contributes to habitat assessment through its unique ability to connect the hydraulic and ecological components of the aquatic environment. Combining modelling and ecological knowledge, ecohydraulic approaches translate physical variables into habitat suitability metrics, such as the Habitat Suitability Index (HSI), which quantifies habitat quality for specific species [31]. The fundamental assumption is that each species and each of its life stages has preferred flow parameters. Habitat suitability can then be described by assigning different depth and velocity values to distinct preference levels, allowing the identification of areas more or less suitable for a given species. This approach allows us to assess how variations in flow affect habitat availability and ecological conditions within the river [7].

In the past, habitat studies often relied on simplified hydraulic descriptions, calculated using averages of velocity and depth. However, over time, it has become clear that fish respond to local hydraulic conditions rather than to average levels. For this reason, a spatially distributed representation of the flow field is necessary to accurately describe habitat conditions. The development of two-dimensional hydraulic models has significantly improved the ability to analyse habitat suitability at ecologically relevant scales. They enable the simulation of the spatial distribution of the depth and velocity in the study reach, and account for the variability of the hydraulic units. This heterogeneity is essential for many fish species, which often require adjacent areas with different flow conditions for feeding, refuge, and migration [30], [32].

The use of two-dimensional modelling is particularly appropriate in regulated rivers, where flow fluctuations from hydropower operations can cause instantaneous changes in depth and velocity. Ecohydraulic modelling is therefore an effective tool for assessing the ecological effects of different flow scenarios and for supporting river management decisions aimed at balancing energy production and ecosystem conservation [7].

Despite the advantages of habitat modelling approaches, it is important to recognise their limitations. Habitat suitability is influenced not only by hydraulic variables but also by other environmental factors, such as substrate, temperature, vegetation cover, and water quality, which are often not included in analyses. For this reason, habitat indices should be interpreted as indicators of potential suitability rather than exact predictions of species occurrence.

## 2.3 Habitat Suitability Theory

Habitat suitability theory assumes that the "living space" of an organism, and consequently the distribution and abundance of aquatic organisms in a habitat, are mainly determined by its physical conditions (Maddock, 1999). In river systems, factors such as water velocity, depth, substrate and water temperature influence ecological patterns and organism distributions.

A fundamental concept underlying habitat suitability theory is Liebig's Law of the Minimum, also referred to as the theory of limiting factors. This principle states

that habitat suitability is limited by the least available environmental factor rather than by the total availability of resources. Consequently, even when most environmental conditions are favourable, a single limiting factor can significantly reduce habitat quality [30].

Habitat suitability is usually presented on a dimensionless, normalised scale ranging from 0 (completely unsuitable or lethal to the species) to 1 (optimal for a specific species or life stage). From an ecological perspective, this concept is related to "holding station" behaviour, whereby fish seek to maximise energy gain by balancing food intake with the energetic cost of maintaining position against the current.

To be ecologically meaningful, habitat suitability should be defined at different spatial scales:

- Microhabitat scale: represents the conditions experienced by an individual at a specific location, such as depth and velocity at that precise point.
- Mesohabitat scale: includes morphological units such as pools, rapids and stream reaches
- Reach or basin scale: relevant for understanding the connectivity of the population within the river network.

### 2.3.1 Habitat suitability methodology

The Habitat Suitability Index (HSI) is a numerical value derived to indicate the suitability of a habitat for a particular species. The methodology was developed in the late 1970s and initiated to demonstrate the necessity of rational and quantified support for water resources management and environmental impact evaluation [31]. It was designed by the U.S. Fish and Wildlife Service and then became a core part of larger systems such as the Instream Flow Incremental Methodology (IFIM) and the Physical Habitat Simulation system (PHABSIM).

Conceptually, the HSI is a synthetic summary of the capacity of habitat to sustain a given species, based on hypothetical relationships between variables and the performance of biological components. Rather than establishing strict cause-and-effect relationships, these models describe hypothesised interactions between species and their habitats in a quantifiable form, suitable for comparison and prediction [33].

The objective of this methodology is to translate the intricate environmental needs of an aquatic species into a quantifiable form. This framework can then be used to identify how altered flow regimes and channel morphology might impact habitat quality [34].

The implementation of an HSI model follows a structured process that begins by defining key habitat parameters that contribute to the habitat suitability index. Basic parameters generally include water depth, velocity, and substrate, but may also include factors such as cover, water temperature, shear stress, and turbulence. These variables are analysed using Habitat Suitability Curves (HSCs), which mathematically represent species preferences.

One key part of this process involves defining a habitat suitability criterion for generating the curves. This definition varies depending on how the criteria were derived. According to the classification proposed by Bovee et al. (1998), three categories can be distinguished:

- Category I (Professional judgment): based on literature review, expert opinion and experience with little or no field data.
- Category II (Utilisation functions): Based on observations of an organism's habitat utilisation during fieldwork, in other words, an index representing the condition in which organisms are observed.
- Category III (Preference functions): obtained by correcting utilisation data to account for environmental availability.

The core principle of HSI modelling is the integration of multiple environmental factors. The factors that influence an organism's choice of habitat are almost always multifaceted and individual variables will only give a limited perspective on the true habitat quality. To account for this complexity, individual Suitability Indices (SI) for each environmental variable are combined into an aggregate habitat Suitability Index (HSI). A commonly used method for the aggregation is the geometric mean, which reflects Liebig's Law by emphasising the influence of the most limiting factor:

$$HSI = \sqrt[n]{\prod_{i=1}^{n} SI_i} \tag{2.1}$$

This formulation implies that if any individual suitability index is zero, the overall habitat suitability is also zero.

Some alternative aggregation methods include the arithmetic mean, which accounts for partial compensation among variables, and the multiplicative product, which assumes independence among variables. More recent approaches incorporate fuzzy logic and machine learning techniques to better represent the non-linear interactions and uncertainties inherent in ecological systems.

From a spatial perspective, the HSI is typically represented as a continuous field, with each computational grid cell assigned a suitability value. This enables the generation of raster maps illustrating habitat conditions across the study area. Such representations facilitate the identification of habitat hotspots, fragmentation patterns and spatial heterogeneity. Evaluating HSI across different flow regimes can highlight habitat expansion and contraction, shifts in the locations of suitable habitats, and thresholds of discharge that have critical influences on the amount of suitable habitat available to each species.

Despite its versatility, the HSI methodology relies on several simplifying assumptions. One key assumption is equilibrium occupancy, in which species distribution is assumed to be in balance with current habitat conditions [11]. This implies that these animals inhabit only the most suitable habitats where the full suite of available resources is accessible and choice is available [30].

Another assumption concerns the independence of environmental variables. In practice, many environmental variables are closely correlated, and the responses of animals are often dictated by a combination of environmental factors, rather than solely by individual variables [12].

In addition, many HSI models assume temporal stability in habitat preferences. These preferences are not constant over seasons or with changes in environmental variables such as light intensity and temperature. It is possible that individuals occupy unsuitable habitat only when density-dependent processes necessitate doing so at high densities [23].

These assumptions have recognised limitations. In general, univariate curves can oversimplify interactions between variables. Furthermore, standard HSI models often neglect broader ecological processes such as connectivity, food availability and predation risk, which are key determinants of habitat selection.

### 1.1.1 Weighted usable area and related index

While HSI provides a measure of habitat suitability at the level of individual computational cells, an aggregate metric is needed to represent the distribution of habitat suitability across the study reach. Weighted Usable Area (WUA) addresses this need [30].

WUA is a composite metric that integrates habitat quality and spatial extent to estimate the total usable habitat for a given species. It determines the amount of "optimal habitat area" that would yield the same habitat value as mixed conditions within a river reach [35].

This weighting approach ensures that WUA reflects habitat quality rather than simply wetted area. This is particularly relevant in regulated rivers, where increased flow can expand the wetted area but simultaneously reduce habitat quality due to unfavourable hydraulic conditions. The WUA is therefore useful for predicting habitat availability as a function of flow and, consequently, for identifying optimal flow intervals.

However, WUA can only quantitatively describe the overall quality of a habitat, without representing its distribution across the spatial area of interest. The configuration and spatial arrangement of the landscape are important ecological characteristics as they influence the patterns of use and behavioural responses of a species.

To determine spatial information about relative habitat quality, habitat suitability is often classified into discrete categories, typically low, medium, and high [36], [37]. Based on this classification, spatial indices such as the Low Suitability Proportion (LSP), the Medium Suitability Proportion (MSP), and the High Suitability Proportion (HSP) are defined. These indices quantify the proportion of the study area belonging to each suitability class and provide complementary information to the WUA.

The combined use of the WUA and these spatial indices allows us for a more comprehensive assessment of habitat conditions, considering both the total extent of suitable habitat and its spatial organisation.

## 2.4 Hydrodynamic modelling

The use of mathematical equations to predict water flow in a river system is referred to as hydrodynamic modelling. Ecohydraulic investigations depend on accurate hydraulic inputs to calculate all habitat suitability functions.

### 2.4.1 Governing equations

The motion of fluids in river systems is described by the Navier-Stokes equations, which express the conservation of mass and momentum for a viscous fluid. Under the assumption of incompressibility, the equations can be divided into three momentum equations and a single continuity equation:

$$\frac{\partial u}{\partial t} + (u \cdot \nabla) u = -\frac{\nabla p}{\rho} + F + \nu \nabla^2 u, \tag{2.2}$$

$$\nabla \cdot u = 0, \tag{2.3}$$

where $u$ is the velocity vector, $p$ is the total pressure, $\rho$ is the fluid density, F represents the body forces on the system and $\nu$ is the kinematic viscosity [9].

However, directly solving the Navier-Stokes equations at the river scale is computationally demanding because it requires resolving turbulent processes. For this reason, these equations are commonly simplified to the Shallow Water Equations (SWE), based on the assumptions of a hydrostatic pressure distribution, negligible vertical accelerations, and horizontal length scales much larger than the vertical dimension. Under these assumptions, the flow can be treated as two-dimensional [9], [38].

The resulting depth-averaged SWE are expressed as:

$$\frac{\partial u}{\partial t} + u\frac{\partial u}{\partial x} + v\frac{\partial u}{\partial y} = -g\frac{\partial \zeta}{\partial x} + F_x, \tag{2.4}$$

$$\frac{\partial v}{\partial t} + u\frac{\partial v}{\partial x} + v\frac{\partial v}{\partial y} = -g\frac{\partial \zeta}{\partial y} + F_y, \tag{2.5}$$

$$\frac{\partial \zeta}{\partial t} + \frac{\partial (hu)}{\partial x} + \frac{\partial (hv)}{\partial y} = 0, \tag{2.6}$$

where $F_x$ and $F_y$ are the x and y components of the body forces, $g$ is the gravitational acceleration, $h$ is the depth, $u$ and $v$ are the depth-averaged velocity components in the x and y direction, respectively, and $\zeta$ is the displacement of the water surface [9].

These equations form the basis of widely used numerical models such as Delft3D and HEC-RAS 2D, enabling the simulation of spatial patterns of depth and velocity required for habitat analysis.

### 2.4.2 Numerical approach

Hydrodynamic models are typically categorised by spatial dimension, with one-dimensional (1D) and two-dimensional (2D) methods being the most prevalent. The selection of the modelling method greatly affects the precision of hydraulic characterisation for habitat evaluation [30].

In one-dimensional models, the flow variables are averaged across cross-sections, and changes in flow are only described along the river course. While computationally efficient and suitable for large-scale applications, they cannot resolve lateral variations or complex flow structures. In contrast, two-dimensional models solve the governing equations over a computational grid, providing spatially distributed maps of depth and velocity. These models operate at a scale relevant to fish microhabitats and are therefore more appropriate for ecohydraulic applications.

This distinction is critical, since habitat suitability depends on local hydraulic conditions. In natural rivers, considerable variability can occur within a single cross-section, making 1D methods generally insufficient. On the other hand, 2D models capture spatial variability and enable more precise evaluation of habitat metrics such as WUA [29].

Growing advances in high-resolution topographic data acquisition, including LiDAR and drone-based photogrammetry, further support the use of 2D modelling by allowing detailed representation of river morphology [16].

### 2.4.3 HEC-RAS software

HEC-RAS, which stands for the Hydrologic Engineering Centre's River Analysis System, is a widely used hydraulic modelling software developed by the U.S. Army Corps of Engineers. It is freely available and supports one-dimensional, two-dimensional and coupled 1D/2D simulations, both with the steady and unsteady solver [39].

In ecohydraulic applications, the unsteady flow solver is particularly important because it allows for the simulation of time-dependent effects on hydraulic conditions and ecological consequences. In 2D mode, HEC-RAS solves the Shallow Water Equations over a computational mesh, producing spatially distributed depth and velocity fields. The numerical solution in HEC-RAS is based on a finite volume method (FVM), which conserves mass and momentum at the cell level and efficiently models wetting and drying processes [38].

HEC-RAS offers different levels of physical complexity. Simplified diffusion wave models can be utilised for large-scale applications with minimal inertial effects, while the full shallow water equations provide a more precise depiction of flow behaviour. Advanced numerical methods, such as Eulerian and Eulerian-Lagrangian techniques, are utilised to achieve a balance between computational efficiency and stability.

A distinctive feature of HEC-RAS is the use of Subgrid bathymetry [39]. Rather than assigning a single elevation value to each computational cell, the model incorporates high-resolution topographic data for each cell to develop relationships for hydraulic properties, such as elevation-wetted perimeter and elevation-volume curves. This technique enables coarse computational grids to accurately depict fine-

scale hydraulic details, thereby improving the portrayal of small-scale elements such as shallow channels and velocity refugia, which are crucial for evaluating habitat suitability.

Overall, the integration of physically based equations, spatially distributed results and effective numerical techniques makes HEC-RAS ideal for ecohydraulic research, especially for assessing habitat suitability metrics such as HSI and WUA.

# Chapter 3
# Materials and methods

## 3.1 Study area

The chosen study site is a section of the Ume River. This is the bypass reach, an alternative river channel constructed to allow water to flow around the main dam, located downstream of the Stornorrfors hydropower plant, 15 km from the city of Umeå (Figure 3.1). The reach extends from the spillways and the fish ladder outlet to the confluence with the power plant discharge channel [9].

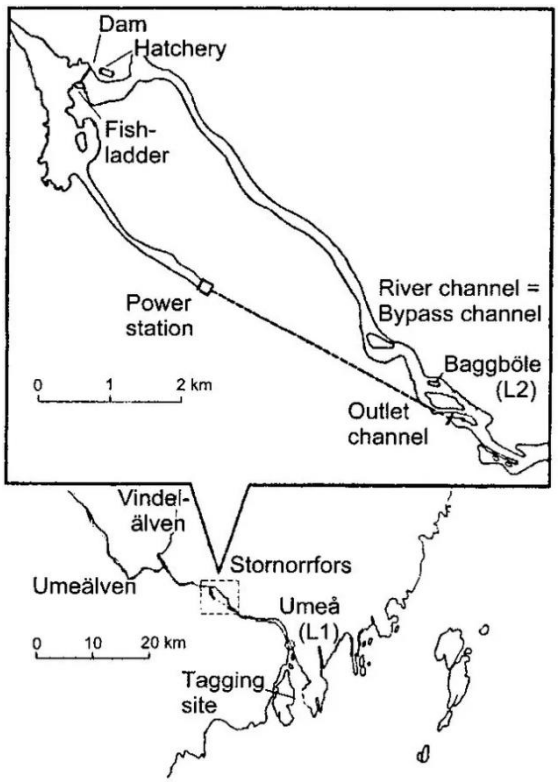



*Figure 3.1.Position of Stornorrfors in Sweden and map of the hydropower plant [42].*

The study reach has an extent of approximately 7-8 km and is characterised by a relatively wide channel with heterogeneous morphology. Its cross-sections vary along its length, with rapids and steeper segments in the upper part [40]. The

peculiarity of this reach is linked to flow management: being a bypass channel, it is seasonally dewatered. From October to May, in fact, almost the totality of the water of the Ume is diverted towards the turbines of Stornorrfors and then returned to the river through an underground tunnel that outlets 4 km further downstream [41], [42].

During the summer months, controlled water releases support fish migration and maintain ecological balance. In this period, the discharge varies between 21 $m^3/s$, which represents the minimum flow required for fish to ascend the fish ladder, and 50 $m^3/s$, flow that is released during weekends for aesthetic and recreational purposes As this is the dam discharge reach, the area is also subject to abrupt variations, especially during spring floods or due to operational needs [9].

## 3.2 Hydraulic model setup

The hydraulic analysis was conducted using HEC-RAS 6.6 in two-dimensional (2D) mode, where computations are performed over a grid to simulate water movement in both horizontal directions. This approach effectively captures complex flow patterns and spatial variations in hydraulic parameters, such as water velocity and depth, across the study area. The 2D approach was selected to ensure a detailed spatial representation of these distributions, which is essential for subsequent ecohydraulic analyses [16].

The model was set up following a structured workflow that included four main phases: firstly, the topographic data were processed and the geometry was created; subsequently, the computational mesh was generated; then, the boundary conditions were defined and, finally, the numerical parameters for the simulation were optimized. Each phase was carefully designed to ensure high model accuracy while at the same time maintaining computational efficiency, useful having to simulate multiple discharge scenarios.

### 3.2.1 Geometry and topographic data

A 2D model is reliable only if the topographic base on which it rests is of quality. To build the model's geometry, a Digital Elevation Model (DEM) was used. The dataset comes from previous studies in which the channel topography was reconstructed using drone-based stereoscopic photogrammetry [9], [40]. This technique is particularly effective in northern river systems, as images were acquired during winter low-flow conditions, when most of the riverbed is exposed. The survey timing was selected to maximise bed visibility and minimise water-surface reflections, which can introduce errors in submerged areas.

The photogrammetric technique provides a spatial accuracy on the order of 0.1 m. However, for this thesis, a pre-processed DEM was used, previously interpolated using the Kriging method to a 2 m spatial resolution (Figure 3.2). The DEM refers to the coordinate system SWEREF 99 TM (EPSG:3006), which was also set in HEC-RAS to ensure consistency with national geospatial standards.

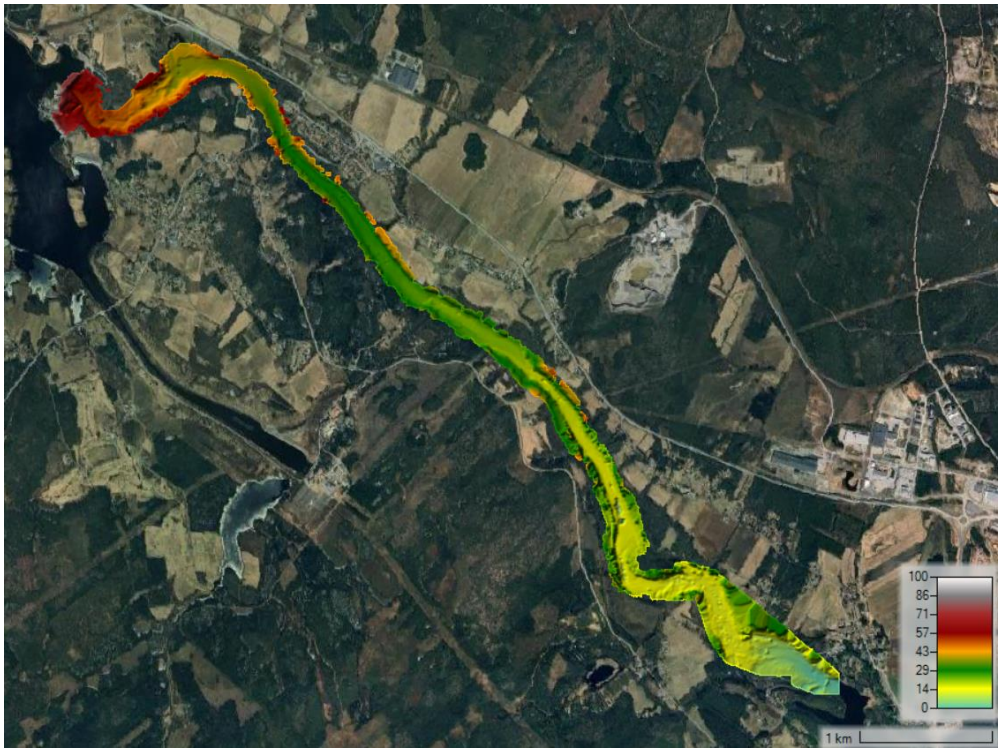



*Figure 3.2. Digital Elevation Model of the study reach in the Ume River. The colour scale represents the elevation.*

The 2 m DEM was imported into the RAS Mapper environment as the "Terrain layer." It served as the static topographic base for all subsequent geometric features, including banklines, mesh, and Manning's roughness zones.

### 3.2.2 River geometry creation

Once the Terrain Layer was established, the river geometry was manually refined within the RAS Mapper environment. The objective of this phase was to define the hydraulic domain and create a realistic representation of the river's shape, as the quality of the topographic representation significantly influences the predictive ability of a 2D model [32].

To define the riverbank lines, a combination of official cartographic data and satellite images was used. The main geometric reference for the river alignment came from raster maps provided by the Swedish Mapping, Cadastral and Land Registration Authority (Lantmäteriet), using the raster dataset LM2026/008876 at a 1:50000 scale. This dataset served as a key reference for outlining the river's planform, ensuring it aligned with validated geographic data.

Where necessary, the bank lines were further refined using high-resolution satellite imagery available through the hybrid basemap of HEC-RAS, based on Google Maps data. This supplementary information proved particularly useful for

meanders and constrictions, where cartographic resolution could not clearly identify small-scale morphological features or local channel variations.

By combining raster cartography and satellite imagery, a robust and spatially coherent model geometry was created (Figure 3.3 and Figure 3.4). This provided a reliable basis for subsequent mesh generation and hydraulic simulation.

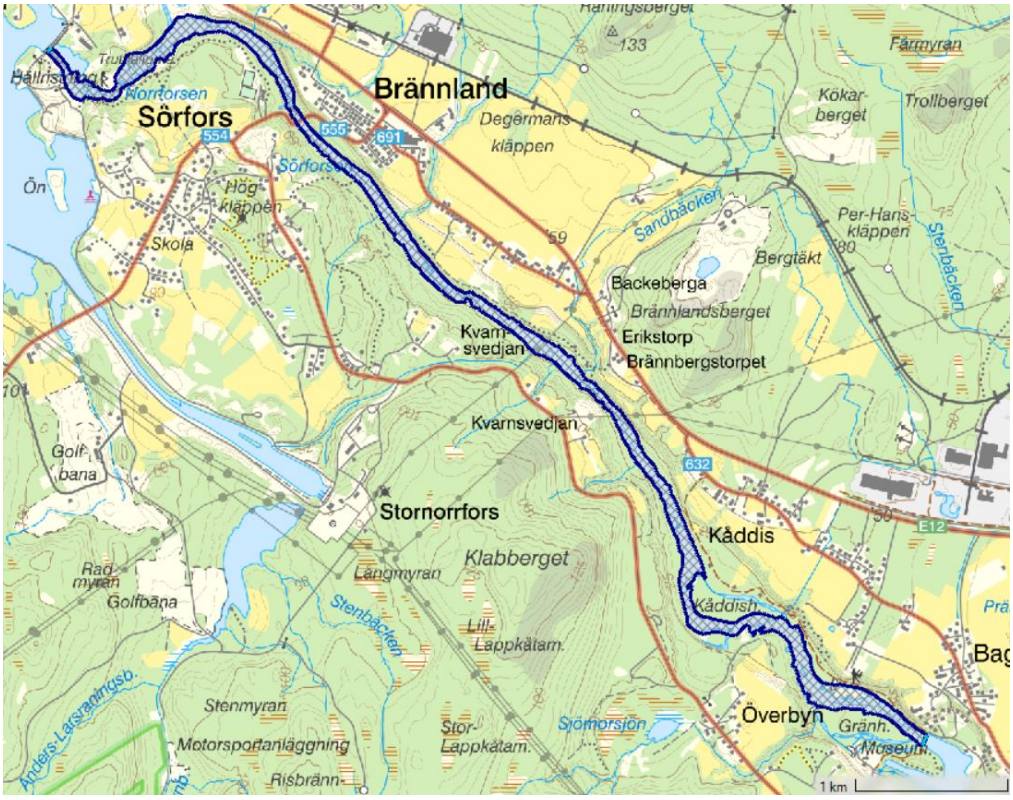



*Figure 3.3. Final banklines overlaid on the Lantmäteriet map*

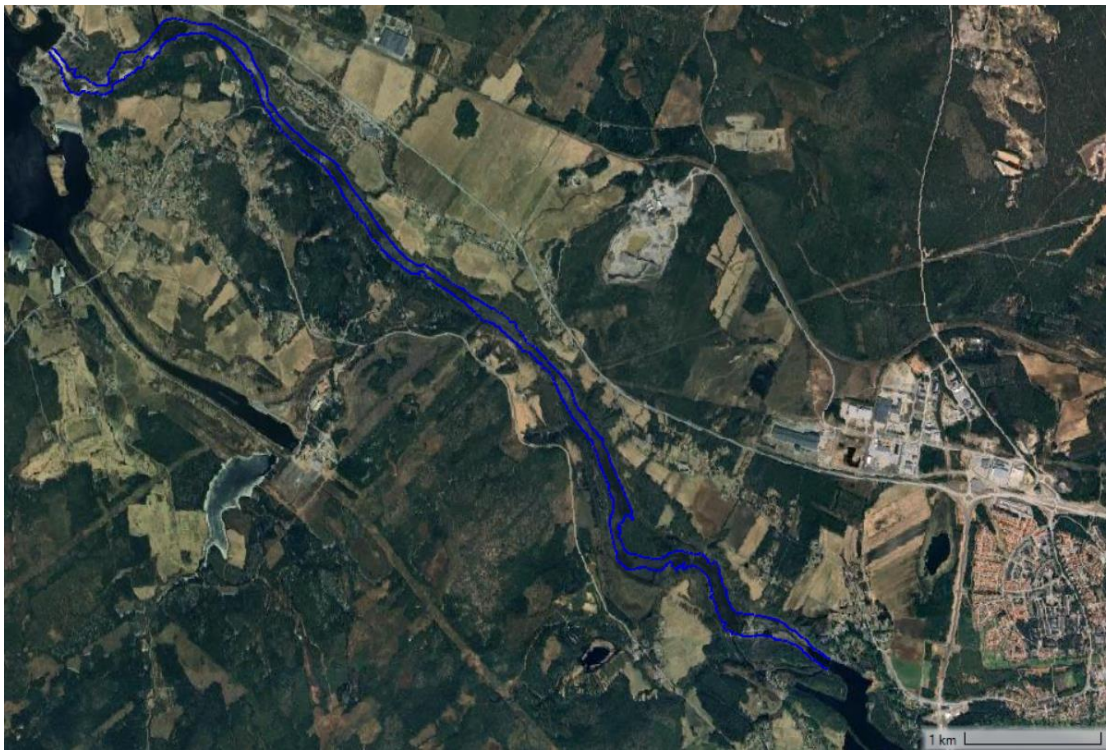



*Figure 3.4. Final banklines overlaid on the Google Maps satellite map*

### 3.2.3 Computational mesh

The computational mesh represents a spatial discretisation of the study domain and plays a crucial role in determining both the accuracy and the stability of the numerical solution, as it controls how flow depth and velocity are computed across the river domain. For this study, a structured 2D mesh was created using HEC-RAS's built-in mesh generator. This approach allows us to obtain an accurate representation of the complex channel geometry, while always maintaining manageable computational needs.

The domain was defined by creating 2D Flow Areas, bounded by previously digitised banklines. The perimeter of the flow area follows the channel boundaries, ensuring that the computational domain represents the active flow zone while excluding unnecessary floodplain areas.

The hydraulic domain was primarily discretised using a 2D mesh with a nominal cell size of 10x10 m. While this grid provides the base resolution, the mesh was further refined using the Enforce Breaklines tool. Specifically, three primary breaklines were added: two that run along the river's edges, corresponding to the banklines, and one following the central axis of the channel. This configuration forces all the cell faces to align with the main flow directions and the surrounding topography, which minimises numerical diffusion and ensures that the velocity vectors truly reflect the river's dynamics.

According to the final statistics generated by HEC-RAS, the mesh has a computational domain of 6338 cells and exhibits the characteristics summarised in Table 3.1.

*Table 3.1. Mesh characteristics extracted from HEC-RAS*

| **Parameter** | **Value** |
|---|---|
| Average Face Length | 11 m |
| Average Cell Size | 114 $m^2$ |
| Maximum Cell Size | 277 $m^2$ |
| Minimum Cell Size | 72 $m^2$ |

The mesh statistics show solid geometric consistency, with cell size variations staying within acceptable limits. The average cell size of 114 $m^2$ is roughly in line with the target resolution, and the size variation reflects the local adjustment introduced by the breaklines and the terrain variability.

The mesh resolution was determined using a sensitivity-oriented approach, ensuring that the selected cell size was adequate to capture the key hydraulic features of the study area while maintaining simulation times reasonable. In addition, the model takes advantage of a high-resolution digital elevation model within a Subgrid bathymetry framework. In this method, high-resolution topographic data were incorporated into each computational cell through a pre-processed hydraulic relationship based on the underlying terrain [38]. This setup helps to preserve fine-scale morphological features relevant for habitat characterisation while maintaining computational efficiency.

The final mesh setup (Figure 3.5) guarantees numerical stability and provides an accurate representation of spatial variations in flow depth and velocity, which are crucial for later ecohydraulic analyses.

For the initial simulations, a uniform Manning's roughness coefficient of 0.06 was applied across the entire domain. This value represents an average roughness coefficient derived from previous studies conducted on the same river [9], [40]. This preliminary assumption was later refined during the model calibration phase.

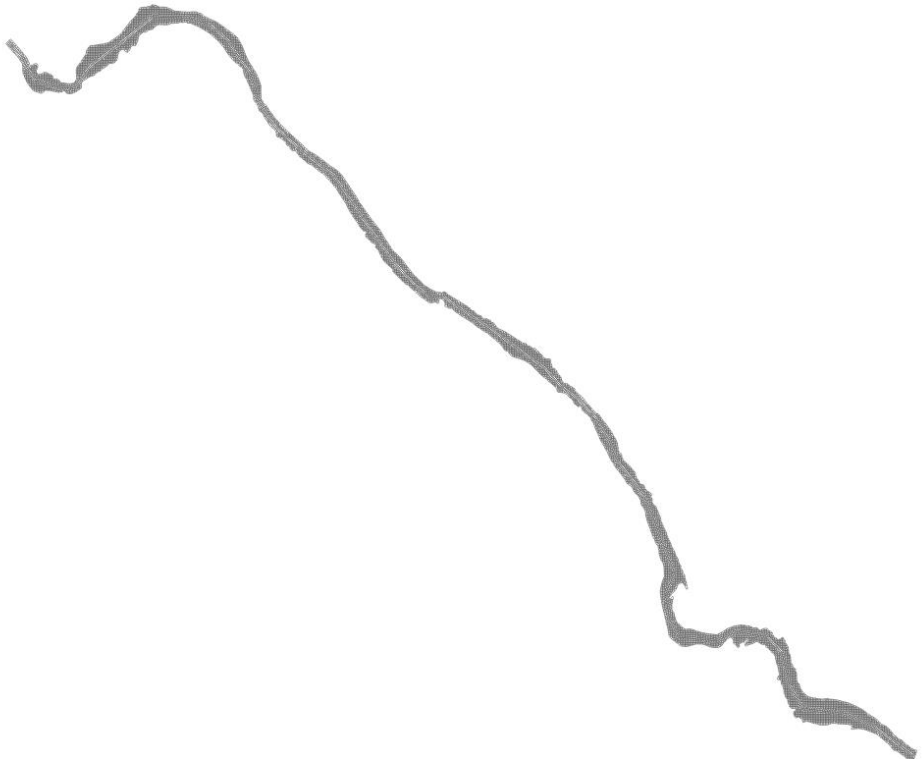


*Figure 3.5. Computational mesh of the study domain generated in HEC-RAS*

### 3.2.4 Boundary conditions

Hydraulic simulations were performed by defining appropriate boundary conditions along the external limits of the 2D flow area. In HEC-RAS, these conditions control interaction between the model domain and the external environment. They are essential for realistic hydraulic behaviour and numerical stability.

Boundary conditions are the key constraints that shape the hydraulic solutions, so it is essential to choose them carefully to accurately represent the physical processes that influence flow behaviour in the study area. According to the HEC-RAS framework, four types of external boundary conditions can be applied to 2D flow areas: flow hydrograph, stage hydrograph, normal depth, and rating curve. Among these, the flow hydrograph can be used to both add and remove flow from the domain, while normal depth and rating curve conditions are only relevant at outflow boundaries [39].

n this study, a flow-based approach is adopted, and two boundary conditions were applied. At the upstream boundary, a flow hydrograph condition was imposed to represent the inflow. This allows us to simulate with both steady and unsteady discharge scenarios, ensuring consistent control of inflow across all simulations.

At the downstream boundary, a normal-depth condition was applied with a friction slope of 0.001. This value was chosen based on previous studies on similar river systems [9], [20], [40]. In normal depth conditions, Manning's equation is used to estimate the water surface elevation at the outlet, providing a stable end and a physically consistent representation of outflow conditions.

In this analysis, no lateral inflow or outflow boundary conditions were applied, as the 2D flow areas are naturally bounded by topographic watershed boundaries and digitalised banklines. These features effectively create a barrier that prevents any lateral flow exchange, thereby preserving the integrity of the computational domain.

The boundary conditions lines were carefully set along the edges of the 2D Flow Area, making sure there were no overlaps or conflicting conditions affecting the same cell faces. Boundary conditions were defined within the RAS Mapper editor environment and subsequently assigned in the Unsteady Flow Data editor. The implementation and spatial location of the boundary conditions are shown in Figure 3.6 and Figure 3.7.

Select Location in table then select Boundary Condition Type

| | River | Reach | RS | Boundary Condition |
|---|---|---|---|---|
| | | | | |
| **Storage/2D Flow Areas** | | | | **Boundary Condition** |
| 1 | Breakline 1 | BCLine: Boundary line 2 | | Flow Hydrograph |
| 2 | Breakline 1 | BCLine: Boundary line 1 | | Normal Depth |

*Figure 3.6. Boundary condition setup in the HEC-RAS Unsteady Flow Data editor*

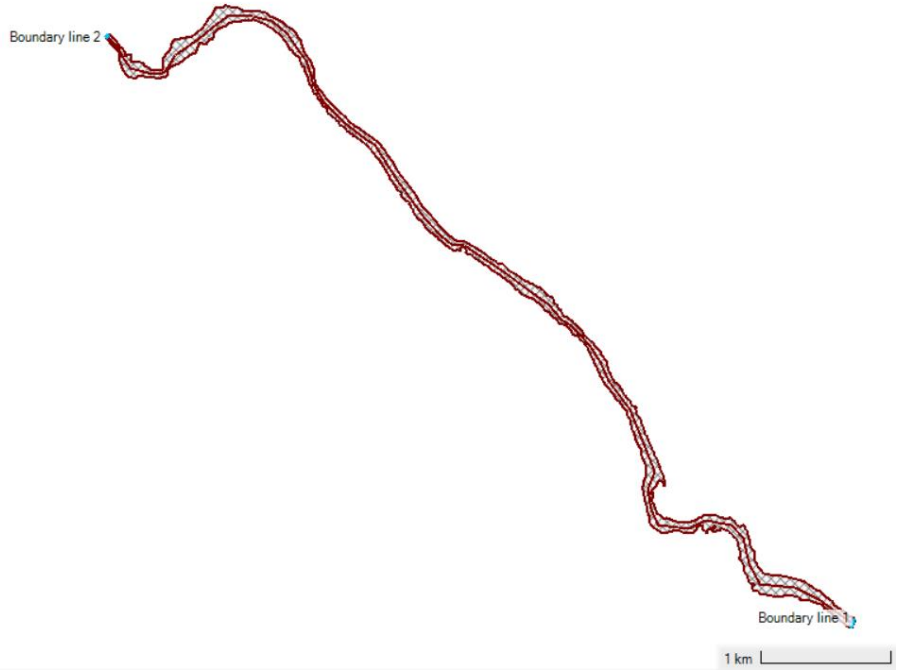



*Figure 3.7. 2D mesh with upstream (Boundary line 2) and downstream (Boundary line 1) boundary lines locations.*

### 3.2.5 Numerical parameters

The hydraulic simulations were conducted under unsteady flow conditions using the two-dimensional Shallow Water Equation solver in HEC-RAS. This solver resolves depth-averaged momentum and continuity equations, ensuring conservation of mass and momentum while accounting for local and convective acceleration terms.

The use of the shallow water framework is essential for capturing hydraulic variables required for ecohydraulic analysis and is consistent with established modelling practices [20].

A simulation time of 24 hours was selected to ensure that any initial transient effects were dissipated and that stable hydraulic conditions were reached throughout the computational area. This duration was sufficient to achieve steady and representative flow conditions for the following habitat analysis.

For temporal discretisation, a computational time of 5 seconds was set. This short time step was chosen to maintain numerical stability and effectively capture rapid variations in hydraulic variables. Mapping outputs were also recorded every 5 seconds to maintain a high level of spatial and temporal detail. Meanwhile, hydrograph and detailed outputs were captured at an interval of 1 minute, providing sufficient temporal resolution for habitat analysis without generating excessive data volume.

To make sure everything was running smoothly, a series of preliminary simulations was conducted. These tests helped assess numerical stability and the system's sensitivity to the chosen time step and output configuration. The results confirmed that the setup delivered stable and reliable solutions without any numerical instabilities or convergence issues.

## 3.3 Model calibration and validation

To ensure the reliability of the hydraulic simulations, the model was calibrated and validated using field measurements from earlier studies [9], [40]. These steps are essential in ecohydraulic modelling because they help ensure that the simulated hydraulic variables align with field observations, thereby increasing the model's reliability for habitat analysis.

Calibration and validation are combined in a single framework because of the strong interdependence between the hydraulic parameterisation and the model's performance. The calibration process focuses on adjusting Manning's roughness coefficients to minimise the difference between simulated and observed water levels. The validation process, on the other hand, assesses the calibrated model's ability to reproduce hydraulic conditions under typical flow scenarios.

For both calibration and validation, observed water levels were used as the primary reference dataset.

### 3.3.1 Validation data

The reference dataset comprises eight pressure loggers (divers) strategically placed across the study area to capture variations in hydraulic conditions. According to Bruman et al. (2020), these loggers were positioned to reflect changes in channel shape and cross-sectional differences, while also accounting for field accessibility (Figure 3.8).




*Figure 3.8. Key locations in the study reach extracted from HEC-RAS*

The water level measurements were collected from mid-May to mid-July 2017 with high accuracy. The sensors provided data with an uncertainty of ±2 cm, and their absolute coordinates were determined using a high-precision GPS pole [9]. For this study, water levels corresponding to a discharge of 50 m³/s ($Q_{50}$) were used as the main calibration benchmark, while the 21 m³/s condition ($Q_{21}$) served as an additional validation case for lower flow scenarios (see Table 3.2).

*Table 3.2. Coordinates and measured water level for the eight validation points*

| Point | X | Y | Measured water elevation ($Q_{50}$) | Measured water elevation ($Q_{21}$) |
|---|---|---|---|---|
| 1 | 747666 | 7093310 | 35.453 | 35.052 |
| 2 | 747954 | 7092890 | 29.514 | 28.675 |
| 3 | 748178 | 7092670 | 29.212 | 28.899 |
| 4 | 748621 | 7092180 | 26.446 | - |
| 5 | 748918 | 7091810 | 24.007 | 23.601 |
| 6 | 749691 | 7091270 | 18.934 | - |
| 7 | 750488 | 7090120 | 15.943 | 15.521 |
| 8 | 751094 | 7089640 | 13.67 | 13.314 |

Simulated water surface elevations were extracted directly from the HEC-RAS computational mesh at the exact location of the pressure loggers. This approach allowed for a direct point-to-point comparison between the observed and the modelled values, all under the same hydraulic conditions. This spatial consistency

minimises potential biases arising from interpolation or misalignment, providing a solid foundation for evaluating the model.

### 3.3.2 DEM anomalies and uncertainties

The DEM used in the hydraulic simulations presents some localised uncertainties due to the conditions under which the photogrammetric survey was conducted. As reported by Burman et al. (2020), ice accumulation during drone-based acquisition led to localised topographic artefacts, creating artificial holes in some parts of the riverbed. These anomalies are particularly noticeable near validation point 7, where the elevation reaches values lower than expected (down to -8 MASL).

These artefacts can impact hydraulic calculations by causing artificial flow concentrations. Because of this, their potential impact was considered during the analysis of the results, as they may introduce local discrepancies between simulated and observed water levels that are not related to the parametrisation.

### 3.3.3 Calibration procedure

The hydraulic model was calibrated using a systematic approach known as "Manning swapping" [40], which focused on reducing differences between simulated and observed water surface elevations at the validation points.

To achieve this, parameter swapping was conducted by iteratively running simulations with Manning's n values ranging from 0.02 to 0.10 at each validation point, using the Q50 discharge scenario. For each simulation, the difference between simulated and observed water surface elevations was evaluated at all eight points.

At each site, the Manning coefficient that minimised the absolute error between observed and simulated water surface elevation was selected as the optimal value. In this way, the spatial variability of hydraulic roughness can be captured across the study reach.

A spatially distributed roughness map was created by assigning calibrated Manning values to sections of the river, determined as the midpoints between each pair of pressure logger locations. Each section was designed to extend halfway to the neighbouring points, ensuring complete spatial coverage of the study area without overlapping regions.

These sections were mapped using a GIS tool (QGIS 3.40.4), in which the n values were spatially attributed and converted to a raster file. The resulting map was then imported into HEC-RAS and used as a Land Cover layer in the RAS Mapper to represent the roughness distribution across the 2D computational domain.

To maintain physical accuracy, the calibrated Manning values were limited within typical ranges reported in literature for natural river channels. According to Chow (1959), as reported in Strum (2001), Manning's coefficients for natural river streams generally range between 0.035 and 0.10. Based on this reference, lower bounds of n=0.035 were imposed, and all the calibrated values falling outside this limit were adjusted to the threshold to maintain physically realistic roughness.

The detailed results of Manning's optimisation and comparison between observed and simulated water surface are presented in Section 4.1.

## 3.4 Scenario simulations

After calibration and validation, the hydraulic model was used to simulate both steady and unsteady flow conditions to support the ecohydraulic assessment. These two types of simulation were designed to provide complementary insights: steady-state simulations were used to evaluate how discharge magnitude affects habitat suitability, while unsteady simulations were used to investigate the impacts of temporal flow variability.

A series of steady-state simulations was performed for discharges $Q_{21}, Q_{30}, Q_{40}$ and $Q_{50}$. These scenarios enable the analysis of how hydraulic parameters, such as water depth and velocity, vary as a function of discharge. This method enables pinpointing the flow conditions potentially most suitable for the aquatic habitat.

In addition to steady conditions, an unsteady simulation was implemented to reproduce the flow variability typical of hydropeaking. The chosen configuration was derived from the scenarios proposed by Burman et al. [9, p. 6], which describe different frequencies of discharge fluctuations within the day. Among these, a scenario with 30 flow changes per day was selected, as it represents a realistic intermediate condition that captures significant temporal variability without being too extreme.

Under this configuration, the discharge changes every 48 minutes. However, to ensure stability and avoid the influence of initial transients, the discharge variations were applied only during the central 12-hour period of the 24-hour simulation. The initial 6 hours were used as a spin-up phase to allow the model to reach stable hydraulic conditions, while the final 6 hours allowed the system to rebalance after the imposed fluctuations. This means the total number of flow changes in the simulation is lower than in a full 24-hour hydropeaking cycle, but it still maintains the timing and frequency of the chosen scenario. The final hydrograph used is represented in Figure 3.9.

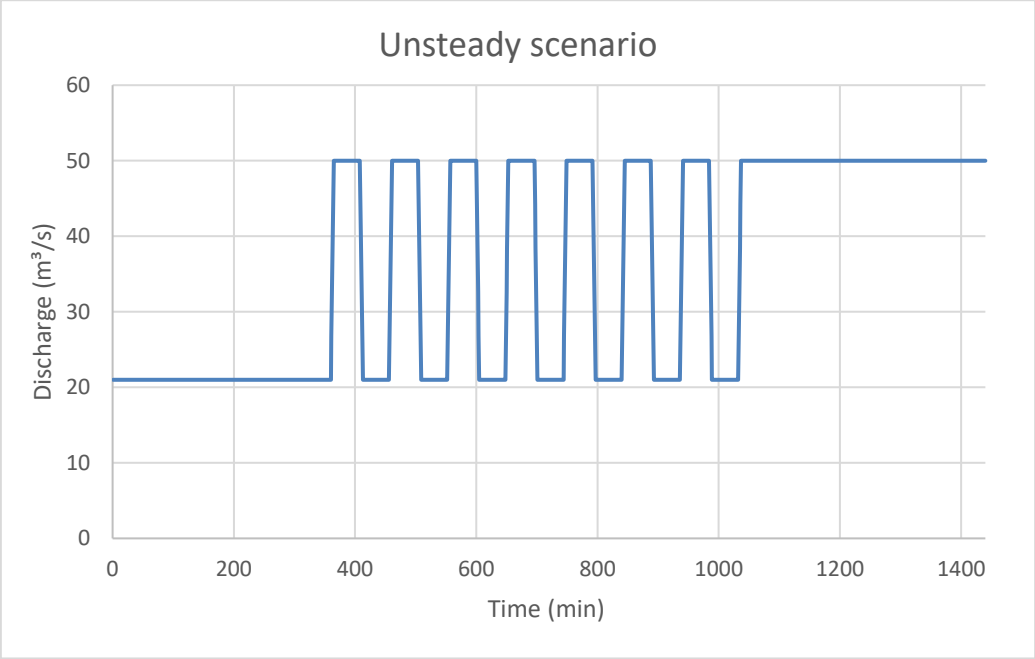



*Figure 3.9. Unsteady flow hydrograph, based on a hydropeaking scenario with 30 flow changes per day*

Each discharge transition was introduced with a ramping time of 5 minutes, as described in the literature [9]. This creates alternating periods of quick flow changes followed by more stable conditions, enabling the model to effectively capture both the transient and stabilised hydraulic responses.

## 3.5 Data extraction and post-processing

After running the hydraulic simulations, model outputs were extracted and processed to derive the parameters required for the ecohydraulic analysis.

Hydraulic variables, including water depth and flow velocity, were obtained directly from the HEC-RAS 2D computational mesh. The analysis was based on computational points (cell centres), which represent the numerical solution's spatial resolution and ensure consistency between the hydraulic model and the subsequent ecological evaluation. To facilitate the data extraction, a point layer aligned with the computational point was created in the RAS Mapper environment. This layer made it easy to systematically gather hydraulic variables at each computational spot, ensuring a clear link between the model's geometry and the extracted datasets.

For steady-state simulations, hydraulic variables were extracted at the final computational time, which reflects fully developed flow conditions for each discharge scenario. In the case of the unsteady simulation, the outputs are obtained from the HEC-RAS binary results file (.hdf), which stores the temporal evolution of the hydraulic variables across the computational domain. This approach enabled the analysis of the spatial and temporal variability in flow conditions associated with hydropeaking dynamics.

The extracted datasets were then processed using MATLAB. A custom routine was used to calculate habitat suitability indices based on depth and velocity data. This

step is crucial because it enables us to convert hydraulic outputs into spatially distributed indicators suitable for ecohydraulic analysis.

The entire data processing workflow ensures a consistent link between hydraulic simulations and subsequent habitat evaluations. This provides a solid and repeatable foundation for the ecohydraulic framework discussed in the next section.

## 3.6 Habitat assessment framework

The quantification of habitat availability of aquatic species requires a structured framework capable of translating the hydraulic model into ecologically meaningful indicators [16]. In this study, an ecohydraulic assessment framework is developed to integrate spatially distributed hydraulic variables, specifically water depth and velocity derived by HEC-RAS simulations, with species-specific habitat preference criteria.

The adopted methodology is based on the principles of the Physical Habitat Simulation (PHABSIM) approach, which remains a reference method for assessing instream flow requirements in river systems [7], [30]. This method operates on the idea that habitat suitability is influenced by how local hydraulic conditions interact with the physiological preferences of the target species. Although PHABSIM has traditionally been implemented using one-dimensional routines, this study extends the concept through a two-dimensional hydraulic modelling framework. Compared to one-dimensional approaches, 2D models provide a more detailed representation of flow heterogeneity, capturing local velocity gradients and traverse flow that are critical for fish [16].

Based on the theoretical background introduced in Chapter 2, the implemented framework focuses on a spatially explicit evaluation of habitat suitability across the computational domain. The analysis was conducted for both steady and unsteady flow conditions, enabling assessments under various discharge scenarios and rapid flow fluctuations.

The workflow is structured into successive steps. First, hydraulic variables are converted into suitability values using habitat preference curves. These values are then combined into the Habitat Suitability Index (HSI), which is subsequently aggregated into spatial metrics such as Weighted Usable Area (WUA) and area-based indicators. This integrated approach facilitates the evaluation of both the total amount of suitable habitat and the spatial organisation and connectivity across the river reach.

### 3.6.1 Habitat Suitability Curves

Habitat Suitability Curves (HSCs) illustrate how the hydraulic conditions relate to target species' preferences for specific environmental features. Often called preference functions, these curves provide a numerical indicator of habitat suitability [12].

In this study, suitability curves for water depth and flow velocity were used as the main indicators of habitat preferences. For any given hydraulic variable x, the suitability index SI(x) is defined as a value ranging between 0 and 1. This index reflects the species' unique ecological preferences and is usually characterised by a piecewise or unimodal trend, depending on the variable considered.

The suitability curves used in this study were created and implemented using a custom MATLAB routine. The numerical values in this function represent well-established fitness relationships, derived from a combination of experimental studies, empirical observations and expert judgment [34], [43], using methods commonly used in ecohydraulic modelling. According to the classification by Bovee et al. (1998), these criteria are classified as Category I. The general structure of the curves is also consistent with the reference curves reported in recent ecohydraulic applications [37].

The curves are created using piecewise linear relationships, with specific threshold values and slope coefficients delineating the unique ecological preferences of different species and life stages. This approach not only captures the ideal ranges but also illustrates gradual shifts toward less suitable conditions, providing a smooth, stable description of habitat suitability.

The MATLAB routine puts these relationships into action by taking local hydraulic variables, water depth (h) and velocity (v), as inputs and returning the corresponding suitability indices namely $SI_d(h)$ for water depth and $SI_v(v)$ for flow velocity. This setup enables us to obtain a reliable, automated assessment of habitat suitability at every computational point across the study area.

The suitability curves used in this study are presented in Figure 3.10 and Figure 3.11, illustrating how depth and velocity relate to their respective suitability values.

From an ecological point of view, these curves illustrate the delicate balance between what organisms can tolerate physiologically and their behavioural preferences. Ideal habitat conditions emerge when hydraulic factors allow for smooth movement, effective feeding and adequate shelter. On the other hand, unsuitable conditions arise when hydraulic stress surpasses the specific limits that different species can handle.

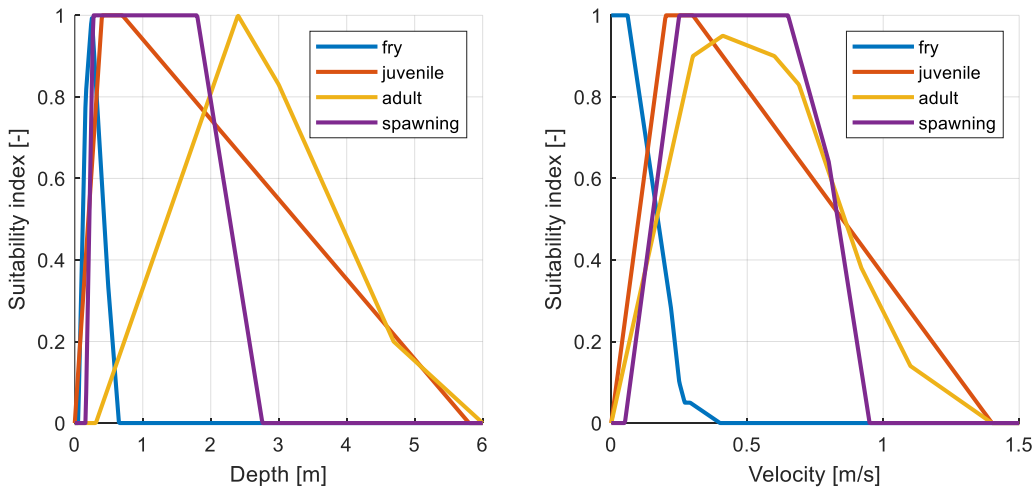



*Figure 3.10. Habitat suitability curves for water depth and flow velocity for Grayling species [34], [43]*

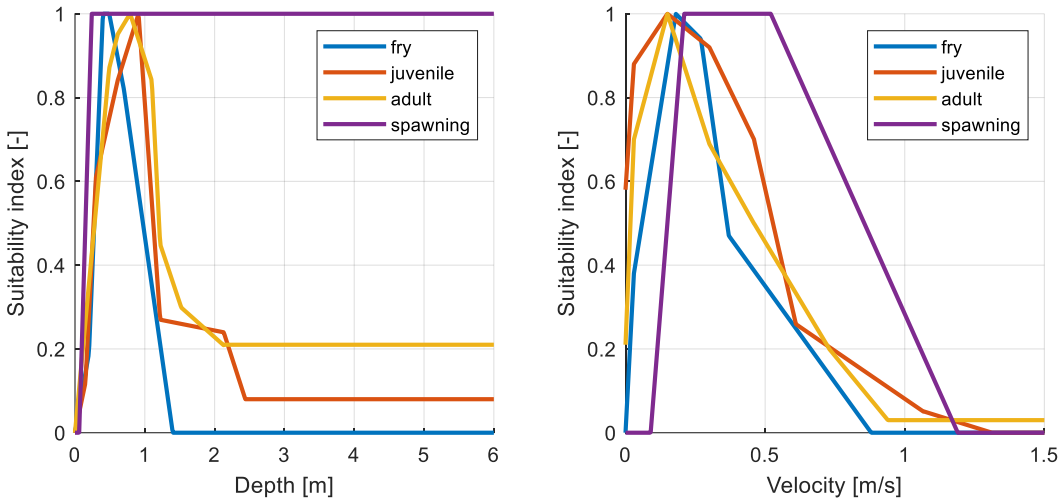



*Figure 3.11. Habitat suitability curves for water depth and flow velocity for brown trout species [34], [43]*

### 3.6.2 Habitat Suitability Index

The Habitat Suitability Index (HSI) is a dimensionless indicator that quantifies the quality of aquatic habitats for specific species. In traditional ecohydraulic modelling, the Habitat Suitability Index (HSI) is typically treated as a multivariate index that accounts for depth (*h*), velocity (*v*), and substrate composition (*s*). Generally, this comprehensive index is expressed mathematically as the geometric mean of these three components [36]:

$$HSI_i = \sqrt[3]{SI_{v,i} \cdot SI_{h,i} \cdot SI_{s,i}} \tag{3.1}$$

where $SI_{v,i}$, $SI_{h,i}$ and $SI_{s,i}$ represent the suitability scores for velocity, depth and substrate, respectively, at the *i*-th computational cell. This formulation assumes that all three elements play equal roles in defining what constitutes an optimal habitat.

In the present study, only hydraulic variables were considered, and substrate effects were not explicitly included. Consequently, the HSI was computed using a simplified formulation based on the geometric mean of depth and velocity suitability [13]:

$$HSI_i = \sqrt[2]{SI_{v,i} \cdot SI_{h,i}} \tag{3.2}$$

where $SI_{v,i}$ and $SI_{h,i}$ are obtained from the habitat suitability curves outlined in Section 3.6.1.

The use of the geometric mean reflects the hypothesis that depth and velocity contribute independently to habitat suitability and that suboptimal conditions in either variable significantly limit overall habitat quality.

The exclusion of substrate from the analysis is justified by data availability and modelling consistency. Reliable spatial information on substrate composition was

not available for the study stretch at a resolution compatible with the hydraulic model. Furthermore, the main goal of this study is to evaluate how hydraulic conditions affect habitat availability, for which depth and velocity represent the dominant controlling factors.

The resulting HSI values range from 0 to 1, with higher values indicating better habitat conditions [30]. This index is calculated at each computational point in the model's domain and serves as the foundation for further spatial analysis.

### 3.6.3 Weighted Usable Area

After computing the HSI for each computational cell, the Weighted Usable Area (WUA) was derived and used to analyse habitat availability at the river reach scale.

The WUA represents a quantitative measure of the total suitable habitat, obtained by combining local suitability values with the spatial extent of individual computation cells. It considers both habitat quality, expressed through the HSI index, and its physical availability, represented by the cell area, thus providing an indicator of habitat conditions at the scale of river reach.

The WUA is defined as follows [36]:

$$WUA = \sum_{i=1}^{n} A_i \cdot HSI_i \tag{3.3}$$

where *n* is the total number of computational cells, $A_i$ is the area of the *i*-th cell and $HSI_i$ is the Habitat Suitability Index at the same location.

The WUA is measured in square meters (m²) and represents the area of fully suitable habitat where the Habitat Suitability Index (HSI) equals 1. This means that areas with lower suitability contribute less to the overall habitat availability.

In this research, WUA was determined for all simulated flow scenarios, encompassing both steady and unsteady conditions. It played a vital role in comparing habitat availability across different hydraulic regimes.

### 3.6.4 Habitat suitability classes

The spatial distribution of habitat suitability was analysed using three additional metrics derived from HSI maps. While WUA provides a synthetic measure of total habitat availability, these indices allow for spatial configuration of suitability to be quantified.

The study area is therefore partitioned into High, Middle, and Low suitability classes, using HSI thresholds that are widely recognised in ecohydraulic studies [36]. This approach highlights the high-quality habitat "hotspots" and, further, pinpoints regions with less-than-ideal hydraulic conditions, improving understanding of the ecological implications of the model results.

The classification criteria are summarised in Table 3.3.3.

*Table 3.3. Classification of habitat suitability criteria used for spatial index calculation*

| Classification | Criteria (HSI) | Index |
|---|---|---|
| High | ≥ 0.7 | HSP |
| Middle | 0.3 - 0.7 | MSP |
| Low | ≤ 0.3 | LSP |

The High Suitability Proportion (HSP) quantifies the fraction of the river reach characterised by near-optimal hydraulic conditions. These areas are particularly relevant for feeding and growth processes, as they provide an energetically efficient habitat. It is defined as:

$$\text{HSP} = \frac{\sum_{i=1}^{n} \left( HSI_{A_i} \mid HSI_i \geq 0.7 \right)}{\sum_{i=1}^{n} A_i} \times 100\% \tag{3.4}$$

where $A_i$is the area of the $i$-th computational cell and $M$is the total number of cells within the modelled domain.

The Medium Suitability Proportion (MSP) represents transitional habitat zones where hydraulic conditions are acceptable but not optimal. These zones often serve as links between high-quality patches or act as secondary habitats during fluctuating flow conditions. It is calculated as follows:

$$\text{MSP} = \frac{\sum_{i=1}^{n} \left( HSI_{A_i} \mid 0.3 \leq HSI_i < 0.7 \right)}{\sum_{i=1}^{n} A_i} \times 100\% \tag{3.5}$$

The Low Suitability Proportion (LSP) refers to regions where hydraulic conditions are generally unfavourable for the target species, often due to high velocity, low depth, or other limiting factors. It is defined as:

$$\text{LSP} = \frac{\sum_{i=1}^{n} \left( HSI_{A_i} \mid HSI_i < 0.3 \right)}{\sum_{i=1}^{n} A_i} \times 100\% \tag{3.6}$$

By analysing the relative contributions of the three habitat classes across different flow scenarios, it is possible to assess changes in overall habitat availability and in the distribution of habitat quality. For example, an increase in habitat uses area (WUA), primarily due to an expansion of MSP, may suggest a deterioration in habitat quality, while an increase in HSP indicates an actual improvement in ecological conditions.

This three-class framework, therefore, allows us to provide a more detailed characterisation of habitat structure and supports a more robust interpretation of the ecological effects associated with flow regulation.

# 3.7 Ecological flow assessment

To convert steady-state simulation outputs into operational water management recommendations, two alternative methodologies for evaluating ecological flow were developed. These methods utilise the reach-scale metrics derived in Section 3.6 to identify the discharge scenarios that best balance habitat availability.

## 3.7.1 Limiting factor analysis

The first method used to identify a conservative ecological flow is the limiting factor method, based on habitat suitability constraints that impact the most vulnerable life stages This approach is based on the ecological assumption that the overall resilience of a fish population's weakest component, which is usually represented by early life stages like fry and juveniles, controls the population's overall resilience [23].

Since different species occupy areas with different orders of magnitude, WUA values were normalised using a Min-Max transformation (Eq. 3.7) to make them comparable on a scale from 0 to 1, where 1 represents the optimal habitat condition for that particular stage.

$$WUA_{norm} = \frac{WUA - WUA_{min}}{WUA_{max} - WUA_{min}} \tag{3.7}$$

The relative change in WUA among the minimum and the maximum discharge scenarios was used to quantify the sensitivity of critical life stages to increasing discharge. Any stage showing a reduction greater than a predefined threshold (-30%) was classified as limiting.

The optimal ecological flow was defined as the discharge that maximises this limiting factor. This conservative criterion ensures that the selected flow preserves the best possible habitat condition for the most vulnerable ecological components, thereby minimising the risk of habitat collapse for those stages.

## 3.7.2 Multi-objective optimisation

To identify a flow rate that ensures global ecological balance, the analysis was transposed into a multi-objective optimisation problem using the Ideal Point Method [34] (Raleigh et al., 1984; Widén et al., 2022).

In this model, each combination of species and life stage represents an objective to be maximised. A theoretical Ideal Point *P (1, 1, …, 1)* was defined in the *n*-dimensional space of objectives, where *n* is the number of life stages considered.

For each discharge scenario, the Euclidean distance between the observed normalised habitat vector and the ideal point was computed:

$$D(Q) = \sqrt{\sum_{i} \left(1 - WUA_{norm,i}(Q)\right)^2} \tag{3.8}$$

The optimal compromise flow rate $Q_{best}$ is defined as the one that minimizes this distance, and it represents the solution that minimizes the overall deviation from optimal conditions for the entire biotic community.

Unlike the limiting factor approach, this method does not focus exclusively on the most vulnerable stage but evaluates the performance of the entire system, capturing trade-offs between competing ecological demands.

# Chapter 4

# Results and analysis

## 4.1 Model calibration and validation

After setting up the hydraulic geometry, mesh and boundary conditions described in Section 3.2, an initial simulation was performed using a constant Manning roughness coefficient of 0.06, as previously chosen. This was useful for evaluating the model's performance and obtaining a first estimate of the spatial distribution of the water surface elevation (WSE) along the entire study stretch, as shown in Figure 4.1.

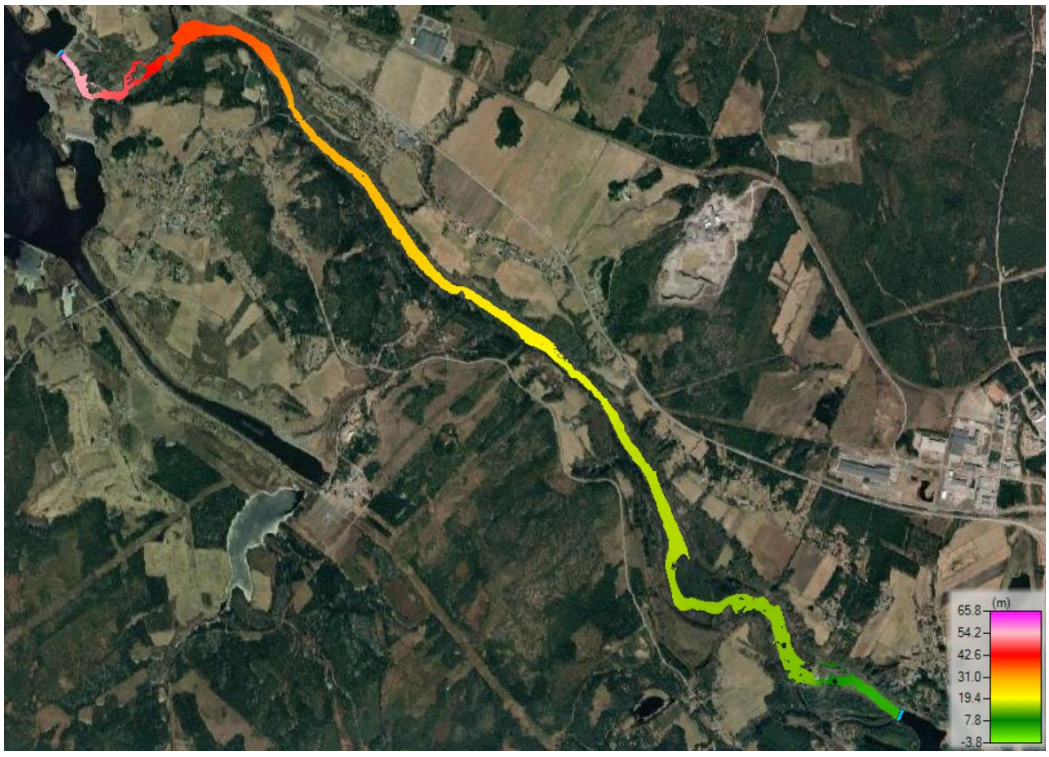



*Figure 4.1. Preliminary WSE distribution obtained from HEC-RAS simulation*

Subsequently, the model was calibrated through an iterative parameter adjustment procedure aimed at minimising the difference between the simulated and observed free surface elevations (ΔWSE). At each iteration, the Manning coefficient was varied while keeping it constant along the stretch, and the results were recorded.

The results of the calibration process are summarised in Figure 4.2, which shows the variation of ΔWSE as a function of Manning roughness for each calibration point along the study reach.

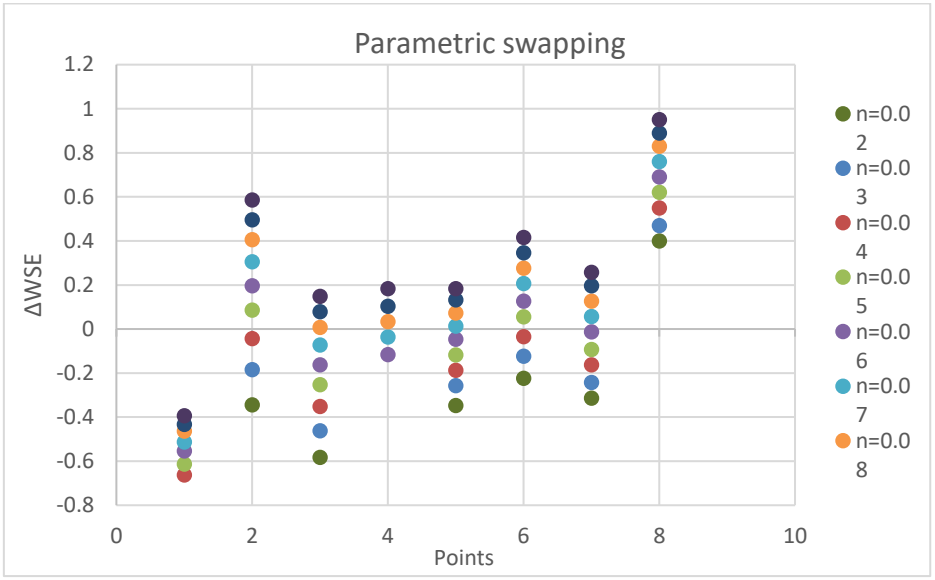



*Figure 4.2. Water surface elevation difference (ΔWSE) obtained from the parametric sweep of Manning's roughness coefficients.*

The results show that the WSE's sensitivity to changes in the Manning coefficient varies spatially along the study stretch. Each calibration point shows a different response, and consequently, minimum ΔWSE values are associated with different Manning coefficients n. For each point, the roughness coefficient showing the smallest error was chosen as the optimal one for that location.

The calibrated Manning's roughness coefficients adopted for the different river sections are reported in Table 4.1.

*Table 4.1. Calibrated Manning's roughness coefficients assigned to the different river sections*

| Point | Final value |
|---|---|
| 1 | 0.10 |
| 2 | 0.04 |
| 3 | 0.07 |
| 4 | 0.08 |
| 5 | 0.07 |
| 6 | 0.04 |
| 7 | 0.06 |
| 8 | 0.035 |

Based on these results, a spatially distributed roughness map was generated with the software QGIS and implemented in HEC-RAS as a Land Cover layer, as shown in Figure 4.3.

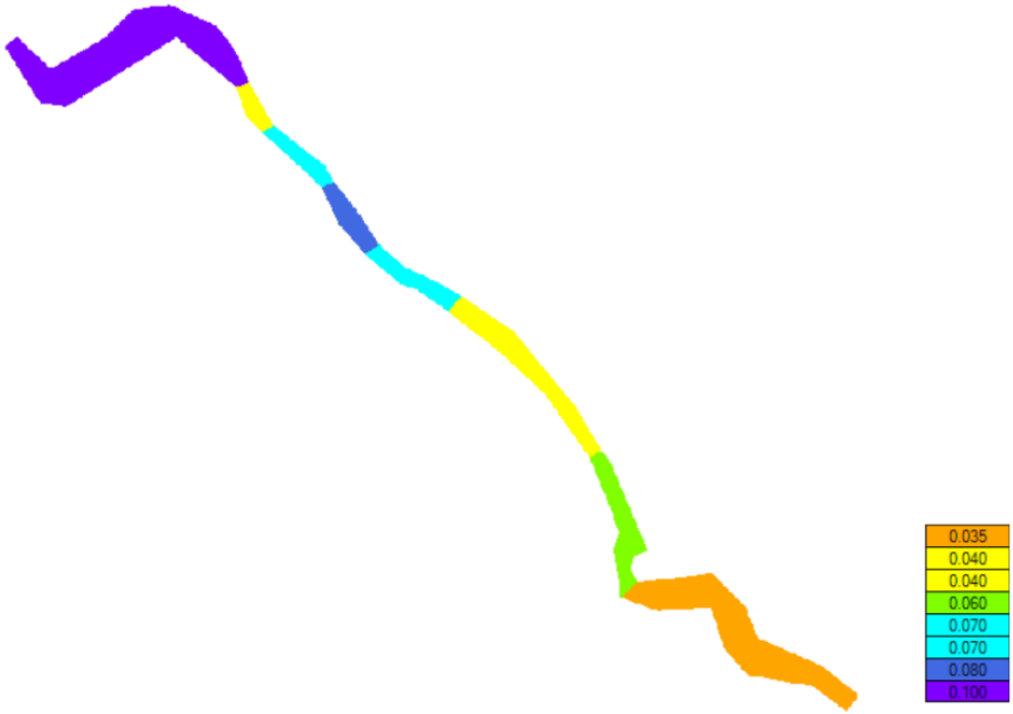



*Figure 4.3. Spatial distribution of calibrated Manning's roughness coefficients implemented as a Land Cover layer*

Once the Manning values were calibrated, the actual model validation was performed by comparing the simulated and observed WSE under the two flow conditions, $Q_{21}$ and $Q_{50}$. For each simulation, the relative percentage errors[2] were calculated for a direct comparison. The validation results are summarised in Table 4.2.

*Table 4.2. Validation results of the hydrodynamic model obtained from the comparison between simulated and observed WSE values*

| No. | Q = 21 m³/s | | | Q = 50 m³/s | | |
|---|---|---|---|---|---|---|
| | Measured (m) | Simulated (m) | Error (%) | Measured (m) | Simulated (m) | Error (%) |
| 1 | 35.05 | - | - | 35.45 | 35.06 | -1.11 |
| 2 | 28.68 | 29.13 | 1.59 | 29.51 | 29.61 | 0.33 |
| 3 | 28.90 | 28.70 | -0.69 | 29.21 | 29.14 | -0.25 |
| 4 | - | - | - | 26.45 | 26.48 | 0.13 |
| 5 | 23.60 | 23.68 | 0.33 | 24.01 | 24.02 | 0.05 |
| 6 | - | 18.62 | - | 18.93 | 18.90 | -0.18 |
| 7 | 15.52 | 15.54 | 0.12 | 15.94 | 15.92 | -0.14 |
| 8 | 13.31 | 13.84 | 3.95 | 13.67 | 14.18 | 3.73 |

Figure 4.4 shows the relationship between the measured and the simulated WSE for both discharge scenarios. The results are plotted with a 1:1 reference line, allowing a direct visual assessment of the model's performance.

[2] The percentage error was calculated as: $Relative\ error\ (\%) = \frac{WSE_{simulated} - WSE_{observed}}{WSE_{observed}} \times 100$

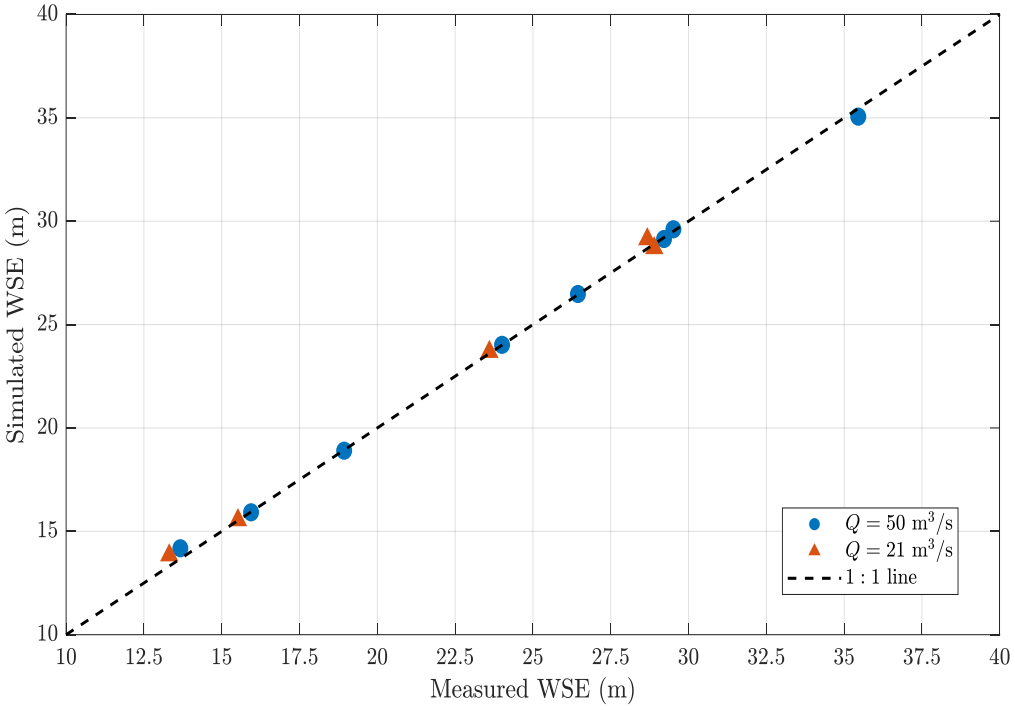



*Figure 4.4. Comparison between measured and simulated WSE*

For both flow conditions, it can be observed that the simulated WSE values closely follow the 1:1 reference line, indicating a good agreement between numerical predictions and field observations.

To further evaluate model performance, a set of statistical indicators was calculated for both scenarios. The results are provided in Table 4.3.

*Table 4.3. Statistics regarding the calibration of the model*

| Property | Q = 50 m³/s | Q = 21 m³/s |
|---|---|---|
| Maximum error [m] | 0.51 | 0.53 |
| Minimum error [m] | 0.01 | 0.02 |
| Mean error [m] | 0.15 | 0.26 |
| Median error [m] | 0.05 | 0.20 |
| Standard deviation [m] | 0.19 | 0.23 |

The statistical analysis indicates that the model showed limited discrepancies between simulated and observed WSE values in both scenarios. The average errors remained below 0.30 m, while the maximum error did not exceed 0.53 m in either scenario and the standard deviation also remained below 0.20 m.

## 4.2 Hydraulic results

Following model calibration and validation, a series of simulations was performed under different flow scenarios. Firstly, four steady-state simulations were performed

under different discharge scenarios, implemented using a constant-flow hydrograph. As described in Section 3.4, the four scenarios were 21, 30, 40 and 50 m³/s. Subsequently, one unsteady simulation was performed using the flow hydrograph described in Figure 3.9.

For each steady-state simulation, the hydraulic outputs of flow velocity and water depth were extracted from the final simulation timesteps at the computational points within the 2D domain. The resulting spatial distribution for a discharge of 21 m³/s is presented in Figure 4.5 and Figure 4.6.

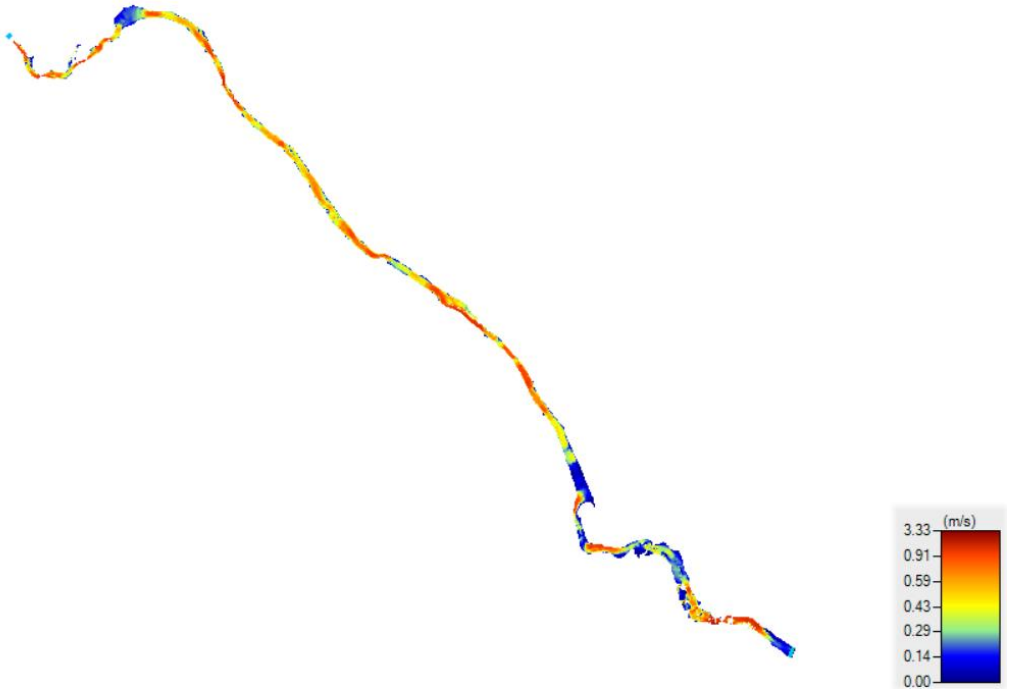


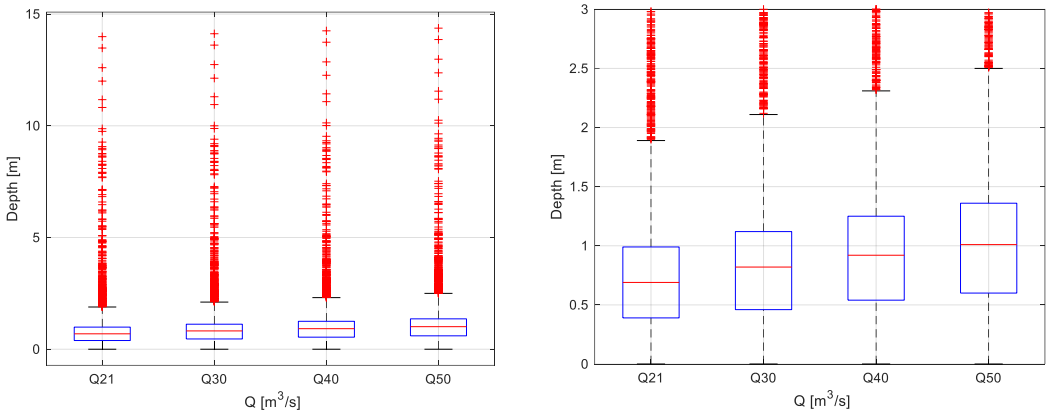

*Figure 4.5. Spatial distribution of flow velocity for Q = 21 m³/s obtained from HEC-RAS*




*Figure 4.6. Spatial distribution of water depth for Q = 21 m³/s obtained from HEC-RAS*

Although the spatial maps of depth and velocity provide a qualitative overview of the hydraulic field, the quantitative variation is better appreciated through statistical analysis of the distributions. Statistical analysis was therefore conducted for each flow scenario to evaluate the variation in depth and velocity as the flow increased.

Figure 4.8 shows the box plots of depths and velocities obtained across the different scenarios analysed.



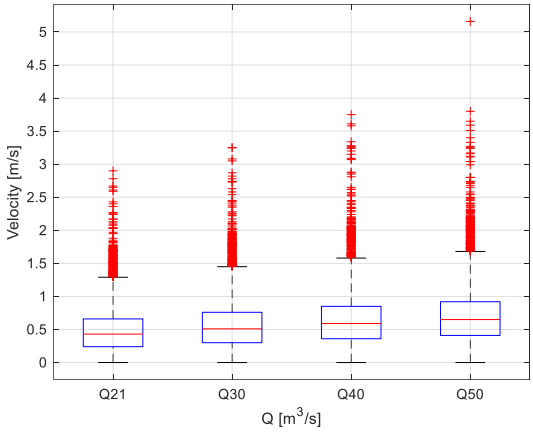



*Figure 4.7. Boxplot of depth and velocities for different flow scenarios: a) complete depth analysis with outliers, b) detail of depth below 3m, c) velocity distribution*

Figure 4.7a shows the actual depth distribution at different flow rates, which is highly asymmetric, with almost all points concentrated below 2 m. In particular, this plot is useful for highlighting the presence of topographic artefacts in the DTM described in Section 3.3.2, which reach a maximum depth of 14 m and appear as outliers relative to the boxplots. Furthermore, these maximum values remain stable across scenarios, ranging from 14 m to 14.4 m, demonstrating that the areas remain fully active even at lower flow rates and that they do not affect the statistical consistency of the mean values.

Figure 4.7b examines the depth behaviour in more detail by zooming in only to depths less than 3 m. In this range, the increase in draft with increasing flow rate is clearly observed. The medians progressively increase from approximately 0.69 m for $Q_{21}$ to approximately 1.1 m for $Q_{50}$.

Finally, Figure 4.7c shows the velocity distribution. A similar, but more dynamic, trend is observed: the median and dispersion increase progressively as the flow rate increases. For $Q_{21}$, the velocities are contained within approximately 0.5-0.6 m/s, while for $Q_{50}$, the distribution shifts toward higher values, reaching maximum values in the order of 5 m/s. This behaviour shows that events with higher flow rates produce more energetic, locally critical flow conditions.

*Table 4.4. Statistical analysis for the hydraulic results: a) Depth and b) Velocity*

**Depth**

| Scenario | Mean [m] | Median [m] | Std Dev [m] | P95 [m] | Max [m] |
|---|---|---|---|---|---|
| Q21 | 0.85 | 0.69 | 0.97 | 2.25 | 13.99 |
| Q30 | 0.95 | 0.82 | 0.98 | 2.37 | 14.12 |
| Q40 | 1.05 | 0.92 | 0.99 | 2.46 | 14.25 |
| Q50 | 1.13 | 1.01 | 1.00 | 2.54 | 14.37 |

**Velocity**

| Scenario | Mean [m/s] | Median [m/s] | Std Dev [m/s] | P95 [m/s] | Max [m/s] |
|---|---|---|---|---|---|
| Q21 | 0.50 | 0.43 | 0.36 | 1.18 | 2.90 |

| | | | | | |
|---|---|---|---|---|---|
| Q30 | 0.58 | 0.51 | 0.40 | 1.33 | 3.25 |
| Q40 | 0.65 | 0.59 | 0.44 | 1.45 | 3.75 |
| Q50 | 0.72 | 0.65 | 0.46 | 1.57 | 5.16 |

To more fully describe hydraulic availability, cumulative distribution functions (CDFs) were also calculated and are shown in Figure 4.8.

The depth CDF (Figure 4.8) shows that over 90% of the computational domain has depths less than 2.5 m in all scenarios analysed. Furthermore, the curves are very close to each other, consistent with the river's structure. A very wide cross-section means that when flow increases, the water expands laterally rather than rises vertically. The tail of the curve graphically shows the "weight" of the anomalies, but since the curve becomes almost flat after 4 m, this means that they represent a very small percentage of the mesh points.

Conversely, the velocity CDF (Figure 4.9) shows a more marked shift to the right, indicating that the river responds to increased flow primarily through an increase in the kinetic energy of the flow, rather than through a significant rise in the water level. The regular shape, however, suggests that this response is uniform.

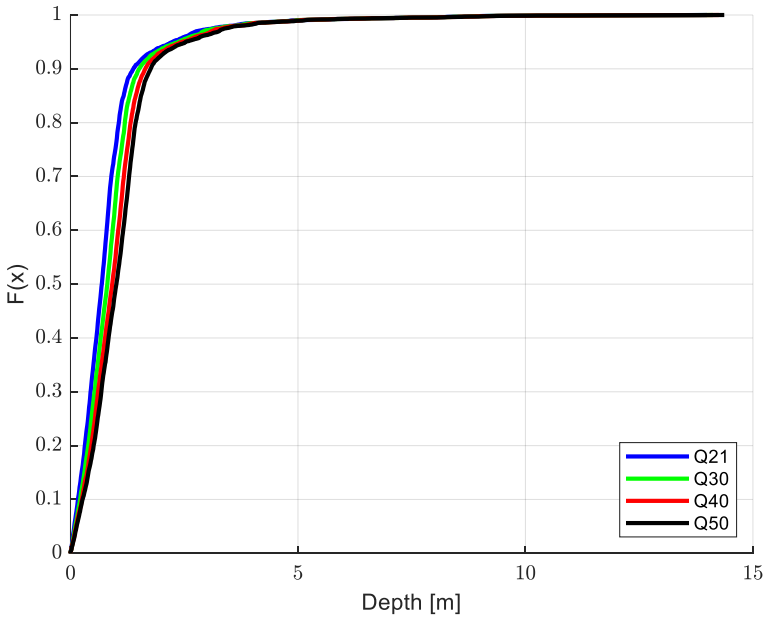



*Figure 4.8. Cumulative Distribution Functions (CDF) for depth*

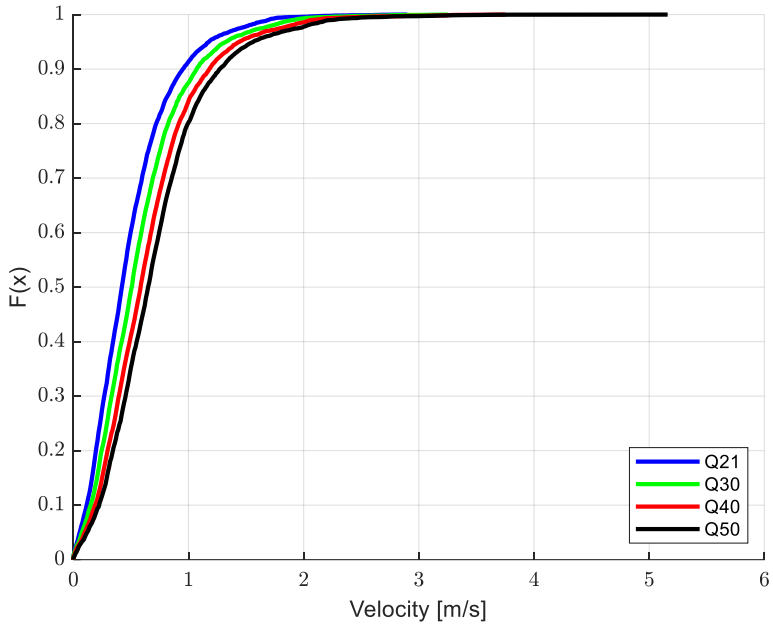



*Figure 4.9. Cumulative Distribution Functions (CDF) for velocity*

## 4.3 Steady-state simulations

### 4.3.1 Habitat suitability spatial distribution

The spatial distribution of the Habitat Suitability Index (HSI) shows numerous differences across species and life stages, as well as across the different flow scenarios considered. The HSI maps provide a spatial representation of how suitable areas are arranged and how their extent and fragmentation vary across scenarios.

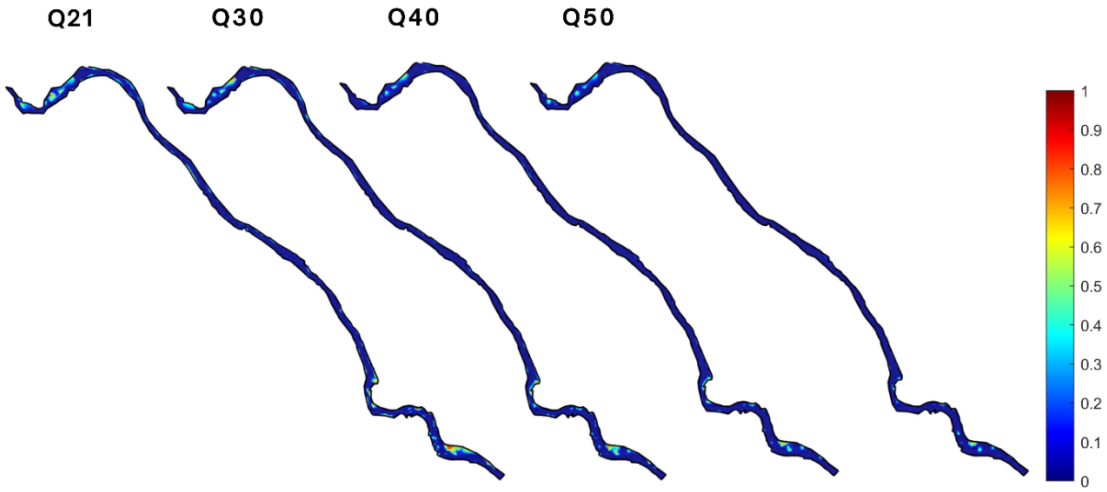



*Figure 4.10. HSI distribution for the fry stage at each discharge scenario for the European grayling*

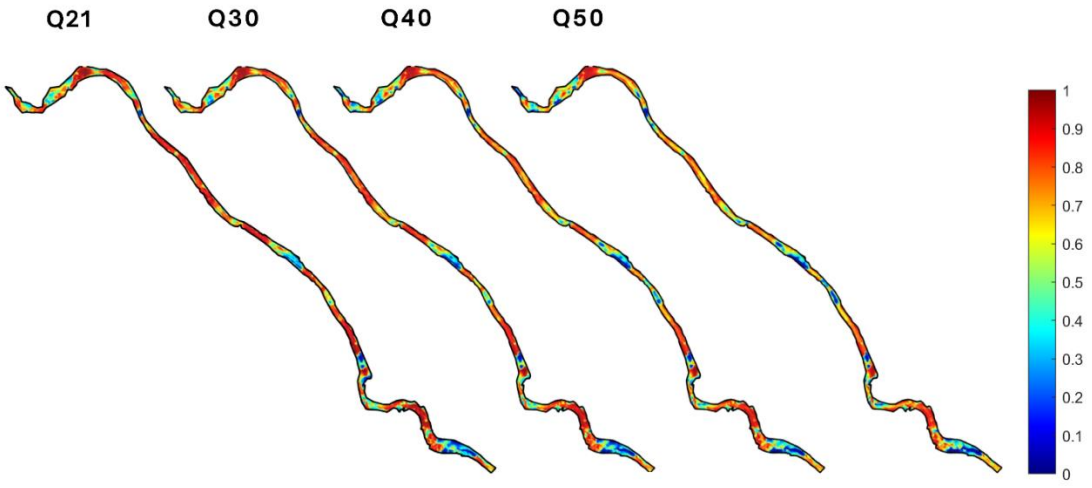



*Figure 4.11. HSI distribution for the juvenile stage at each discharge scenario for the European grayling*

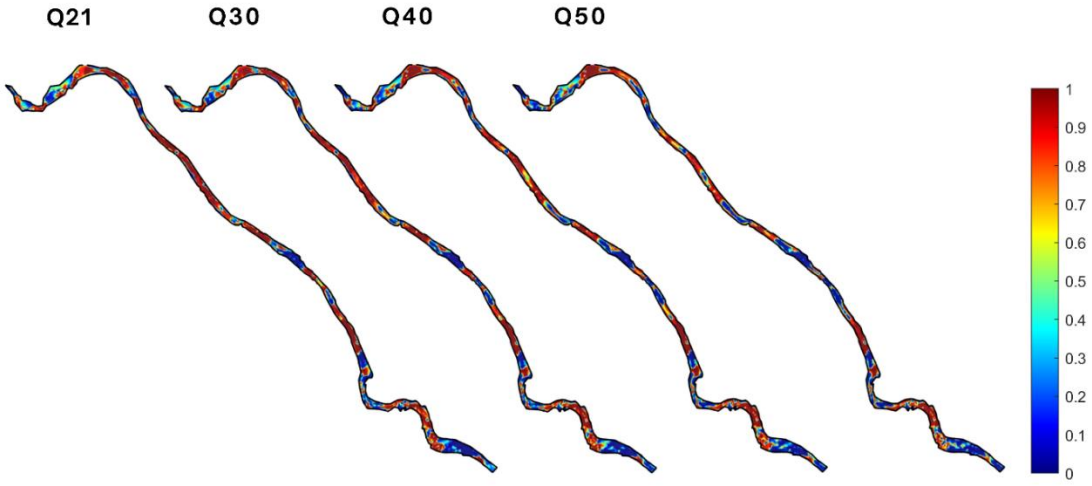



*Figure 4.12. HSI distribution for the spawning stage at each discharge scenario for the European grayling*

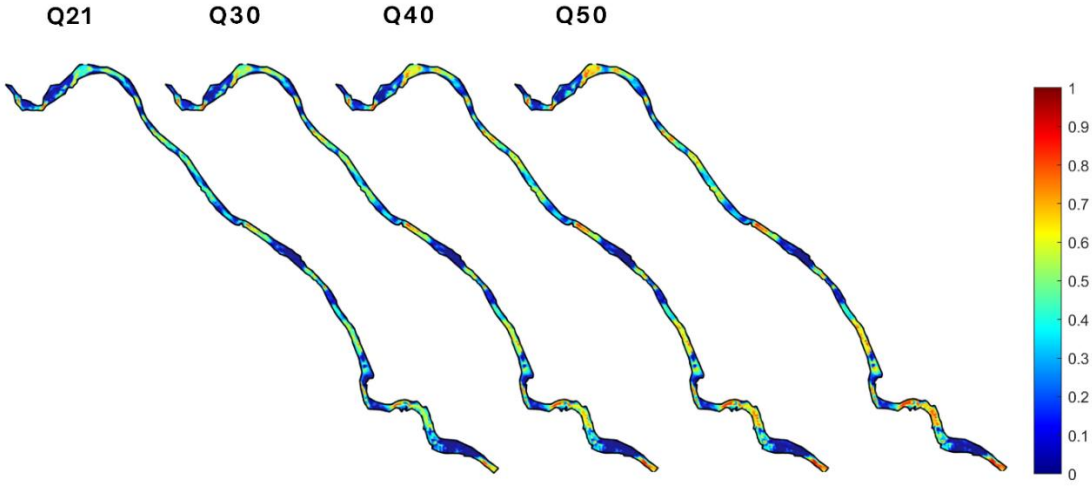



*Figure 4.13. HSI distribution for the adult stage at each discharge scenario for the European grayling*

Regarding the European grayling, the fry and juvenile stages exhibit a negative response to increased discharge. Specifically, the fry stage (Figure 4.10) represents

the most vulnerable phase: even under the $Q_{21}$ scenario, suitable habitat appears limited and fragmented, confined primarily to the marginal upstream and downstream areas of the study reach. As discharge increases, these zones progressively contract until they nearly disappear in the $Q_{50}$ scenario, suggesting that high velocities and elevated hydraulic energy levels are incompatible with the ecological requirements of grayling fry.

The juvenile stage (Figure 4.11) also shows a progressive contraction of high-HSI areas as discharge increases, though with a higher tolerance than fry. Favourable conditions tend to concentrate increasingly in lateral areas and zones protected by river bends, where flow velocities remain relatively moderate. Despite this reduction, juveniles maintain a wider distribution of suitable areas, indicating a higher capacity to occupy a broader range of conditions.

Conversely, a reverse trend is observed for adults (Figure 4.13): the increase in discharge leads to an expansion of high-suitability areas, indicating a preference for conditions characterised by greater depth and higher flow energy. In this case, the increase in discharge makes the channel progressively more suitable, suggesting that adult European grayling can benefit from higher-flow scenario.

The spawning stage (Figure 4.12) exhibits a non-linear response to discharge. In the $Q_{21}$ scenario, suitable habitat appears fragmented and restricted to the most morphologically stable areas. Optimal conditions appear to be reached in the intermediate scenarios ($Q_{30}$ - $Q_{40}$) where high-suitability areas become more extensive and connected. Then, a reduction in maximum HSI zones is observed at $Q_{50}$, suggesting that excessively energetic hydraulic conditions may compromise substrate stability or the persistence of spawners.

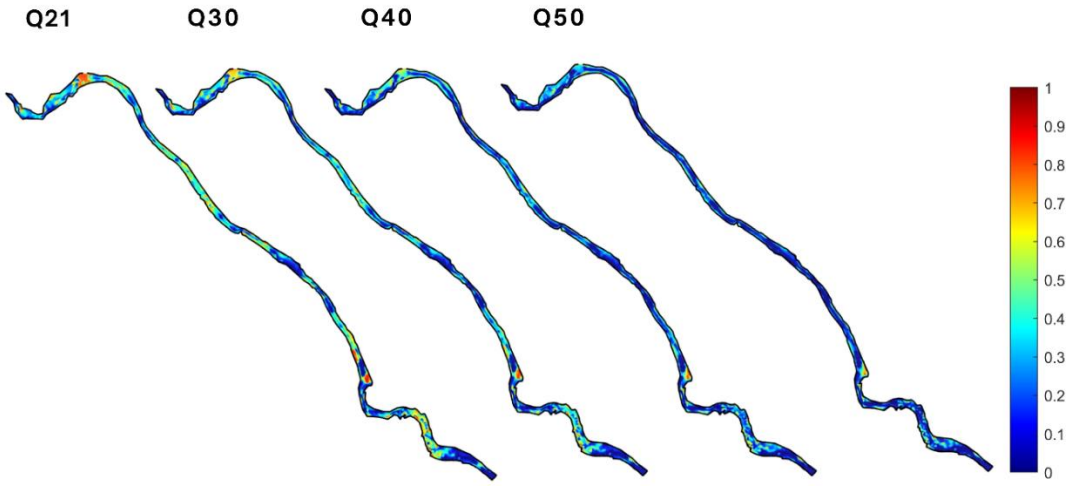



*Figure 4.14. HSI distribution for the fry stage at each discharge scenario for the brown trout*

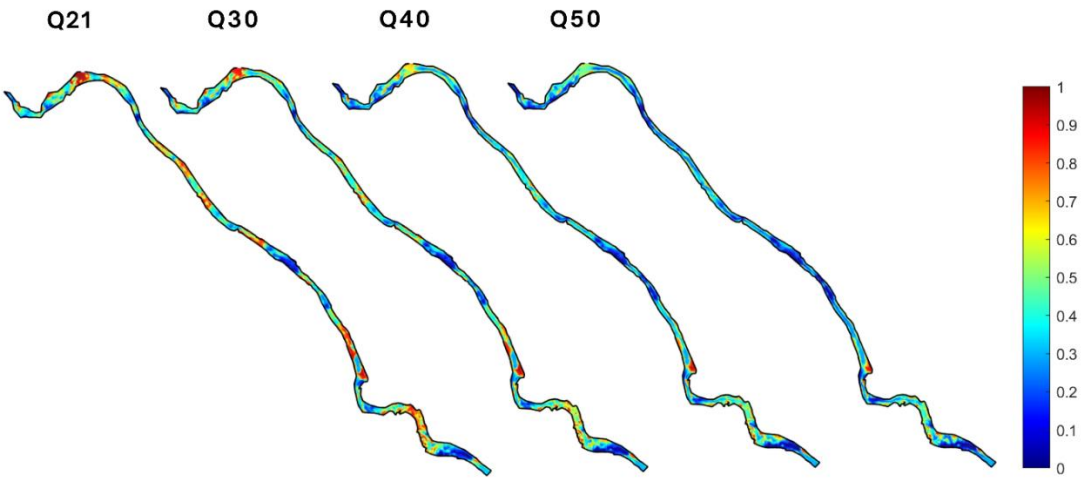



*Figure 4.15. HSI distribution for the juvenile stage at each discharge scenario for the brown trout*

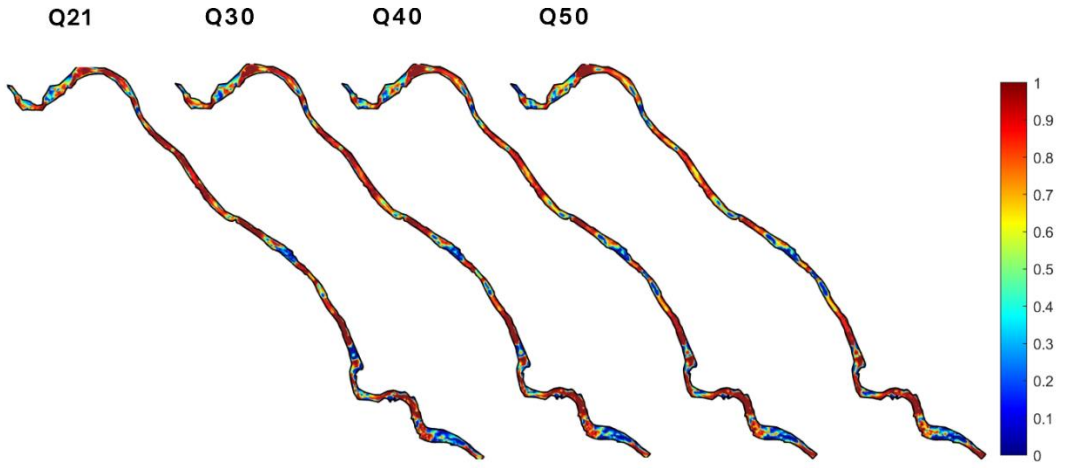



*Figure 4.16. HSI distribution for the spawning stage at each discharge scenario for the brown trout*

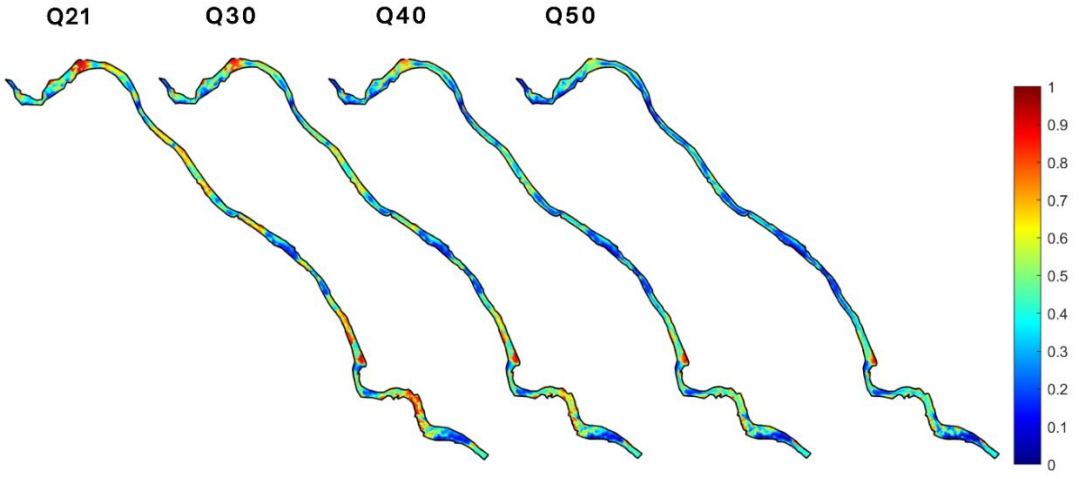



*Figure 4.17. HSI distribution for the adult stage at each discharge scenario for the brown trout*

The fry and juvenile stages of the brown trout display a pattern similar to that observed for the grayling, characterised by a progressive reduction in habitat

suitability as discharge increases. However, this contraction is more pronounced in trout. For the fry stage (Figure 4.14), suitable habitat is already confined to narrow, protected marginal niches at $Q_{21}$. Moving to the $Q_{30}$ and $Q_{40}$ scenarios, these areas are drastically reduced, disappearing almost entirely at $Q_{50}$. This highlights the extreme sensitivity of trout fry to increased flow velocities.

The juvenile stage (Figure 4.15) also shows progressive fragmentation of suitable areas as discharge rises. While habitat is widely distributed and of high quality at $Q_{21}$, high-HSI zones decrease significantly in high-flow scenarios due to excessive hydraulic energy. Compared to the fry, juveniles maintain a wider spatial distribution of suitable habitat, but the reduction due to increased water flow remains evident.

In contrast, the adult stage of brown trout (Figure 4.17) follows an opposite trend compared to adult grayling: a progressive decrease in suitable areas is observed as discharge increases. This shows that adult trout are being affected more negatively than adult grayling by the high-flow conditions. Fewer high-HSI areas imply a preference for lower-energy-flow conditions than in the adult grayling.

The spawning stage (Figure 4.16) likewise exhibits a bell-shaped suitability response relative to discharge. Optimal conditions are found in the intermediate scenarios ($Q_{30}$ - $Q_{40}$), which are characterized by maximum connectivity between high-suitability areas. A moderate deterioration in habitat quality occurs at $Q_{50}$ in the central sections of the channel, likely due to the excessive increase in flow velocity.

Overall, the HSI maps emphasise that each life stage occupies a distinct hydraulic niche, reflecting different habitat preferences for water velocity and depth. Generally, early life stages prefer areas with low velocity and limited hydraulic energy, whereas adult stages are associated with deeper zones and moderate velocity.

Although discharge variation strongly influences the magnitude of HSI values, the spatial organisation of habitat suitability does not change randomly in the cases considered. Higher-suitability zones are usually aggregated around the designated hydraulic and morphological unit of the reach. An increase in flow magnitude has been shown to change the shape and quantity of the patches, without altering their spatial locations randomly. This would mean that a reach contains a few functional units that become more or less useful depending on flow magnitude, species and life stages.

### 4.3.2 Quantitative habitat analysis

The quantitative analysis of the Weighted Usable Area (WUA) provides a numerical synthesis of patterns observed in the HSI maps, highlighting the differing responses of the two species and their life stages to discharge variations.

The results (Figure 4.18) indicate that the relationship between available habitat and discharge is not uniform but depends heavily on both the species and the life stage analysed.

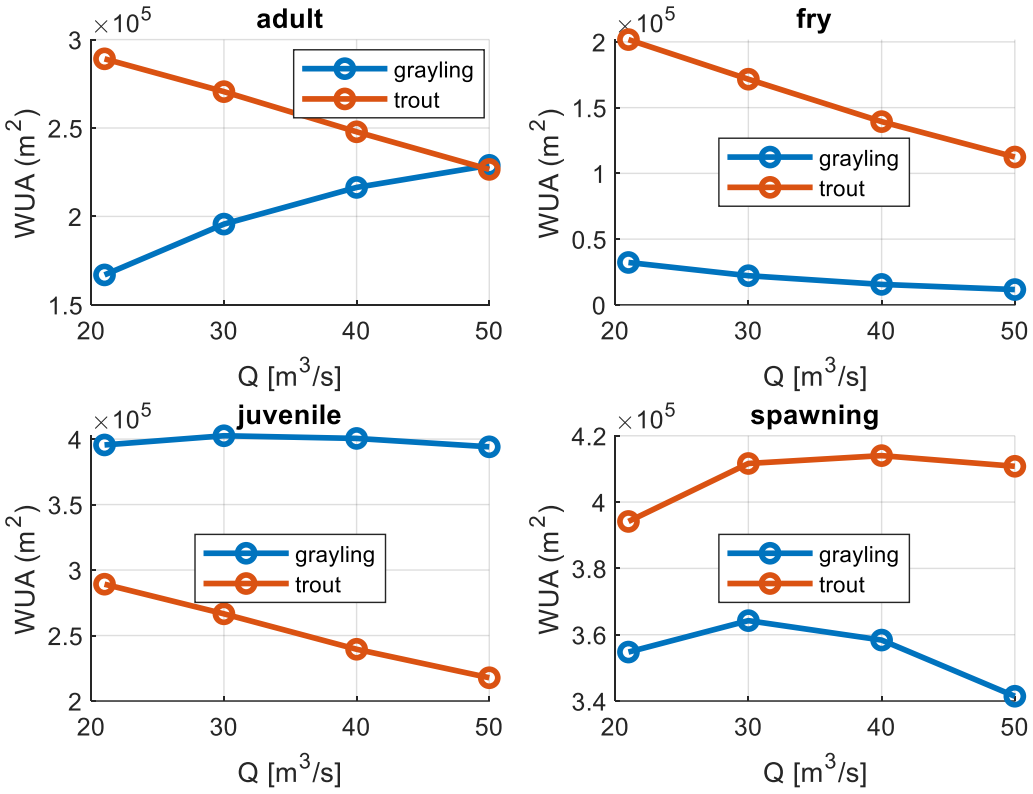



*Figure 4.18. Variation of WUA with the discharge: comparison between the two species*

For the adult stages, opposing dynamics emerge between the European grayling and brown trout. For the adult European grayling, the WUA increases progressively with discharge, confirming the expansion of suitable areas in the main channel observed in the HSI maps. In contrast, adult brown trout show a progressive reduction in WUA as discharge increases, highlighting a greater sensitivity to high-velocity conditions. Despite these opposing trends, both species reach similar WUA values, approximately $2.3 \times 10^5$ m², under the $Q_{50}$ scenario.

For the fry stages, both species exhibit a marked decrease in WUA as discharge grows. This confirms that suitable habitats for fry are confined to low-velocity marginal areas and tend to contract in high-flow scenarios. However, brown trout maintain systematically higher WUA values than European grayling across all analysed scenarios.

The juvenile stage shows more pronounced differences between the two species. Juvenile European graylings maintain high and relatively stable WUA values across all discharge scenarios, suggesting that the studied reach provides favourable habitat for this growth phase. Conversely, juvenile brown trout show a progressive reduction in WUA as discharge increases, confirming higher sensitivity to high velocities compared to the European grayling.

Regarding the spawning phase, both species exhibit a non-linear, bell-shaped WUA trend. Optimal habitat conditions are associated with intermediate discharge scenarios: European grayling reaches its maximum WUA at $Q_{30}$, while brown trout get to the peak at $Q_{40}$. Beyond these thresholds, the WUA decreases rapidly, suggesting that excessively energetic hydraulic conditions may compromise the suitability of spawning grounds.

The patterns observed in WUA values indicate life-stage-specific flow requirements. High discharge shows a very high loss of available habitat for the fry life stage, whereas for the spawning life stage, habitat appears to be optimised at moderate flows. Adult European grayling seems to favour higher discharge levels, whereas adult brown trout seem to be increasingly penalised at higher flows.

### 4.3.3 Qualitative habitat analysis

Since WUA graphs only show the total available area, the habitat was subdivided into quality classes to further investigate its functional value. The three suitability classes considered are:

- HSP: High Suitability Proportion (green), representing high-quality habitat.
- MSP: Medium Suitability Proportion (yellow), representing moderate-quality habitat.
- LSP: Low Suitability Proportion (red), representing poor or unsuitable habitat.

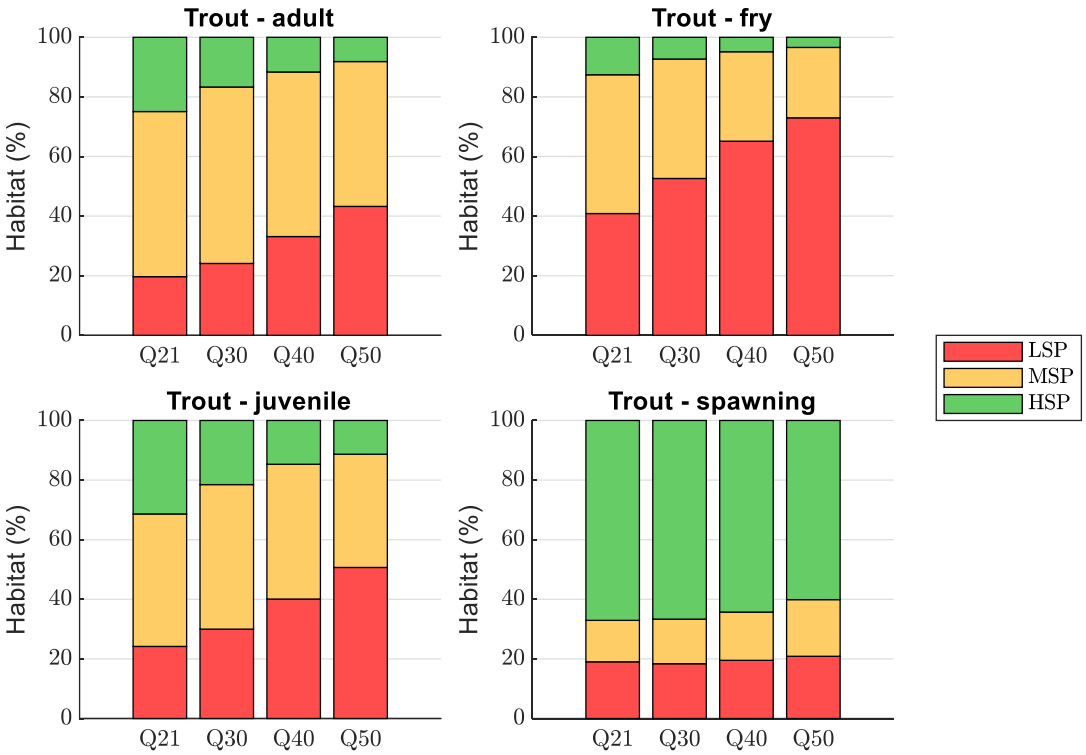



*Figure 4.19. Habitat quality composition for brown trout: percentage distribution of High (HSP), Medium (MSP), and Low (LSP) Suitability Proportions as a function of discharge.*

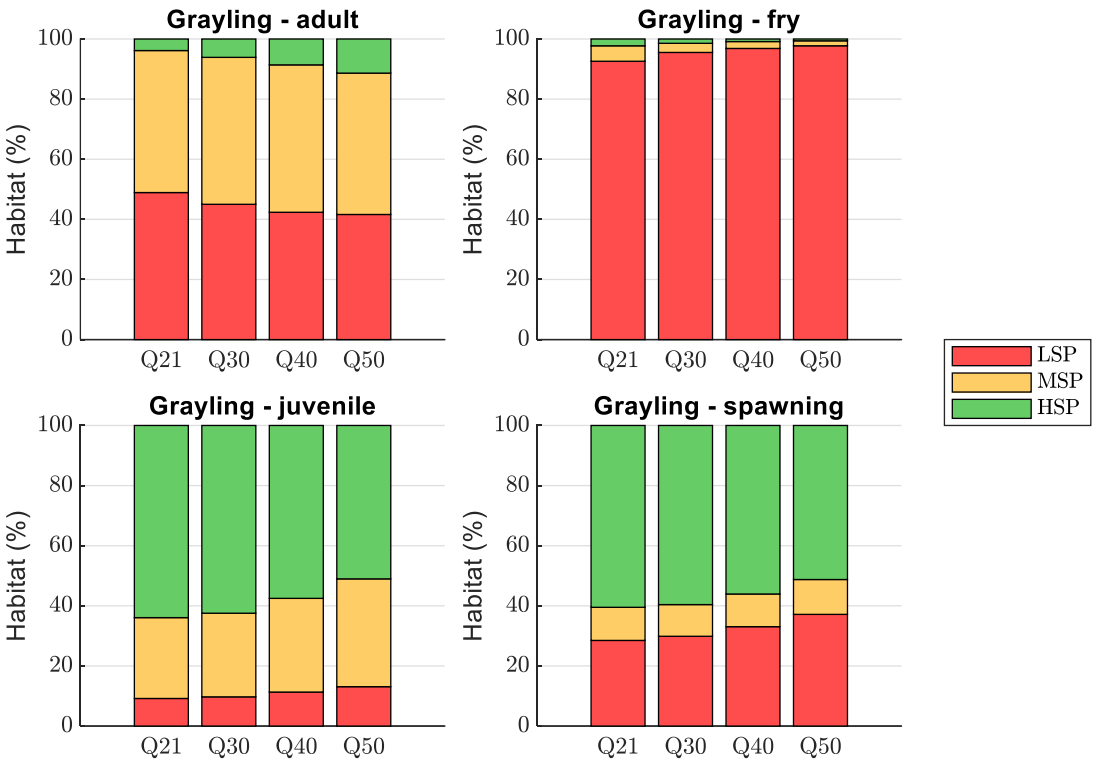



*Figure 4.20. Habitat quality composition for European grayling: percentage distribution of High (HSP), Medium (MSP), and Low (LSP) Suitability Proportions as a function of discharge.*

As observed for habitat availability, the quality is also influenced by discharge variations. For brown trout, a progressive decline in habitat quality is evident as discharge increases. A clear reduction in the HSP component, in favour of an increase in LSP, is noticeable across the adult, fry, and juvenile stages. Specifically, for fry, the low-quality habitat (LSP) increases from 40% at $Q_{21}$ to over 70% at $Q_{50}$. This indicates that the reduction in WUA is accompanied by a deterioration in the quality of the remaining habitat.

Spawning emerges as the most resilient stage, maintaining a constant optimal habitat percentage above 60% across all scenarios. This suggests that spawning areas are either protected or located in zones where the hydraulic conditions remain favourable even at high discharges. Therefore, despite minor spatial changes, overall habitat quality does not seem to vary significantly.

The European grayling, however, shows more variable dynamics across life stages. The fry stage is clearly the most critical: the habitat is almost entirely dominated by LSP, and the already small fraction of quality habitat almost disappears as discharge increases. This indicates that the reach is nearly inhospitable for newborns.

Juvenile and spawning stages of European grayling show high levels of quality habitat, as already evidenced by the WUA curves, which nevertheless reduce as discharge increases. However, as discharge rises, the percentage of high-quality habitat declines. This means that, even though WUA may remain relatively high, the internal quality composition of the habitat may be degrading.

For adults, the opposite pattern is observed. The high-quality habitat component nearly doubles as discharge rises. Furthermore, it is noteworthy that despite

differences in previous scenarios, the $Q_{50}$ scenario results in a habitat class distribution for adult grayling that is nearly identical to that of adult trout.

### 4.3.4 Habitat response to discharge variations

The graph analysing the movement of the centroids (Figure 4.21) serves to understand how the "centre of gravity" of hydraulically suitable habitat shifts as discharge varies. In practice, each point represents a weighted average of the HSI within the depth-velocity space for each species and life stage. It is important to emphasise that these points do not indicate an active choice by the fish but rather describe where the best statistical conditions are concentrated within the studied river reach.

The Figure 4.20 shows that increasing discharge systematically shifts the habitat toward more energetic conditions, specifically deeper areas with higher velocities. The only stage that deviates from this trend is the grayling fry. Its centroid remains fixed within a narrow range, with velocities below 0.2 m/s and depths below 0.4 m.

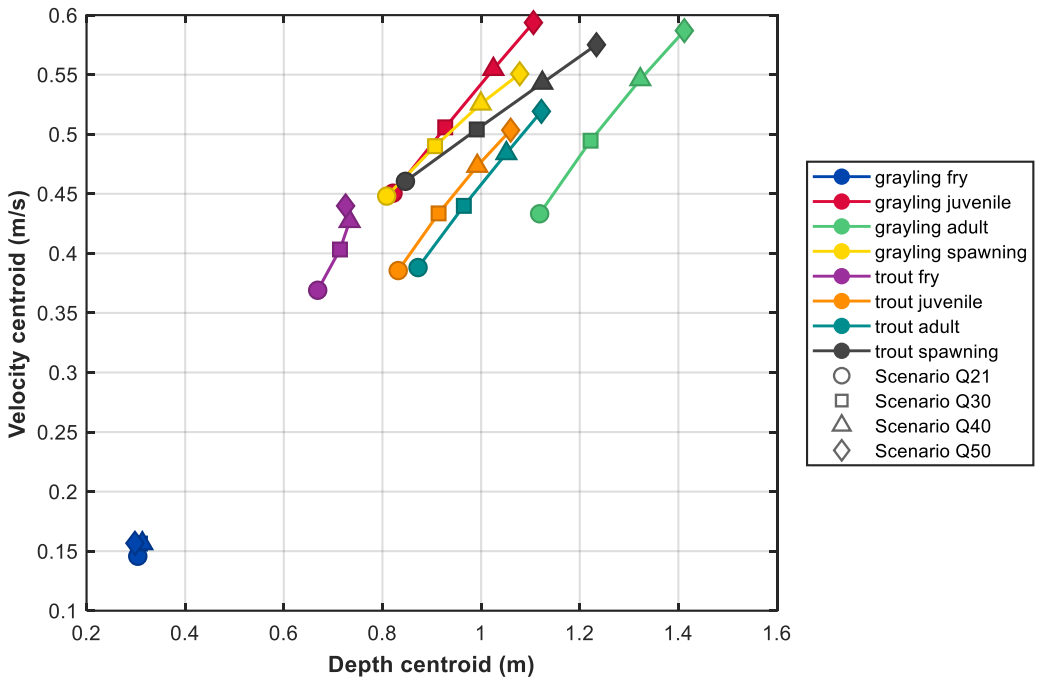



*Figure 4.21. Hydraulic niche shift analysis: displacement of habitat centroids in the depth-velocity space for each species and life stage across the simulated discharge scenarios*

### 4.3.5 Optimal discharge identification

The first phase of the integrated analysis involved aggregating the habitat responses of all life stages into a single synthetic indicator. For each species, the Total Weighted

Usable Area was calculated as the sum of the WUA values for all life stages in each discharge scenario.

*Table 4.5. Weighted Usable Area (WUA) values (m2) for European grayling life stages across the four steady-state discharge scenarios*

| Stage | WUA Q21 | WUA Q30 | WUA Q40 | WUA Q50 |
|---|---|---|---|---|
| adult | $1.67 \cdot 10^5$ | $1.96 \cdot 10^5$ | $2.16 \cdot 10^5$ | $2.29 \cdot 10^5$ |
| fry | $0.32 \cdot 10^5$ | $0.22 \cdot 10^5$ | $0.16 \cdot 10^5$ | $0.12 \cdot 10^5$ |
| juvenile | $3.96 \cdot 10^5$ | $4.03 \cdot 10^5$ | $4.00 \cdot 10^5$ | $3.94 \cdot 10^5$ |
| spawning | $3.55 \cdot 10^5$ | $3.64 \cdot 10^5$ | $3.58 \cdot 10^5$ | $3.41 \cdot 10^5$ |
| Total | $9.49 \cdot 10^5$ | $9.85 \cdot 10^5$ | $9.91 \cdot 10^5$ | $9.76 \cdot 10^5$ |

*Table 4.6. Weighted Usable Area (WUA) values (m²) for brown trout life stages across the four steady-state discharge scenarios*

| Stage | WUA Q21 | WUA Q30 | WUA Q40 | WUA Q50 |
|---|---|---|---|---|
| adult | $2.89 \cdot 10^5$ | $2.71 \cdot 10^5$ | $2.48 \cdot 10^5$ | $2.27 \cdot 10^5$ |
| fry | $2.02 \cdot 10^5$ | $1.72 \cdot 10^5$ | $1.39 \cdot 10^5$ | $1.12 \cdot 10^5$ |
| juvenile | $2.89 \cdot 10^5$ | $2.67 \cdot 10^5$ | $2.40 \cdot 10^5$ | $2.18 \cdot 10^5$ |
| spawning | $3.94 \cdot 10^5$ | $4.12 \cdot 10^5$ | $4.14 \cdot 10^5$ | $4.11 \cdot 10^5$ |
| Total | $1.17 \cdot 10^6$ | $1.12 \cdot 10^6$ | $1.04 \cdot 10^6$ | $0.97 \cdot 10^6$ |

Notably, except for the fry stage, brown trout generally exhibit higher WUA values across life stages compared to European grayling. As illustrated in Figure 4.22, the trend of the Total Combined WUA (obtained by summing values for both target species) shows a constant decline as discharge increases. Although the European grayling (Table 4.5) benefits from a moderate increase in habitat up to $Q_{40}$ the sharp contraction in habitat availability for the brown trout (Table 4.6) dominates the aggregated data. Consequently, from the perspective of the system's total carrying capacity, lower discharge regimes $Q_{21}$ appear to ensure the greatest extent of physical habitat usable on a global biotic scale.

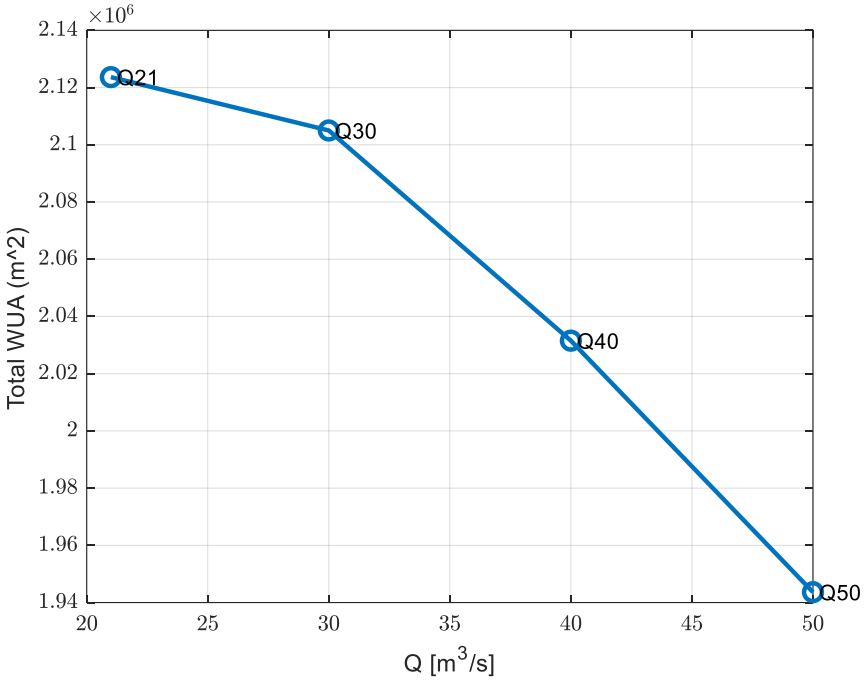



*Figure 4.22. Total Weighted Usable Area (Grayling + Trout) as a function of discharge*

While this approach is commonly adopted for its simplicity, it possesses a significant limitation. By summing the habitat availability of all stages, the method inherently assigns greater weight to those characterised by larger spatial extents. Consequently, ecologically critical stages that occupy smaller areas, such as fry habitats, may be underrepresented despite their key role in recruitment and long-term population persistence.

To investigate conflicts between the two species, a multi-objective optimisation analysis was conducted by constructing a Pareto Front. For each discharge scenario, the aggregated WUA of the two species was compared to identify efficient solutions, defined as conditions in which habitat gains for one species can be achieved only at the expense of the other.

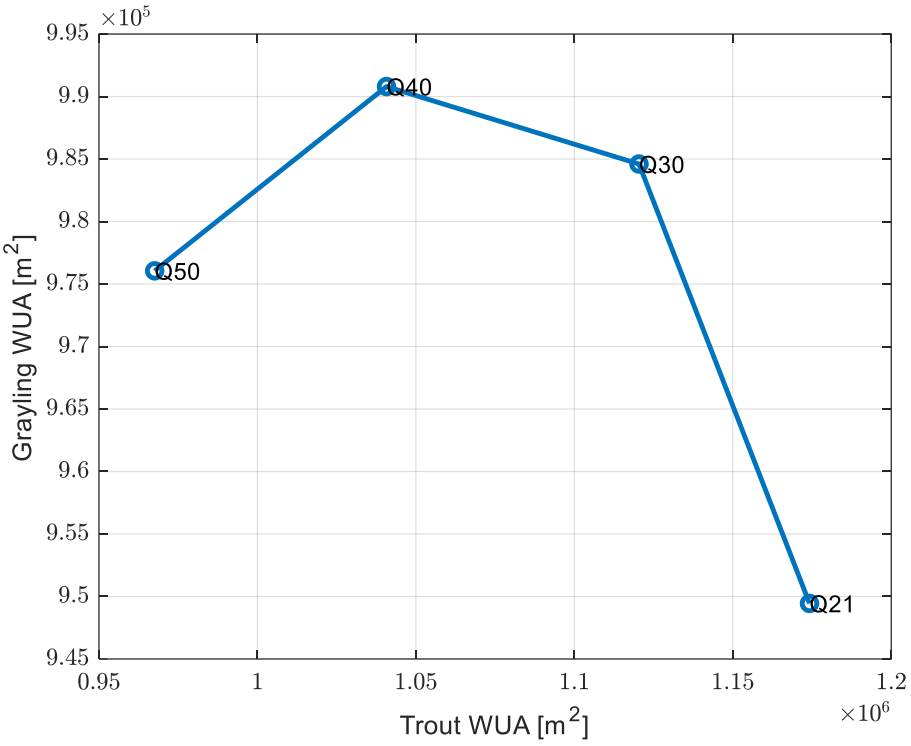



*Figure 4.23. General Pareto trade-off curve*

The global Pareto analysis (Figure 4.23) confirms the existence of a strong ecological conflict between intermediate and extreme discharges. The $Q_{21}$ scenario represents the optimum for brown trout but coincides with the minimum habitat value for the European grayling. Conversely, the $Q_{40}$scenario maximizes habitat for the European grayling but results in a significant loss for the trout. Interestingly, the $Q_{50}$ scenario is found to be inefficient (dominated): by moving from $Q_{50}$ to $Q_{40}$, habitat availability increases for both species simultaneously.

However, the trade-off depends heavily on the specific life stage, as shown in the disaggregated analysis.

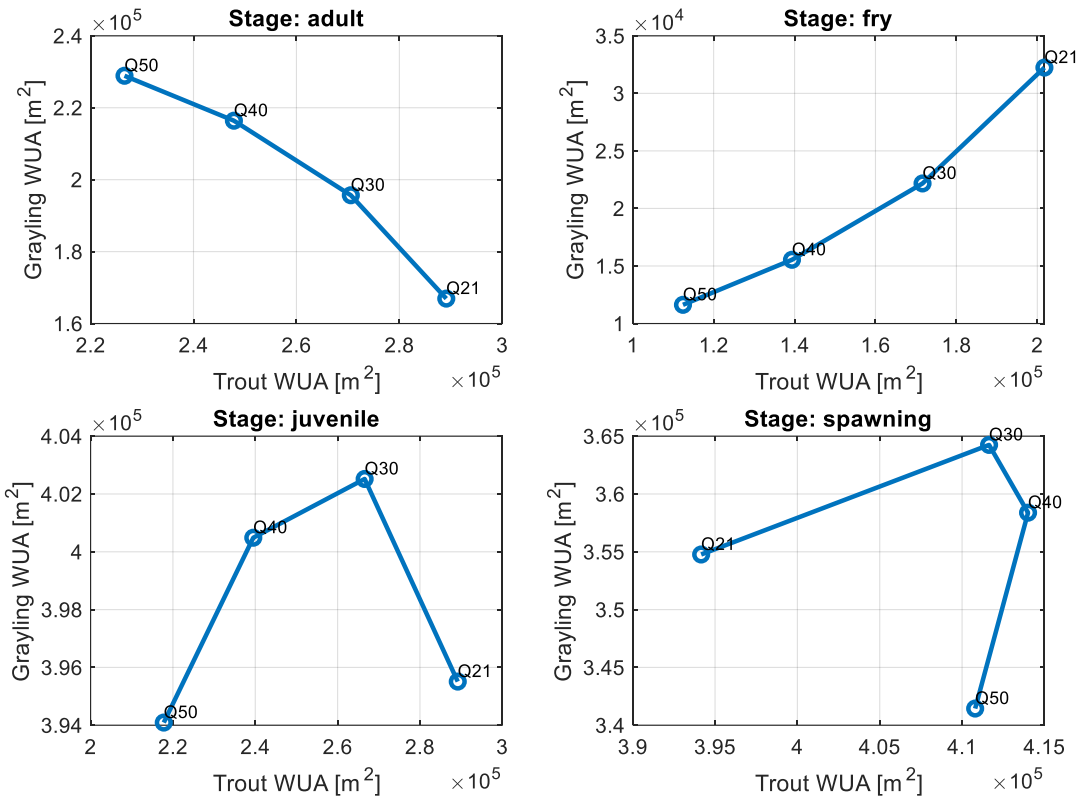



*Figure 4.24. Pareto trade-off curve per life stages*

The Pareto analysis revealed diverse dynamics across stages. The adult and fry stages both exhibit a linear trade-off, though they differ conceptually. For adults, conditions improve for grayling but worsen for brown trout as discharge increases. For fry, synergy is observed: both species benefit from reduced discharges, and they show a mutual loss of habitat as flow increases.

The juvenile and spawning stages show more complex, non-linear trends. For juveniles, $Q_{21}$ represents a peak in availability for European grayling, while trout continue to favour lower flows. For spawning, the conflict eases between $Q_{30}$ and $Q_{40}$, scenarios that appear to offer an acceptable compromise for both species. These results demonstrate that no single discharge maximises habitat suitability across all ecological objectives, highlighting the necessity for compromise-based optimisation approaches.

To identify the best compromise of discharge and overcome the limitations of simple aggregation, a Limiting Factor Analysis was conducted. This approach identifies ecological "bottlenecks", which are life stages that experience the greatest spatial restriction in specific scenarios.

The analysis identified fry habitats as the primary critical point for both species. As illustrated in Figure 4.25, normalized habitat availability suffers a drastic collapse as discharge increases, with a loss exceeding 60% when moving from $Q_{21}$ to $Q_{30}$, and nearly reaching zero at $Q_{50}$.

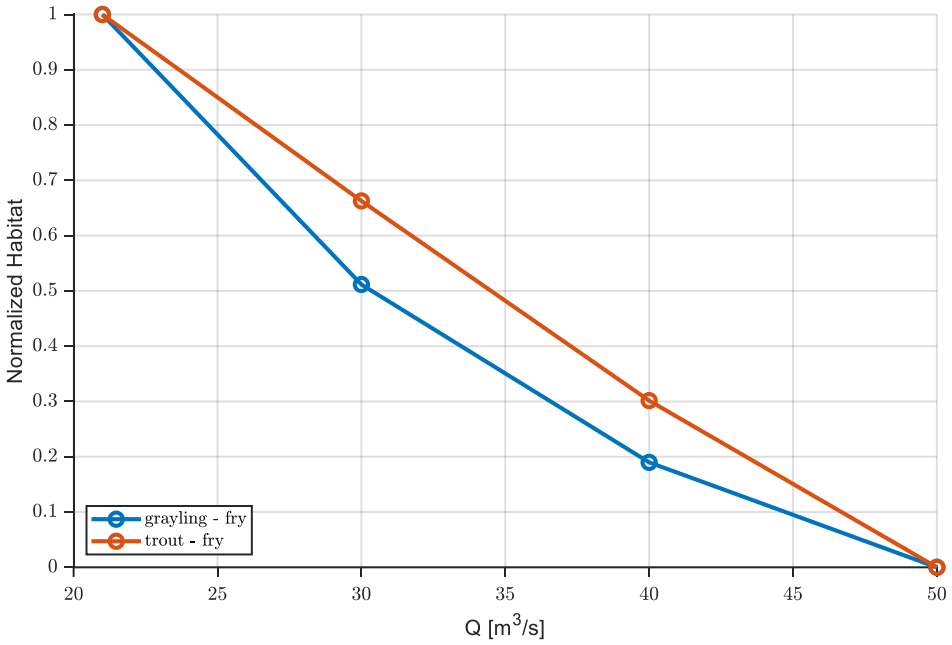



*Figure 4.25. Limiting factor analysis*

According to the limiting factor criterion, the optimal ecological discharge corresponds to the flow that maximises the minimum normalised habitat availability among the vulnerable phases. Within this conservative framework, $Q_{21}$ emerged as the most protective discharge scenario, ensuring maximum preservation of fry and juvenile habitats while minimizing the risk of habitat collapse during high-flow conditions. This result underscores the ecological importance of marginal, low-velocity habitats, which are fundamental for survival during early life stages.

While the limiting factor approach prioritises protecting vulnerable stages, it may undervalue the ecological benefits associated with higher discharges for other habitat components. To achieve a more balanced evaluation, a multi-objective trade-off analysis using the Ideal Point Method was conducted (Figure 4.26).

The results identified $Q_{30}$ as the optimal compromise solution. Unlike the conservative limiting-factor approach, this method balances habitat losses affecting sensitive fry stages with habitat gains observed in juvenile and spawning areas under moderate flow conditions.

The compromise solution thus represents the discharge that minimises overall ecological conflict, ensuring the best possible balance between the competing requirements of the different components within the river reach.

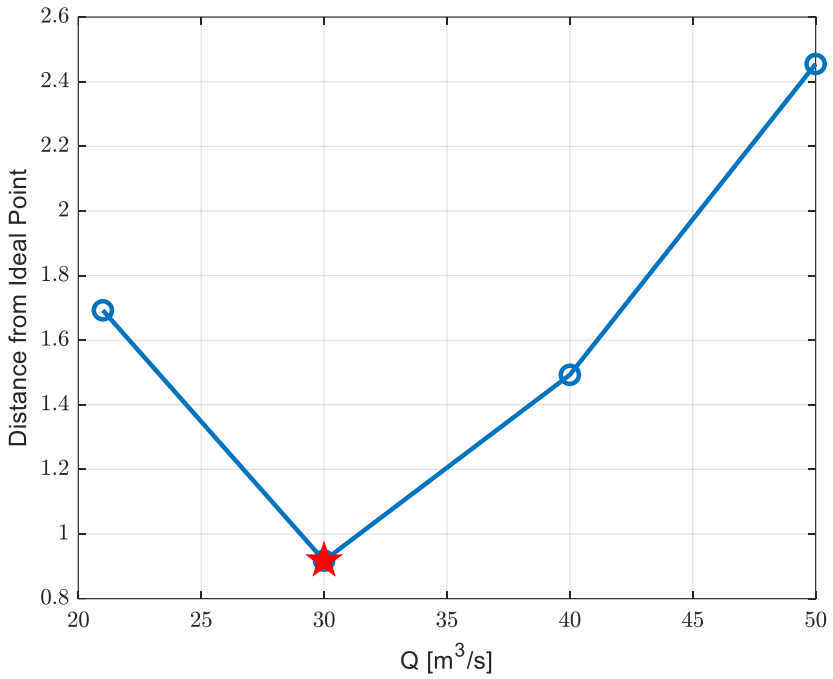



*Figure 4.26. Multi-objective compromise*

## 4.4 Unsteady simulation

Following the steady-state analysis, the river's behaviour was also investigated under unsteady flow conditions, using the HEC-RAS flow hydrograph described in Section 3.4. The implementation of an unsteady flow simulation represents a fundamental addition to the analysis. While steady-state scenarios provide a good quantification of the quantity and quality of available habitat, unsteady-flow analysis allows us to assess the stability and persistence of these habitats.

### 4.4.1 Temporal evolution of habitat availability

The variable-regime analysis allows us to assess species' sensitivity to the frequency of hydraulic variations. During the non-stationary phase of the simulation, the central 12 hours, the model simulated 15 cyclical flow variations between $Q_{21}$ and $Q_{50}$. This behaviour is clearly reflected in the oscillations of the WUA curves, highlighting a specific dynamic response for each life stage.

The summary results of the simulation are shown in Table 4.7, which highlights the net variations (ΔWUA), obtained as the difference between the initial and final values, the standard deviation and the habitat instability expressed as the coefficient of variation[3] (CV).

[3] Coefficient of variation (CV) is defined as the ratio between the standard deviation and the mean, and it is used to express the relative variability of a dataset: $CV = \frac{\sigma}{\mu}$

*Table 4.7. Summary of dynamic habitat response during the unsteady simulation*

| Species | Stage | WUA Initial | WUA Final | ΔWUA% | Std Dev | CV |
|---|---|---|---|---|---|---|
| Grayling | adult | 222186.2 | 264278.9 | 18.9 | 13153.0 | 0.05 |
| | fry | 56705.82 | 35186.3 | -37.9 | 7127.6 | 0.19 |
| | juvenile | 461330.1 | 454544.9 | -1.5 | 7293.3 | 0.02 |
| | spawning | 410257.1 | 402308.9 | -1.9 | 9920.1 | 0.03 |
| Trout | adult | 350064.4 | 295762.3 | -15.5 | 20493.3 | 0.07 |
| | fry | 229195.6 | 159952.4 | -30.2 | 24778.6 | 0.15 |
| | juvenile | 346190.4 | 288976.6 | -16.5 | 21919.2 | 0.08 |
| | spawning | 457075.8 | 471579.8 | 3.2 | 7689.9 | 0.02 |

The boxplots in Figure 4.27 and Figure 4.28 provide a synthetic view of habitat availability during the central ramping period of the hydrograph. They allow the distinction between life stages with persistent habitat availability and those characterised by stronger temporal variability.

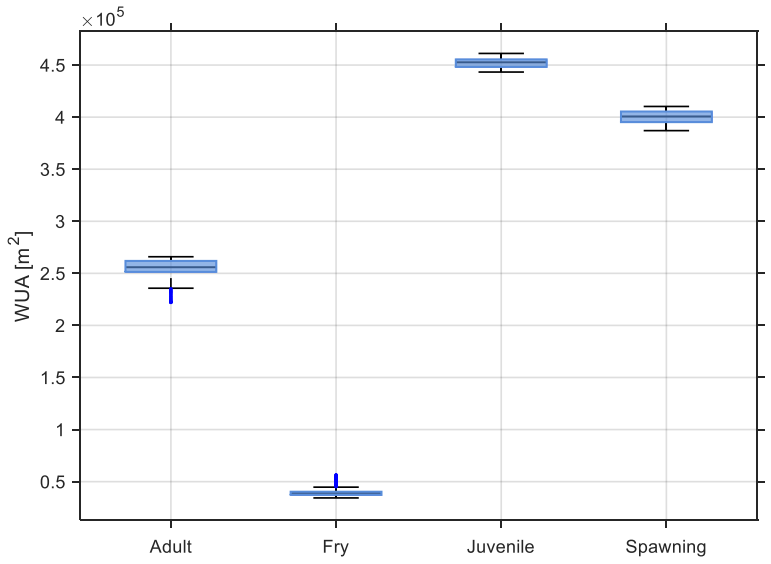



*Figure 4.27. Distribution of WUA values during the central 12 h of ramping for the different life stages of European grayling*

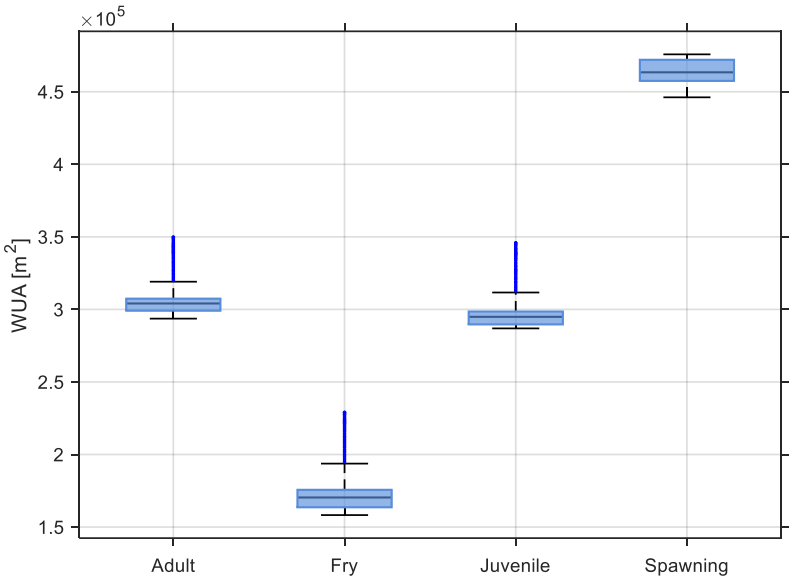



*Figure 4.28. Distribution of WUA values during the central 12 h of ramping for the different life stages of brown trout*

For European grayling, fry show the lowest WUA values and face the greatest ecological limitations. They remain distinctly separated from other stages. Adult, juvenile, and spawning stages have higher WUA values, with juvenile and spawning habitats showing particularly stable distributions. This indicates that the unsteady regime mainly affects the earliest life stage, while later stages are less sensitive to short-term flow fluctuations.

For brown trout, the boxplots show a wider range of responses across life stages. Spawning maintains the highest WUA values and a stable distribution, confirming resilience under tested unsteady conditions. Adults and juveniles show intermediate values, while fry is more limited and variable. Thus, compared with European grayling, brown trout shows greater sensitivity to unsteady flow, affecting not only fry but also adult and juvenile habitats.

Overall, the WUA boxplots show that habitat response to flow variability cannot be assessed only by comparing initial and final values. The temporal distribution of WUA is also important. Habitats with similar average availability may still differ greatly in stability and ecological reliability.

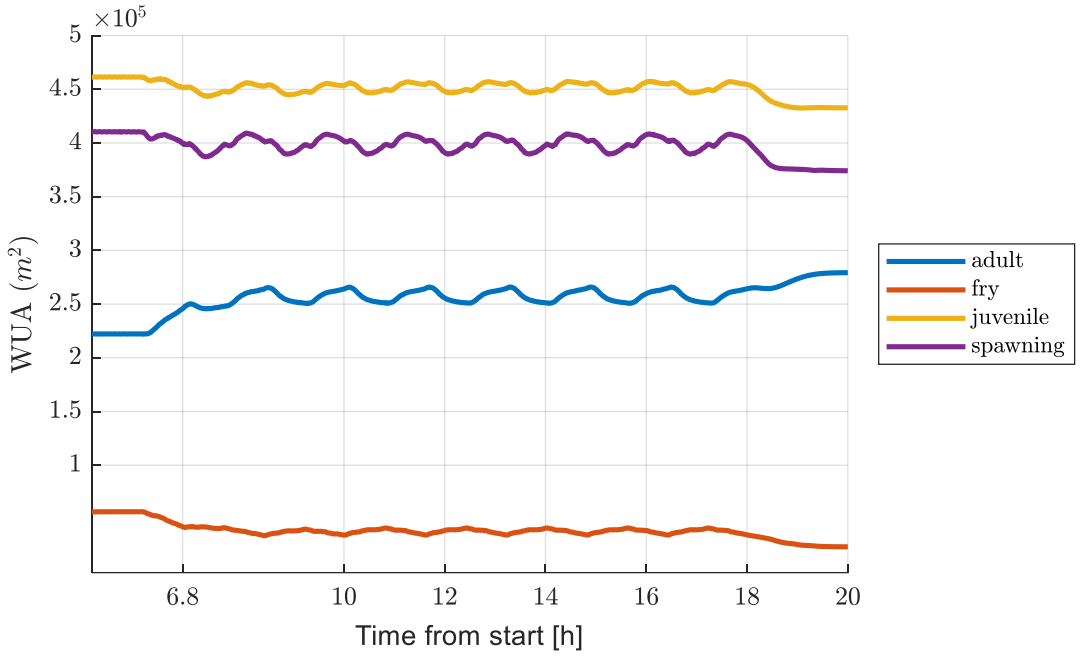



*Figure 4.29. Evolution of WUA over time for European grayling: comparison between the stages*

The dynamic analysis for grayling (Figure 4.29) confirms the generational conflict already observed in the stationary simulations for European grayling. This graph shows a clear divergence between adults and fry.

For adults, increasing flow leads to incremental benefits, as they reach a maximum WUA at $Q_{50}$. Conversely, for fry, increasing flow causes an immediate contraction of habitat. Visual analysis reveals a systematic phase opposition: every peak in flow that favours adults is matched by a loss for fry. Furthermore, fry also have the highest coefficient of variation in the dataset (CV = 0.19), indicating that habitat for newborns is not only decreasing but is extremely unstable. This high variability may increase the vulnerability of fry to displacement or drift during transient flow conditions.

Juvenile and spawning stages demonstrate more restricted WUA fluctuations. The low CV values illustrate the stability of WUA over time and the increased hydraulic resistance of these stages to short-term flow fluctuations. This suggests that these stages are less sensitive to variability than fry.

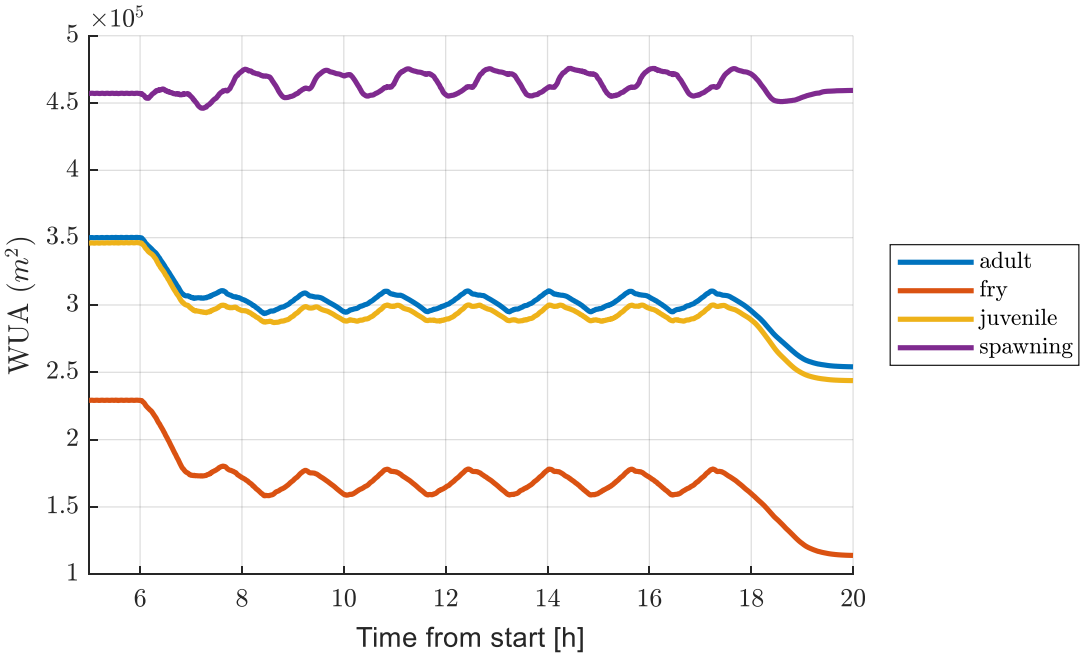



*Figure 4.30. Evolution of WUA over time for brown trout: comparison between the stages*

For brown trout (Figure 4.30), it is possible to observe a more widespread vulnerability to increased flows. For the fry, juvenile, and adult stages, the hydrograph shows a sudden reduction in habitat as early as the first hours of transition. A negative step is observed: once the flow rate increases, the system no longer recovers to its initial values, stabilising on a lower plateau of habitat availability.

This behaviour demonstrates that the response to unsteady flow does not merely involve a consistent fluctuation around an averaged value. In several cases, especially for brown trout fry, juveniles, and adults, the initial jump from low to high discharge may be particularly critical in reducing available habitat.

The spawning stage is the only exception: the curve shows an opportunistic dynamic, in which flow peaks push the WUA above the initial condition (ΔWUA = 3.2%). This occurs because fluctuations force the system to pass through intermediate flow ranges ($Q_{30}$ and $Q_{40}$) that had proven to be optimal for these stages in stationary analyses.

### 4.4.2 Habitat quality dynamics

To understand whether the variation in WUA is accompanied by a real change in environmental conditions, the percentage distribution of suitability classes was also analysed. Figure 4.30 and Figure 4.31 show the variation over time of the three classes: HSP (High Suitability, green), MSP (Medium Suitability, yellow), and LSP (Low Suitability, red).

The analysis for brown trout (Figure 4.31) highlights a clear decline in quality. For the fry and adult stages, the increase in flow causes a drastic expansion of the LSP class, indicating that an increasing proportion of the available area is likely to be hydrologically unsuitable and of poor quality. For fry, the reach reaches up to 75% of the available area, confirming that this stage is highly sensitive to unsteady flow

conditions. Similarly, in line with the decline in WUA recorded in temporal curves, degradation in habitat quality can also be observed across adult and juvenile life stages.

In contrast, the spawning stages maintain a dominant and stable HSP component, above 60% throughout the simulation. This indicates that their habitat remains resilient under unsteady flow conditions.

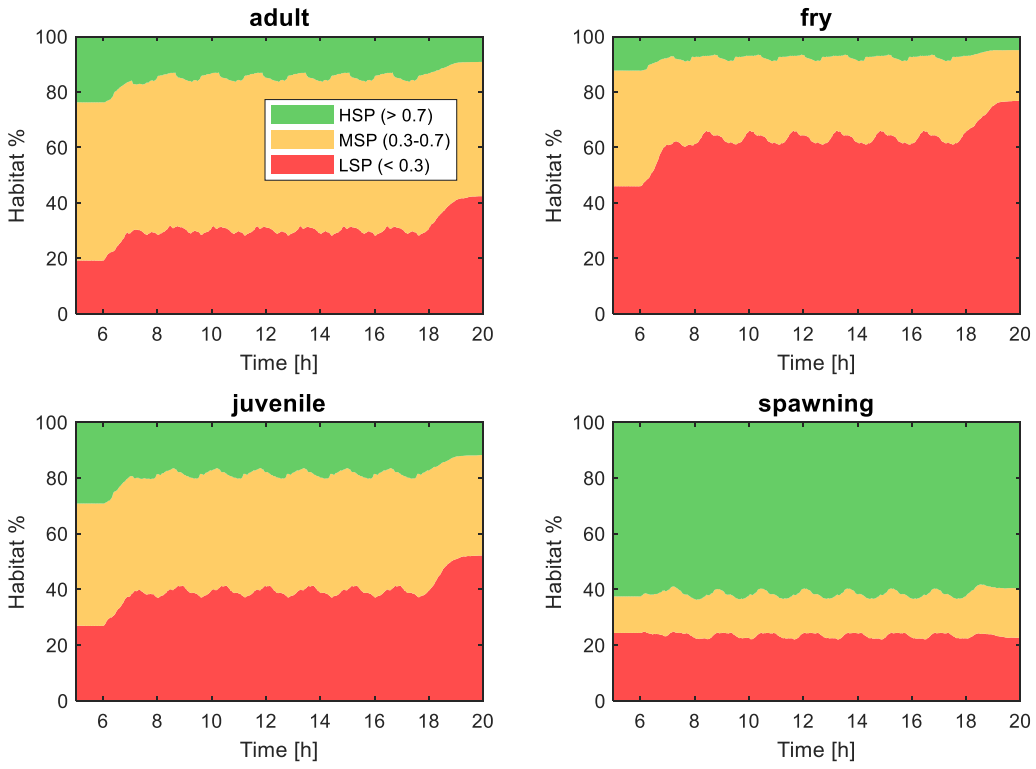



*Figure 4.31. Temporal dynamics of habitat quality for Brown Trout during the unsteady simulation, showing the evolution of suitability classes (HSP, MSP, LSP) over time*

European grayling (Figure 4.32) presents specific challenges during the fry stage, where the LSP class consistently dominates over 90% of the area. This indicates an almost complete absence of safe shelter for fry during transients. In contrast, the adult stage shows a qualitative improvement: as flow increases, the HSP component triples, confirming that the flood regime creates high-energy niches ideal for adult European grayling. The juvenile and spawning life stages appear to have more

constant quality distribution, with less temporal variation. This is consistent with their low ΔWUA% and the stable WUA curves.

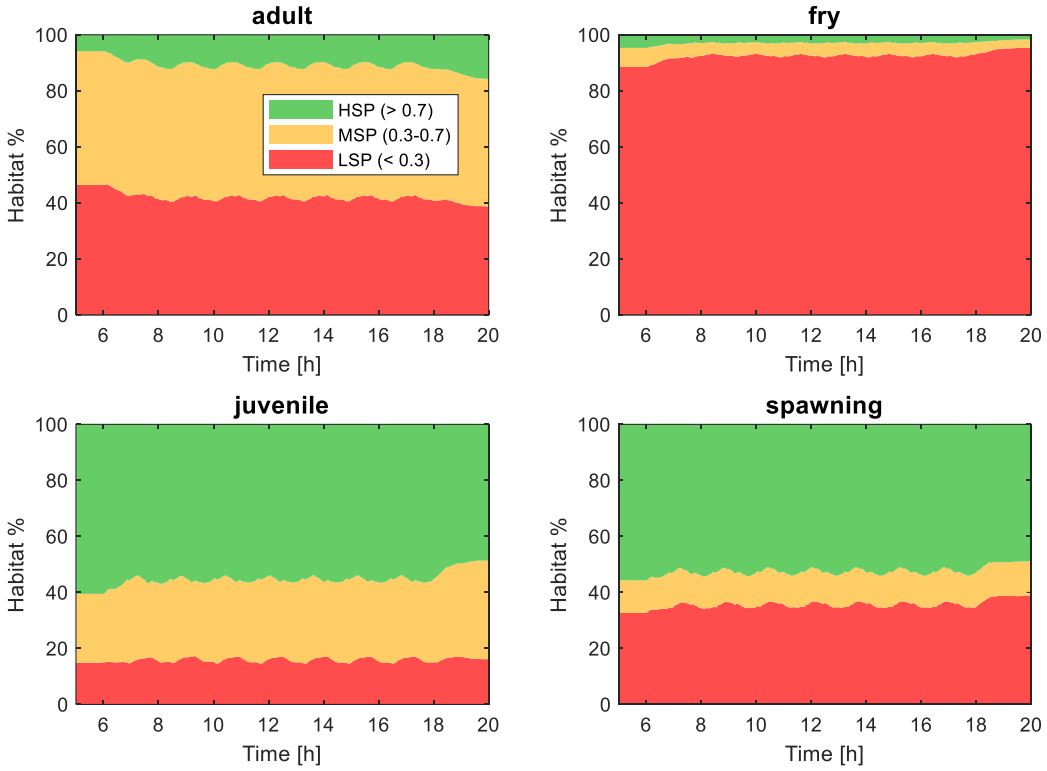



*Figure 4.32. Temporal dynamics of habitat quality for European Grayling during the unsteady simulation, showing the evolution of suitability classes (HSP, MSP, LSP) over time*

These results show that changes in habitat quantity and habitat quality do not always evolve in the same way. In some cases, WUA variations are accompanied by clear shifts in suitability classes, while in others the total habitat area remains relatively stable but its quality changes. Therefore, combining WUA dynamics with suitability-class distributions provides a more complete interpretation of the ecological response to unsteady flow.

The habitat-class boxplots provide a compact summary of the temporal variability of HSP, MSP and LSP during the central ramping period. They support the

interpretation derived from the time series by showing how persistent each suitability class is during the unsteady simulation.

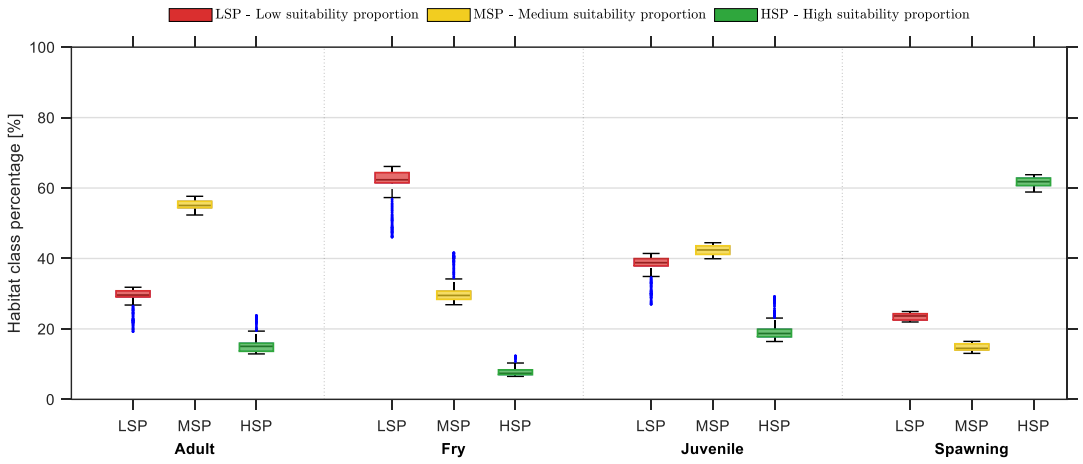



*Figure 4.33. Habitat class boxplot for brown trout*

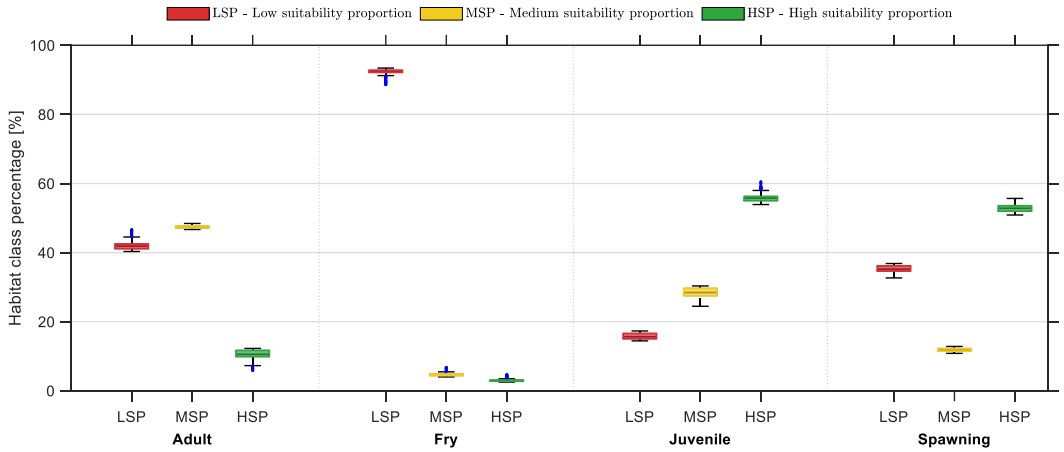



*Figure 4.34. Habitat class boxplot for European grayling*

For brown trout (Figure 4.33), the distributions confirm a tendency towards habitat degradation at the fry, juvenile, and adult stages, with the LSP component remaining relevant during the oscillating-flow phase. The fry stage is the most sensitive, with high proportions of low-suitability habitat and limited high-suitability conditions. By contrast, spawning maintains a consistently high HSP component, confirming the stability of reproductive habitat under the tested unsteady regime.

For European grayling (Figure 4.34), the boxplots emphasise the contrast between fry and adults. Fry habitat is persistently dominated by LSP, confirming that poor-quality conditions are not occasional but maintained throughout the analysed period. Adult habitat shows the opposite behaviour, with a much higher proportion of HSP, supporting the idea that flow variability can improve habitat quality for this life stage. Juvenile and spawning stages occupy an intermediate position, with less pronounced changes and more stable quality distribution patterns.

Overall, the unsteady simulation demonstrates that the ecological relevance of flow variability differs across life stages. Flow peaks increase and stabilise habitat

availability for adult grayling, while reducing and destabilising it for fry. In brown trout, fry, juvenile and adult stages are negatively affected by high-flow events, whereas spawning habitat remains suitable and may even improve slightly due to the repeated crossing of intermediate discharge ranges.

# Chapter 5

# Discussion

This work focused on the creation and validation of an ecohydraulic model of the bypass reach of the Ume River and on the analysis of habitat availability for two target species, brown trout (*Salmo trutta*) and European grayling (*Thymallus thymallus*), at different life-cycle stages. The main aim was to understand how discharge variation, which regularly affects the analysed reach, influences the quality, quantity and temporal stability of the available habitat.

## 5.1 Model reliability

The first objective of this research was to develop a model capable of accurately simulating the hydraulic conditions of the analysed river. In this regard, HEC-RAS proved to be an effective tool for modelling the system, reproducing field-observed water levels with high reliability.

The analysis of the results clearly shows that the maximum errors occur at points 1, 2, and 8. This behaviour is consistent with what was reported by Burman et al. (2019) and can be interpreted as an indication of the model's ability to reproduce, to a good extent, the system's behaviour. This discrepancy, also noted by Andersson & Angele (2018), can be explained by the formation of an upstream pool, which can lead to large variations in free-surface water levels at the model's initial points. At point 8, the difference in water surface level can be attributed to local ice buildup [40], which can cause large local variations and, consequently, uncertainty in calibration. Despite these few localised deviations, the model performs well, with a maximum measured error of 0.53 m and an excellent correlation along the 1:1 line. The order of magnitude of this error is in line with the literature, where Burman et al. (2020) report maximum errors of 0.74 m under comparable conditions.

Compared with previous models developed by Burman et al. (2019, 2020), differences were observed in the Manning coefficients assigned to each reach section. This discrepancy is common in ecohydraulic models and may be due to several factors. It may be related both to the use of different software, HEC-RAS in the present study and Delft3D in the reference papers, which can lead to different numerical resolutions, and to variations in mesh resolution, which therefore require different values to compensate for unresolved effects.

From the analysis of the cumulative distribution functions of the hydraulic parameters, it can be observed that the river system responds to increasing discharge mainly through changes in kinetic energy rather than in water depth. In a wide channel, water tends to spread and flow rapidly in the horizontal direction, without substantially increasing the water level. This behaviour implies that, from an ecological perspective, the discriminating variable is flow energy. The progressive reduction of low-energy areas may represent a critical factor for the most vulnerable organisms.

## 5.2 Ecological differences between species and life stages

The analysis of the quantity and distribution of suitable habitats clearly shows that each species and each life stage occupies a specific hydraulic niche. This confirms one of the fundamental principles of ecohydraulics: a single hydraulic condition cannot be considered optimal for all components of the system simultaneously [6], [30].

The most relevant result is the identification of fry as the limiting element of the system. In both steady and unsteady analyses, these stages exhibit the greatest habitat losses and the highest temporal instability.

Early life stages are particularly sensitive to increasing discharge. This result is consistent with Armstrong et al. (2003) and Heggenes (1996), who reported that fry are restricted to low-velocity areas and strongly depend on hydraulically protected habitats. In this study, this vulnerability is evident from several perspectives. First, fry show a strong reduction in habitat availability, with WUA decreasing rapidly as discharge increases. Second, they exhibit limited capacity for adaptation, as evidenced by an almost negligible shift in the niche centroid. This behaviour was well described by Padoan et al. (2025), who noted that juvenile stages are more vulnerable to flow changes due to their reduced hydraulic mobility. The fact that the centre of their habitat remains static makes fry highly exposed: if velocity increases, fry do not move to seek refuge, but lose access to their suitable microhabitat, increasing the risk of drift-related mortality.

For these reasons, fry can be considered the ecological bottleneck of this river system and should be the focus of management efforts to reduce the risk of negative effects on population recruitment.

In contrast, adult stages show greater tolerance or adaptive capacity under high-energy conditions, as they can utilize a broader range of depths and velocities for foraging and energetic efficiency compared to the more restricted requirements of early life stages

Another important aspect is the comparison between the two species, which is a key element for identifying a single flow strategy for the system. The analysis shows that European grayling has a greater tolerance to higher discharge levels and may even benefit from them. Brown trout, on the other hand, tends to experience a reduction in habitat with increasing discharge in almost all its life stages, showing greater sensitivity to high velocities. The literature indicates that adults of this species tend to select deeper, slower habitats, such as pools, to minimise energy expenditure

and reduce predation risk, thereby preferring more moderate flow regimes compared with grayling [23].

This behaviour suggests that the two species, across most of their life stages, respond differently to the same hydraulic variation.

## 5.3 Optimal discharge and ecological conflicts

The identification of an optimal discharge for the river reach represents one of the central themes of the study. However, the analysis of the behaviour of each species and life stage has shown that this cannot be achieved in absolute terms, since hydraulic requirements vary drastically throughout the biological cycle. It is therefore necessary to identify a discharge that maximises the system's functionality as much as possible, while being aware that the concept of optimal discharge depends on the criterion used and the priorities defined during the analysis.

By analysing the total Weighted Usable Area, it is possible to evaluate how the maximum usable area available to the whole system changes with discharge. This allows the discharge that maximises total habitat availability to be identified. From this analysis, it can be observed that low-discharge scenarios, $Q_{30}$ and especially $Q_{21}$, tend to maximise the overall availability of habitat. However, this aggregated interpretation must be interpreted with caution, as it tends to favour stages with greater spatial extent, risking an underestimation of the most ecologically fragile components.

This bias in habitat assessment was also discussed by Bovee et al. (1998), who argued that integrated approaches may overestimate favourable conditions for some classes at the expense of others.

This aspect emerges clearly in the case of grayling fry. Although they represent the most vulnerable stage, their numerical contribution to the total WUA is minimal and risks being overlooked. For this reason, a limiting factor analysis was also adopted. This type of logic is widely used in flow requirement analysis models [30]. This analysis prioritises the most sensitive stage and adopts as optimal the discharge that is most protective for that stage, in this case $Q_{21}$, because it ensures the greatest conservation of low-velocity marginal areas, which are necessary for fry survival.

However, such a conservative approach tends to underestimate the needs of adult European grayling stages, which prefer more energetic hydraulic conditions. If all species and life stages are considered in a balanced way, a different situation emerges. The compromise configuration appears to be $Q_{30}$. This method is consistent with the multi-objective approaches proposed in the literature for managing environmental flow regimes [14].

Overall, the results confirm what Bunn & Arthington (2002) highlighted: the management of flow regimes is an inherently multi-objective problem, and there is no single optimal solution.

It should also be noted, however, that the different life stages of a fish are not all present at the same time. Therefore, a more advanced strategy could be, as proposed by Hayes et al. (2019), to identify "emergence windows" during which a minimum discharge is maintained to support fry, while adopting more dynamic regimes for the rest of the year to favour adult stages.

## 5.4 Effects of hydropeaking

The simulations under unsteady conditions show that discharge fluctuations significantly affect both habitat quality and stability. This is consistent with the findings of Burman et al. (2021) and Maddock et al. (2013), who reported negative effects of hydropeaking on salmonid migration and survival.

In particular, rapid habitat loss is observed for brown trout fry, juveniles, and adults from the first flow variation. As highlighted by Burman et al. (2020), the river system exhibits hysteresis and intrinsic inertia, meaning that habitat availability is not fully recovered during subsequent phases of the hydraulic cycle.

An interesting exception is represented by the brown trout spawning stage. In contrast to what was observed in the other stages, it shows a positive response, suggesting that transient conditions create favourable periods. This phenomenon is related to the dynamic nature of the Potential Spawning Area, which, as documented by Burman et al. (2021), varies over time throughout the hydropeaking cycle in response to changes in velocity and depth. However, the observed improvement should not be interpreted as a generally positive effect of hydropeaking, but rather as the consequence of repeated transitions through discharge ranges favourable to spawning.

This result allows highlighting the partial divergence observed in this study compared with the literature. On the one hand, the results are consistent with those of Hayes et al. (2019), who identify fry as a particularly vulnerable life stage. On the other hand, they are not consistent regarding spawning, which does not appear vulnerable in this study. This variation may be due to the hydromorphological characteristics of the analysed river reach and, in the case study, to the association of spawning sites with hydraulically favourable conditions even within discharge fluctuations. Since the simulation accounts for the hydraulic consequences on habitat suitability but not for the direct effects on reproduction, such as substrate mobility, nest erosion, fine sediment deposition, or egg mortality, a positive spawning response must be interpreted with caution.

Therefore, the effect of hydropeaking cannot be considered uniform across all species and life stages. Instead, the response is strongly stage specific. Fry stages are the most sensitive, while juvenile, adult, and spawning stages show different responses depending on the species and on the overlap between the simulated hydraulic cycle and their respective hydraulic niche.

The boxplot analysis further shows that the ecological response to hydropeaking depends not only on net habitat loss, but also on the temporal stability of suitable conditions. Life stages with similar average WUA values may differ in variability, indicating that habitat availability can be more or less reliable during the ramping phase. This is particularly relevant for fry, for which even short periods of habitat instability may have strong ecological effects due to their limited swimming capacity and dependence on low-velocity refugia. Overall, the boxplots highlight the importance of considering habitat stability, in addition to habitat magnitude, when assessing unsteady flow regimes.

## 5.5 Practical implications, study limitations and future directions

The results of this study have practical implications for the management of regulated river reaches affected by hydropower operations. By linking two-dimensional hydraulic modelling with habitat suitability assessment, the approach provides a quantitative basis for identifying how different discharge scenarios influence habitat availability for multiple species and life stages. This is particularly relevant in bypass reaches such as the one downstream of the Stornorrfors dam, where flow releases are directly controlled by dam operation and therefore represent a potential management tool.

From a river management perspective, the results indicate that environmental flow decisions should not be based only on total habitat availability but should also consider the vulnerability of the most sensitive life stages. In this study, fry stages, especially grayling fry, emerged as the main ecological bottleneck because of their dependence on low-velocity marginal habitats. This suggests that low-discharge scenarios may be particularly important during sensitive periods of emergence or early development. At the same time, the results show that a single fixed discharge cannot simultaneously satisfy all ecological requirements. Therefore, a more flexible, seasonal flow strategy, combining protective low flows during critical periods with more dynamic regimes during less sensitive periods, may offer a more balanced compromise between ecological needs and hydropower operations.

The modelling framework applied in this thesis can also support restoration planning and decision-making. Spatially distributed maps of habitat suitability enable identification of areas where suitable habitats are concentrated, where low-energy refugia are lacking, and where habitat quality is most affected by increased flow. This information could be used to guide complementary restoration actions, such as improving marginal habitats, increasing hydraulic shelter, or prioritising areas where small morphological interventions could improve habitat availability for vulnerable stages.

Despite these implications, the study presents some limitations that must be considered when interpreting the results. First, the calibration of the hydraulic model was carried out based on observed water levels. Although the good agreement between simulated and measured WSE confirms the ability of the model to reproduce the general hydraulic behaviour of the reach, it does not necessarily guarantee the same accuracy in the spatial distribution of velocities. This aspect is particularly relevant for habitat analysis, since velocity is one of the most discriminating variables for juvenile stages and for the definition of low-energy areas.

Moreover, the limited number of points available for calibration and validation, together with the presence of missing values in some sections, reduces the possibility of fully assessing the spatial accuracy of the model. The validation, therefore, makes it possible to verify the general consistency of the water surface profile but does not allow for a detailed characterisation of local uncertainty across all morphological units of the reach.

A further source of uncertainty is related to the quality of the DTM used. As highlighted by the statistical analysis of water depths, the presence of anomalous

values up to approximately 14 m indicates the existence of local topographic artefacts. Although these anomalies represent a very limited portion of the domain and do not seem to substantially alter the average trends, they could locally influence the distribution of depth, the classification of habitat suitability, and the extreme values of hydraulic statistics.

The calibrated Manning coefficients must also be interpreted with caution. They represent effective model parameters and may compensate not only for the actual bed roughness, but also for uncertainties related to topography, mesh, vegetation, grain size, and boundary conditions. Consequently, the adopted roughness map should be considered functional to the hydraulic calibration, rather than a unique physical representation of the actual roughness.

From an ecological perspective, the analysis of habitat suitability was based only and exclusively on hydraulic parameters, without considering other fundamental ecological drivers. Factors such as water temperature, substrate grain size, or biological interactions play a fundamental role in site selection and survival. The absence of these variables, together with the lack of consideration of morphological changes, may lead to a partial representation of reality, since species often select complex combinations of physical and structural parameters rather than isolated variables. Moreover, the Habitat Suitability Curves (HSCs) adopted in this study were derived from published literature and expert-based sources rather than from site-specific observations collected within the Umeälven reach. Therefore, the represented hydraulic preferences may not fully reflect the actual behaviour and habitat requirements of local brown trout and European grayling populations. In addition, no independent biological observations, such as fish density surveys, habitat occupancy data, or spawning success measurements, were available to validate model predictions. Consequently, HSI and WUA values should be interpreted as indicators of potential physical habitat rather than direct measures of species presence, abundance, or ecological status.

This limitation is particularly relevant for the spawning stage. Reproductive suitability does not depend only on depth and velocity, but also on substrate grain size, bed stability, fine sediment transport and the risk of nest erosion. In addition, derived hydraulic parameters such as bed shear stress were not considered in the analysis, despite their importance in determining spawning redd stability and the energetic cost of station-holding for reproducing fish. Therefore, the positive response observed for spawning, especially under unsteady conditions, must be interpreted with caution: it indicates the maintenance of favourable hydraulic conditions, but does not necessarily demonstrate reproductive success.

Furthermore, the two-dimensional model, although suitable for the reach-scale analysis performed, does not fully represent microhabitat complexity and fine-scale hydraulic processes. The computational grid of 10 m × 10 m, while appropriate for covering the entire river stretch, lacks the spatial resolution necessary to solve the flow field at the fish scale of approximately 1 m. As a consequence, the model is unable to capture small local refugia, such as low-velocity zones behind boulders, near river margins, or beneath undercut banks, which may be particularly important for vulnerable stages.

These limitations are further amplified by the inherent simplifications of the two-dimensional modelling approach. As suggested by Burman et al. (2023), some

transient processes, such as the decrease in discharge during hydropeaking, may have a fundamentally three-dimensional nature, linked to vertical mixing and turbulence that cannot be captured by 2D models. Therefore, the model may only partially reproduce the hydraulic mechanisms governing habitat availability and refuge formation during rapid flow fluctuations.

Finally, the hydropeaking conditions, which are very important for the dynamic analysis of the river, were simulated through an idealised hydrograph. Although useful as a management benchmark, this stepwise scenario does not fully represent the natural variability of hydropower plant operations, failing to capture real-world fluctuations in peak frequency, duration, and ramping rates, as well as potential hysteresis phenomena in habitat recovery. Consequently, the simulated habitat responses should be interpreted as indicative trends rather than exact predictions of ecological conditions under real hydropeaking regimes.

About future developments, the research could evolve in the following directions:

- Integration of ecological variables: the inclusion of thermal models and substrate maps would greatly improve the ecological realism of HSI assessments.
- High-resolution modelling: the adoption of 3D models or more refined meshes would make it possible to identify more accurately the velocity shelters created by boulders and mesoscale obstructions.
- Population dynamics: it would be appropriate to integrate habitat models with long-term simulations and individual-based models (IBMs), in order to assess the effects of the flow regime not only on space availability, but also on actual population dynamics and recruitment over time.
- Seasonal analysis: as suggested by Hayes et al. (2019), the development of flow criteria specific to different "time windows" would allow the most sensitive stages to be protected, without excessively penalising hydropower production during the rest of the year.

•

# Chapter 6

# Conclusion

This thesis has investigated the application of two-dimensional ecohydraulic modelling for habitat suitability assessment in the regulated reach of the Ume River downstream of the Stornorrfors dam. The study is motivated by the ecological challenges associated with flow regulation in river systems, where alterations in hydraulic conditions can significantly affect habitat availability and quality. The objective of this study has, therefore, been to connect hydraulic modelling and ecological analysis to identify the effects of changing discharge levels on brown trout (*Salmo trutta*) and European grayling (*Thymallus thymallus*), considering four life-cycle stages: fry, juvenile, adult, and spawning.

The study shows that habitat availability in the bypass reach depends not only on discharge volume but also on how discharge redistributes hydraulic energy along the river reach. The ecohydraulic model showed that increasing flow does not elicit a uniform ecological response; rather, it produces clear contrasts among species and life stages.

The main ecological result of the study is the identification of early life stages, particularly grayling fry, as the most vulnerable components of the system. Their dependence on low-velocity marginal habitats makes them highly sensitive to both increasing discharge and short-term fluctuations. For this reason, they represent the main ecological bottleneck of the studied reach and should be taken into account in the management of environmental flows.

The comparison between discharge scenarios confirms that no single discharge scenario can maximise habitat suitability for all ecological components simultaneously. Low discharges, particularly $Q_{21}$, provide the greatest protection for the most sensitive life stages. While an intermediate discharge such as $Q_{30}$ represents a more balanced compromise when all species and life stages are considered together. This clearly shows that the management of ecological flow in regulated rivers cannot be based solely on maximum suitable habitat area; it must also consider environmental vulnerability, habitat quality, and reliability.

The simulations under unsteady conditions also demonstrate that hydropeaking fluctuations can reduce habitat stability, even when average availability appears acceptable. This was further highlighted by the boxplot analysis, which showed that the persistence and variability of suitable habitat can differ substantially among life stages, even when overall WUA values appear comparable. This aspect is particularly

important for early life stages, which have limited mobility when suitable hydraulic conditions disappear. Consequently, the ecological impact of flow regulation should be evaluated not only in terms of minimum and maximum values, but also by considering the timing of variations, their frequency, and the rate at which flows change.

Overall, the thesis demonstrates that two-dimensional ecohydraulic modelling can provide useful quantitative support for the management of regulated rivers. It offers a spatially explicit framework for comparing different discharge scenarios and identifying ecological trade-offs between species and life stages. However, the results should be interpreted only as indicators of potential hydraulic habitat suitability, not as direct predictions of fish presence or reproductive success. For this reason, future management should combine hydraulic habitat modelling with ecological information on substrate, temperature, refuge availability, sediment dynamics and the seasonal requirements of the different life stages.

In conclusion, the sustainable management of Ume River requires an adaptive, compromise-based approach to flow regimes. Maintaining environmental flows during critical periods for sensitive life stages, while allowing more fluctuating flow regimes during non-critical early-life periods, could be a more environmentally successful alternative to a uniform discharge throughout the year. This approach would better reflect the complexity of fish habitat requirements and the ecological consequences of flow regulation in rivers influenced by hydropower plan.

# Declaration of Generative AI Use

Artificial intelligence tools were employed exclusively as supporting instruments during the development of this thesis. Their use was limited to an initial screening of scientific papers in order to identify material relevant to the research topic, to assist in reformulating and improving clarity and language of the manuscript and to support the development of MATLAB code through error checking and debugging activities.

AI systems were not used to generate scientific results, perform independent analyses, or draw research conclusions. All methodological decisions, modelling approaches, data processing procedures, interpretations, and final considerations presented in this work remain entirely responsibility of the author.

# Bibliography


[1] USGS, 'How Much Water is There on Earth? | U.S. Geological Survey'. Accessed: Mar. 23, 2026. [Online]. Available: https://www.usgs.gov/water-science-school/science/how-much-water-there-earth

[2] UN-Water, 'UN-Water input on Freshwater-Biodiversity Linkages: Response to the Zero-Draft Document from the Open-Ended Working Group on the Post-2020 Global Biodiversity Framework', UN-Water. Accessed: Mar. 23, 2026. [Online]. Available: https://www.unwater.org/publications/un-water-input-freshwater-biodiversity-linkages-response-zero-draft-document-open

[3] WWF, '2024 Living Planet Report', World Wildlife Fund. Accessed: Mar. 17, 2026. [Online]. Available: https://www.worldwildlife.org/publications/2024-living-planet-report/

[4] WWF, 'The World's Forgotten Fishes'. Accessed: Mar. 23, 2026. [Online]. Available: https://wwf.panda.org/discover/our_focus/freshwater_practice/the_world_s_forgotten_fishes

[5] D. Dudgeon *et al.*, 'Freshwater biodiversity: importance, threats, status and conservation challenges', *Biol. Rev.*, vol. 81, no. 2, pp. 163–182, 2006, doi: 10.1017/S1464793105006950.

[6] S. E. Bunn and A. H. Arthington, 'Basic Principles and Ecological Consequences of Altered Flow Regimes for Aquatic Biodiversity', *Environ. Manage.*, vol. 30, no. 4, pp. 492–507, Oct. 2002, doi: 10.1007/s00267-002-2737-0.

[7] S. J. Cooke *et al.*, 'The role of ecohydraulics in addressing the freshwater biodiversity crisis', *Water Biol. Secur.*, vol. 5, no. 2, p. 100475, Apr. 2026, doi: 10.1016/j.watbs.2025.100475.

[8] Å. Widén, B. M. Renöfält, and R. Jansson, 'Environmental flows in a future climate: Balancing hydropower production and ecosystem rehabilitation in the Ume River system, Sweden', *Sci. Total Environ.*, vol. 955, p. 176622, Dec. 2024, doi: 10.1016/j.scitotenv.2024.176622.

[9] A. J. Burman, A. G. Andersson, J. G. I. Hellström, and K. Angele, 'Case Study of Transient Dynamics in a Bypass Reach', *Water*, vol. 12, no. 6, p. 1585, Jun. 2020, doi: 10.3390/w12061585.

[10] G. Englund and B. Malmqvist, 'Effects of Flow Regulation, Habitat Area and Isolation on the Macroinvertebrate Fauna of Rapids in North Swedish Rivers', *Regul. Rivers Res. Manag.*, vol. 12, no. 4–5, pp. 433–445, 1996, doi: 10.1002/(SICI)1099-1646(199607)12:4/5<433::AID-RRR415>3.0.CO;2-6.

[11] J. Heggenes, 'Habitat Selection by Brown Trout (salmo Trutta) and Young Atlantic Salmon (s. Salar) in Streams: Static and Dynamic Hydraulic Modelling', *Regul. Rivers Res. Manag.*, vol. 12, no. 2–3, pp. 155–169, 1996, doi: 10.1002/(SICI)1099-1646(199603)12:2/3<155::AID-RRR387>3.0.CO;2-D.

[12] D. Ayllón, A. Almodóvar, G. G. Nicola, and B. Elvira, 'Interactive effects of cover and hydraulics on brown trout habitat selection patterns', *River Res. Appl.*, vol. 25, no. 8, pp. 1051–1065, 2009, doi: 10.1002/rra.1215.

[13] F. Padoan, G. Calvani, G. De Cesare, and P. Perona, 'Hydraulic drive framework on habitat suitability enhances movement bias of brown trout in stream networks', *Sci. Rep.*, vol. 15, no. 1, p. 16688, May 2025, doi: 10.1038/s41598-025-00216-x.
[14] Å. Widén, B. M. Renöfält, E. Degerman, D. Wisaeus, and R. Jansson, 'Let it flow: Modeling ecological benefits and hydropower production impacts of banning zero-flow events in a large regulated river system', *Sci. Total Environ.*, vol. 783, p. 147010, Aug. 2021, doi: 10.1016/j.scitotenv.2021.147010.
[15] Å. Widén, B. Malm Renöfält, E. Degerman, D. Wisaeus, and R. Jansson, 'Environmental Flow Scenarios for a Regulated River System: Projecting Catchment-Wide Ecosystem Benefits and Consequences for Hydroelectric Production', *Water Resour. Res.*, vol. 58, no. 1, p. e2021WR030297, 2022, doi: 10.1029/2021WR030297.
[16] A. Adeva-Bustos, K. Alfredsen, H.-P. Fjeldstad, and K. Ottosson, 'Ecohydraulic Modelling to Support Fish Habitat Restoration Measures', *Sustainability*, vol. 11, no. 5, p. 1500, Mar. 2019, doi: 10.3390/su11051500.
[17] Vattenfall, 'Våra kraftverk: Stornorrfors - Vattenfall'. Accessed: Mar. 23, 2026. [Online]. Available: https://powerplants.vattenfall.com/sv/stornorrfors/
[18] Umeå universitet, 'Restoration project recreates variation in the Vindel River, Sweden', ScienceDaily. Accessed: Mar. 23, 2026. [Online]. Available: https://www.sciencedaily.com/releases/2015/11/151103090541.htm
[19] Rewilding Sweden, 'Removal of four barriers, Sweden - Open Rivers Programme', Open Rivers Programme - European Open Rivers Programme. Accessed: Mar. 23, 2026. [Online]. Available: https://openrivers.eu/projects/202407585-removal-of-four-barriers-sweden/
[20] A. J. Burman, R. D. Hedger, J. G. I. Hellström, A. G. Andersson, and L. E. Sundt-Hansen, 'Modelling the downstream longitudinal effects of frequent hydropeaking on the spawning potential and stranding susceptibility of salmonids', *Sci. Total Environ.*, vol. 796, p. 148999, Nov. 2021, doi: 10.1016/j.scitotenv.2021.148999.
[21] D. S. Hayes *et al.*, 'Life Stage-Specific Hydropeaking Flow Rules', *Sustainability*, vol. 11, no. 6, p. 1547, Jan. 2019, doi: 10.3390/su11061547.
[22] HELCOM, 'Salmon and Sea Trout Populations and Rivers in the Baltic Sea – HELCOM assessment of salmon (Salmo salar) and sea trout (Salmo trutta) populations and habitats in rivers flowing to the Baltic Sea', Helsinki Commission (HELCOM), Baltic Sea Environment Proceedings No. 126A, 2011.
[23] J. D. Armstrong, P. S. Kemp, G. J. A. Kennedy, M. Ladle, and N. J. Milner, 'Habitat requirements of Atlantic salmon and brown trout in rivers and streams', *Fish. Res.*, vol. 62, no. 2, pp. 143–170, May 2003, doi: 10.1016/S0165-7836(02)00160-1.
[24] M. Kottelat and J. Freyhof, *Handbook of European freshwater fishes*. Cornol, Switzerland; Berlin, Germany: Kottelat; Freyhof, 2007.
[25] P. Louhi, A. Mäki-Petäys, and J. Erkinaro, 'Spawning habitat of Atlantic salmon and brown trout: general criteria and intragravel factors', *River Res. Appl.*, vol. 24, no. 3, pp. 330–339, 2008, doi: 10.1002/rra.1072.
[26] iFikse, 'Brown Trout (Salmo trutta)', iFiske.se. Accessed: Apr. 10, 2026. [Online]. Available: https://www.ifiske.se/en/fish-brown-trout.htm

[27] M. Nykänen and A. Huusko, 'Suitability criteria for spawning habitat of riverine European grayling', *J. Fish Biol.*, vol. 60, no. 5, pp. 1351–1354, 2002, doi: 10.1111/j.1095-8649.2002.tb01730.x.
[28] iFikse, 'Grayling (Thymallus thymallus)', iFiske.se. Accessed: Apr. 10, 2026. [Online]. Available: https://www.ifiske.se/en/fish-grayling.htm
[29] I. Maddock, 'The importance of physical habitat assessment for evaluating river health', *Freshw. Biol.*, vol. 41, no. 2, pp. 373–391, 1999, doi: 10.1046/j.1365-2427.1999.00437.x.
[30] I. Maddock, A. Harby, P. Kemp, and P. J. Wood, *Ecohydraulics: An Integrated Approach*. John Wiley & Sons, 2013.
[31] A. M. Mouton, M. Schneider, J. Depestele, P. L. M. Goethals, and N. De Pauw, 'Fish habitat modelling as a tool for river management', *Ecol. Eng.*, vol. 29, no. 3, pp. 305–315, Mar. 2007, doi: 10.1016/j.ecoleng.2006.11.002.
[32] D. W. Crowder and P. Diplas, 'Using two-dimensional hydrodynamic models at scales of ecological importance', *J. Hydrol.*, vol. 230, no. 3–4, pp. 172–191, May 2000, doi: 10.1016/S0022-1694(00)00177-3.
[33] Atlantic Ecology Division (AED), and US EPA, 'Habitat Suitability Index (HSI)'. Accessed: Feb. 06, 2026. [Online]. Available: https://archive.epa.gov/aed/html/research/scallop/web/html/hsi.html
[34] R. F. Raleigh, L. D. Zuckerman, and P. C. Nelson, 'Habitat suitability index models and Instream flow suitability curves: Brown trout', 1984.
[35] K. D. Bovee, B. L. Lamb, Bartholow, J. M., Stalnaker, C. B., Taylor, J., and Henriksen, J., 'Stream habitat analysis using the instream flow incremental methodology', U.S. Geological Survey, Biological Resources Division, USGS/BRD-1998-0004, 1998.
[36] G. Yang *et al.*, 'Application of a fish habitat model to assess habitat fragmentation using high flow and sediment transport in the Rumei Dam in Lancang River (China)', *Ecohydrology*, vol. 17, no. 4, p. e2583, Jun. 2024, doi: 10.1002/eco.2583.
[37] P. Zhou *et al.*, 'Impacts of channel complexity and main-to-anabranch width ratio on fish habitat suitability across varying flow regimes', *Ecol. Eng.*, vol. 226, p. 107931, May 2026, doi: 10.1016/j.ecoleng.2026.107931.
[38] USACE, 'HEC-RAS Hydraulic Reference Manual', Hydrologic Engineering Center (HEC), Davis, CA, Dec. 2020. [Online]. Available: https://www.hec.usace.army.mil/confluence/rasdocs/ras1dtechref/6.6
[39] USACE, 'HEC-RAS 2D User's Manual', Hydrologic Engineering Center (HEC), 2024. Accessed: Apr. 16, 2026. [Online]. Available: https://www.hec.usace.army.mil/confluence/rasdocs/r2dum/latest
[40] A. J. Burman, A. G. Andersson, and J. G. I. Hellström, 'INHERENT DAMPING IN A PARTIALLY DRY RIVER', presented at the 38th IAHR World Congress, Sep. 2019, pp. 5091–5100. doi: 10.3850/38WC092019-0281.
[41] A. J. Burman, A. G. Andersson, and J. G. I. Hellström, 'Hydraulic classification of hydropeaking stages in a river reach', *River Res. Appl.*, vol. 39, no. 4, pp. 692–702, 2023, doi: 10.1002/rra.4098.
[42] P. Rivinoja, S. McKinnell, and H. Lundqvist, 'Hindrances to upstream migration of atlantic salmon ( *Salmo salar* ) in a northern Swedish river caused by a

hydroelectric power-station', *Regul. Rivers Res. Manag.*, vol. 17, no. 2, pp. 101–115, Mar. 2001, doi: 10.1002/rrr.607.

[43] W. Yao, 'Application of the Ecohydraulic Model on Hydraulic and Water Resources Engineering', PhD Thesis, Technische Universität München, 2016. [Online]. Available: https://mediatum.ub.tum.de/1303204